Aalto University
School of Engineering

Matias Purtanen

External Compression in Medium-Speed Engines

Thesis of diploma, which has been given in for the degree of Master of Science in Technology.

In Vaasa 4.3.2018
Supervisor: Ville Vuorinen (Prof.)
Advisor: Christer Hattar (M.Sc.Tech.)

Aalto-yliopisto
Insinööritieteiden korkeakoulu

Aalto-yliopisto, PL 11000, 00076 AALTO
www.aalto.fi

Diplomityön tiivistelmä

Tekijä Matias Purtanen		
Työn nimi Ulkoinen puristus keskinopeusmoottoreissa		
Koulutusohjelma Energy Technology		
Pääaine Energy Technology		**Koodi** ENG21
Työn valvoja Prof. Ville Vuorinen		
Työn ohjaaja DI Christer Hattar		
Päivämäärä 4.3.2018	**Sivumäärä** 82 + 15	**Kieli** Englanti

Tiivistelmä

Tämä diplomityö tutkii vaihtoehtoisten polttomoottorien tyyppiä, joita kutsutaan ulkoisen puristuksen moottoreiksi. Huomattava osa paloilman puristuksesta tehdään työsylinterin ulkopuolella, eli ulkoisesti. Moottoreissa käytetään toisentyyppistä kaksitahtityökiertoa. Pakokaasuja ei huuhdella sylinteristä, sen sijaan kaasunvaihto tehdään venttiileillä, niin kuin nelitahtimoottorissa. Näillä moottoreilla on potentiaalia parantaa polttomoottorin hyötysuhdetta samalla tavoin kuin Atkinson- ja Miller-työkierto.

Tämän diplomityön tarkoituksena on selvittää näiden vaihtoehtoistyyppisten moottorien suorituskykypotentiaali keskinopeusmoottorien reunaehdoilla. Kirjallisuuskatsauksella selvitetään teoria, ja minkälaisia ulkoisen puristuksen moottorikonsepteja on kehitetty. Tarkempaan tutkimukseen on valittu kaksi konseptia: Z-moottori ja Hoos Variant-moottori. Näitä konsepteja tutkitaan 1-ulotteisen moottorisimulaation avulla käyttäen GT-Power-ohjelmistoa. Herkkyysanalyysillä selvitetään kuinka herkkiä konseptit ovat eri moottoriparametreille. Konseptit optimoidaan ja niitä verrataan nelitahtiseen keskinopeuksikseen referenssi-Wärtsilä-moottoriin. Vertailulle on määritelty standardireunaehdot, jotta se olisi järkevä.

Standardireunaehdoilla lopputulos on, että referenssimoottorilla on parempi hyötysuhde kuin Z-moottorilla ja Hoos Variant-moottorilla. Pääsyynä on erittäin korkeat lämpöhäviöt, johon pääsyynä on moottorien käyttämä työkierto. Pääongelma työkierrossa on, että moottorin sylinterissä on jatkuvasti erittäin kuumia jäännöskaasuja, joka aiheuttaa kohtuuttoman suuren lämpökuorman moottorille. Kuitenkin, standardireunaehdoilla hyvän turboahtamisen hyötysuhteen ja ainutlaatuisen työkierron ansiosta konsepteilla on huomattavasti marginaalia nostaa sylinterin maksimipainetta. Jos tämä marginaali hyödynnetään käyttämällä nopeaa palamistyyppiä, kuten homogeenista puristussytytystä, on kummankin moottorikonseptin hyötysuhde huomattavasti parempi kuin referenssimoottorin.

Loppupäätelmänä on, että näiden moottorikonseptien kehityksen aloittaminen ei ole kannattavaa Wärtsilälle. Jos Wärtsilä päättää tutkia näitä moottoreita tarkemmin, ylimääräisiä simulaatiotutkimuksia suositellaan, jotta tämän työn päätelmät voidaan vahvistaa.

Avainsanat Keskinopeusmoottorit, ulkoinen puristus, moottorikonseptit, kaksitahtimoottorit, turboahtaminen, mäntäkompressori, ahtoilma, Z-moottori, Hoos-moottori

Aalto University
School of Engineering

Aalto University, P.O. BOX 11000, 00076 AALTO
www.aalto.fi

Abstract of master's thesis

Author Matias Purtanen		
Title of thesis External Compression in Medium-Speed Engines		
Degree programme Energy Technology		
Major Energy Technology		**Code** ENG21
Thesis supervisor Ville Vuorinen (Prof.)		
Thesis advisor Christer Hattar (M. Sc.Tech.)		
Date 4.3.2018	**Number of pages** 82 + 15	**Language** English

Abstract

This Master's thesis is a study of an alternative type of internal combustion engines. Such engines are referred to as the external compression engines. A significant part of the compression of the combustion air is done outside the working cylinder, in other words externally. The external compression engines use an alternative type of two-stroke cycle. Instead of exhaust gas scavenging, gas exchange is done with poppet valves, like in a four-stroke engine. External compression engines have potential to increase an internal combustion engine's efficiency in a similar way as the Atkinson and Miller cycle.

The purpose of this thesis is to find out the engine performance potential of such engines, within medium-speed engine boundary conditions. The thesis starts with a review of the related theory and the different external compression engine concepts. Two engine concepts, the Z-engine and the Hoos Variant engine are studied using 1-D engine performance simulations utilizing GT-Power simulation software. A sensitivity analysis is done to find out how sensitive the concepts are to different engine parameters. The concepts are optimized and compared to a reference Wärtsilä four-stroke medium-speed engine. Standard boundary conditions are defined so that the comparison will be sensible.

The result of the final comparison is that with the standard boundary conditions, both the Z-engine and the Hoos Variant are less fuel efficient than the reference Wärtsilä engine. The main reason is very high heat transfer losses during the whole working cycle in the concepts, which is caused by the working cycle of the concepts. The major problem with this working cycle is that the cylinder is constantly operating with extremely hot residual gases, which causes an unreasonably high heat load. However, due to the efficient turbocharging and the unique two-stroke cycle, with the standard boundary conditions, the concepts have significant margin to increase the maximum cylinder pressure. If this margin is utilized with a fast heat release, such as HCCI, then both concepts are significantly more efficient than the reference engine.

The conclusion is that it is not recommended for Wärtsilä to start the development of these engine concepts. If Wärtsilä decides to investigate the subject further, certain additional simulation studies are recommended to substantiate the conclusions of this thesis.

Keywords Medium-speed engines, external compression, engine concepts, two-stroke engines, turbocharging, piston compressor, charge air, Z-engine, Hoos engine

Preface

This Master's thesis work was a great and challenging opportunity for me. In addition to learning a lot about engines and engine simulations, I had to learn the fundamentals again through practice. With limited simulation experience, I was slightly worried to start studying these exotic engine concepts. This worry was completely unnecessary, as building and running an unconventional engine model proved to be extremely interesting and rewarding.

This Master's thesis was done as an assignment for Wärtsilä Finland Oy. Thanks go to Jari Hyvönen and all of my colleagues. Special thanks go to Jesper Engström, whose help with GT-Power was irreplaceable. Big thanks go to my advisor Christer Hattar, who gave me this opportunity, is a true inspiration for me and gave me essential guidance throughout the thesis work. Big thanks also go for the interesting off-topic conversations; it is great to meet someone who "speaks the same language". I also want to thank everyone else at Wärtsilä, who took their time to help this clueless thesis worker.

I thank the people at Gamma Technologies support for further help with their simulation software. I want to thank Timo Janhunen from Aumet Oy and Sami Nyyssönen from VTT Oy for collaboration. Thanks also go to Frank Hoos. At Aalto University, I want to thank my supervisor Ville Vuorinen for guidance and help with the thesis work.

I want to thank friends and family for supporting me, like with everything, also during my study years. Thanks go to my Wasa fellows, and the pastor of Lauttasaari. Marti also wants to thank his friends out there in the world. Also the ones who know I don't care. Big thanks go to Tornio Roastmasters, who support me each day, even though the method is sometimes interesting.

Invictus of Tornio kiittää ja kuittaa.

Vaasa 4.3.2018

Matias Purtanen

Matias Purtanen

Table of Contents

Symbols

ºCA	Degrees of crank angle
ºCA aTDC	Degrees of crank angle after top dead centre
bar (a)	Absolute pressure in bar
g/kWh	Grams Per Kilowatt-Hour
kJ/kg	Kilojoules per kilogram
rpm	Revolutions per minute
delta p	Pressure difference over the cylinder (p_3-p_5)
M	Specific molar mass
$\dot{m}$	Mass flow rate
$\dot{N}$	Molar mass flow rate
P_C	Total compression work
$P_{iT,C}$	Compressor isothermal work
$P_{s,C}$	Compressor isentropic work
$P_{s,T}$	Turbine isentropic work
p	Pressure
p_1	Suction air pressure
p_3	Charge air pressure
p_5	Exhaust pressure before first turbine
p_6	Ambient exhaust pressure
p_{comp}	Compression pressure
p_{max}	Maximum cylinder pressure
R	Specific gas constant
T	Temperature
T_1	Suction air temperature
T_5	Exhaust gas temperature
T_{comp}	Compression temperature
$\dot{V}$	Volume flow rate
$\eta_{iT,C}$	Compression isothermal efficiency
$\eta_{s,C}$	Compression isentropic efficiency
$\eta_{s,T}$	Turbine isentropic efficiency
γ	Specific heat ratio
λ	Relative air-fuel ratio
π	Pressure ratio

Abbreviations

aTDC	After Top Dead Centre
BDC	Bottom Dead Centre
BMEP	Brake Mean Effective Pressure
BSFC	Brake Specific Fuel Consumption
CAC	Charge Air Cooler
CMEP	Compressor Mean Effective Pressure
ECE	External Compression Engine
EGR	Exhaust Gas Recirculation
FMEP	Friction Mean Effective Pressure
HCCI	Homogeneous Charge Compression Ignition
IC	Intercooler
IMEP	Indicated Mean Effective Pressure
ISFC	Indicated Specific Fuel Consumption
IVO	Intake Valve Opening
NA	Naturally Aspirated
NOx	Nitrogen Oxides
PC	Piston Compressor
PR	Pressure Ratio
PM	Particulate Matter
TC	Turbocharger
TDC	Top Dead Centre
VT	Valve Train
W20	Wärtsilä 20-engine
W20 FS	Four-stage turbocharged Wärtsilä 20-engine

1 Introduction

1.1 Background

Internal combustion engines can be classified by their operating speed: high-speed engines, medium-speed engines and low-speed engines. The medium-speed engines stand in the context of this Master's thesis. Medium-speed internal combustion engines are mainly used in marine vessels as main propulsion engines or auxiliary power generation sets, and as main power generators in power plants.

Medium-speed engines are defined by their operating speed: 300—1200 rpm. Medium-speed engines are commonly four-stroke engines with non-premixed combustion, running on heavy fuel oil or light fuel oil. Due to the stricter emission limits, engines utilising premixed combustion and using natural gas as fuel, have gained a foothold in the market in the recent years. (Mollenhauer and Tschöke 2010, p. 576, p. 582.)

The customers of medium-speed engine manufacturers value excellent fuel efficiency in steady-load operation. Even a slight improvement in fuel efficiency results to significant yearly savings in fuel costs for a medium-speed engine operator. The development of the internal combustion engine is essential to medium-speed engine manufacturers in order stay competitive in the market, and to face the growing pressure to decrease the engines' environmental impact. (Mollenhauer and Tschöke 2010, p. 576, p. 582.)

The development of the four-stroke internal combustion engine has been mainly limited to the development of combustion, mixture formation, alternative fuels and turbocharging. The working process of the four-stroke engine remains largely unchanged. Two significant technologies in the recent years, which improve engine efficiency and emissions are relevant to this thesis: Homogeneous Charge Compression Ignition (HCCI) and Miller cycle. HCCI is regarded as the ideal combustion, which combines the best parts of spark-ignited and compression ignition combustion. The greatest challenge of HCCI has been combustion phasing and speed control, which is why it has been limited to low loads in the four-stroke engines. Miller cycle is the only significant technology in the recent years, which has changed the working process of the internal combustion engine. However, an engine implementing Miller cycle is still considered a four-stroke engine. (Stanglmaier and Roberts 1999, Anderson et al 1998.)

This thesis studies alternative types of engines, referred to as the external compression engines (ECE). The external compression engines have some similarities to the Miller cycle; however, the working process of these engines is completely different to that of the four-stroke engine. The external compression engines could also be a way to enable HCCI operation at full cylinder output. These engines could have potential to improve the fuel efficiency and decrease the amount of harmful emissions of the internal combustion engine.

1.2 External compression engines

External compression is defined as the compression done outside the engine cylinder, for example the compression done in a turbocharger compressor. The total engine compression is defined to include the external compression and the compression done inside the cylinder. In a naturally aspirated engine, all compression is done in the cylinder, where also combustion and expansion take place (Heywood 1988, p. 27). In a four-stroke engine with

Miller cycle, an additional part of the total compression work is moved from the engine's cylinder to the turbocharger compressor (Anderson et al 1998). However, the turbocharger compressor's share of the total engine compression remains small.

In external compression engines, a significant part of the total engine compression is done externally. The purpose is to minimize the work required by the total compression by moving most of the compression work outside of the working cylinder. Instead of the hot working cylinder, compression can be done for example in efficient piston compressors, or in multiple cooled compressor stages. Engine overall efficiency is improved by decreasing the engine total compression work. (Tiainen et al. 2003.)

The external compression engines have some similarities to the Miller cycle, which is usually implemented in four-stroke engines. The external compression engines use a considerably higher charge air pressure, and the intake stroke is shortened so much that an alternative type of two-stroke cycle can be used (Tiainen et al. 2003). The share of the external compression is significantly larger than in a four-stroke engine with Miller cycle, hence the name: external compression engines. (Anderson et al. 1998.)

External compression engine concepts have been developed since the invention of the internal combustion engine. In many cases, engine simulations predict them to be more efficient than the four-stroke engine. Despite numerous prototypes, the simulation results are not backed by engine test results (Janhunen and Nyyssönen 2017, Philips et al. 2011, Coney et al. 2003). None of them have made their way into the market.

Since the early days of the internal combustion engine, supporting technology such as controllers, valvetrain and injectors have developed significantly. With the ever-stricter emission regulations and pressure to be fuel efficient, the situation today could be different. Perhaps in the time of the first concepts, the emissions and fuel consumption requirements have not been strict enough, or the technology not advanced enough for there to be an incentive to bring these concepts to the market.

External compression engine concepts could be suitable for HCCI combustion, which is already starting to make its way to the automotive market (Mazda 2017). The external compression concepts have some features which could be advantageous with HCCI combustion, such as internal exhaust gas recirculation and in theory, an adjustable compression temperature. HCCI is difficult to operate in four-stroke engines, but as most of the external compression engines are two-stroke engines, HCCI could be realisable at full load. (Kuleshov et al. 2015)

To take the edge from the four-stroke engine in the medium-speed market, the external compression engines must do many things right. In addition to brake specific fuel consumption, reliability, simplicity, ease of maintenance and compact size are important aspects for medium-speed engines. External compression engines would have to have a considerable advantage in one or more of these aspects than the four-stroke engine for the development work to be worth the effort and cost. (Mollenhauer and Tschöke 2010, p. 582.)

This thesis focuses on two interesting external compression engine concepts: the Z-engine and the Hoos engine. The Z-engine is a concept developed in 2001 by Mr. Timo Janhunen (M. Sc. Tech.). The Z-engine uses a combination of a turbocharger and a piston compressor

to produce charge air, and its gas exchange cycle is an alternative type of two-stroke cycle. A New generation of combustion engine, referred to as the Hoos engine, was developed by Mr. Frank Hoos in 2015. The concept uses a four-stage turbocharging setup to produce a very high charge air pressure, and a two-stroke working cycle very similar to the one in the Z-engine. (Grönlund and Larmi 2004, Hoos 2015.)

1.3 Content, method and objective of the thesis

The objective of this Master's thesis is to evaluate the engine performance potential of the two external compression engine concepts, the Z-engine and the Hoos engine, with medium-speed engine boundary conditions. The method of study is 1-D engine simulations using the software GT-Power from Gamma Technologies (Gamma Technologies 2017). It is also important to understand the sensitivity of these engine concepts to important engine design and operating parameters.

The most important question is, whether the concepts are more fuel efficient than a comparable four-stroke engine. The fact that none of the concepts have made it to the market, suggests that they have bottlenecks. If this is the case, the aim is to find out, what these bottlenecks are. It is also important to find out, whether the concepts could even be realised with existing Wärtsilä solutions and hardware. Existing Wärtsilä solutions are mainly referring to components such as engine crank train or valve train. Answering these questions should provide an understanding to whether it is sensible for Wärtsilä to start developing these engine concepts.

Therefore, the research questions of the thesis are:

1. Are the Z-engine and Hoos engine concepts more fuel efficient than a comparable four-stroke medium-speed engine?
2. What are the possible bottlenecks of the concepts?
3. Can the concepts be realised with existing Wärtsilä designs and solutions?
4. Is it a good idea for Wärtsilä to start developing these engine concepts?

The theory related to external compression is reviewed to understand the reason, why external compression would increase and internal combustion engine's fuel efficiency. A literature study is made to see, what kind of different external compression engine concepts have been developed, to see where the concepts stand among the others. Both engine concepts will be optimized to best extent that is sensible. The concepts' engine performance will be compared to a reference Wärtsilä four-stroke engine, the Wärtsilä 20.

This thesis focuses on external compression, internal combustion engines; external combustion engines like the Stirling engine are not considered. The concept review considers other existing external compression engine concepts; however, they are not studied. The scope of the thesis is limited to studying the two engine concepts, the Z-engine and the Hoos engine. The simulations are limited to 1-D-simulations due to the software used, no 3-D simulations are done. The engine simulations are limited to steady-state runs at full load. Transient load and part load studies are not a part of this thesis. This study does not limit the combustion type used in the engine concepts. The comparisons are done by simulating a non-premixed combustion, however also premixed combustion is studied.

2 Theory

This chapter describes the theory and some concepts that are related to this thesis. Finally, the purpose behind external compression engines, and why they would increase the engine overall efficiency is explained.

2.1 Basic definitions

For clarity, some basic definitions used in the thesis are described. A medium-speed engine has the following main components: the turbocharger (TC) compressor, the charge air cooler (CAC), the charge air receiver, the working cylinders and the turbocharger turbine. The flow system which connects the turbine and the working cylinders is referred to as the exhaust manifold.

The air which flows into the turbocharger compressor in suction air pressure p_1 (commonly ~1 bar (a)), and in ambient temperature T_1, is referred to as the suction air. The suction air is compressed up to the charge air pressure p_3 in the turbocharger compressor, or in the case of the external compression engines in a series of compressors. After being cooled to the charge air temperature T_3, the charge air flows into the charge air receiver, where it remains in the charge air pressure to be used for combustion in the working cylinders. In practice there is always a pressure drop in the charge air cooler, so the pressure in the charge air receiver is slightly lower than after the turbocharger compressor. To be specific, p_3 refers to the charge air pressure in the charge air receiver.

In the working cylinder, the charge air is compressed to the compression pressure p_{comp}, which is the pressure around top dead centre (TDC) before ignition and combustion. The temperature at the end of compression in the working cylinder is referred to as the compression temperature T_{comp}. The maximum cylinder pressure in the working cylinder, during combustion is referred to as p_{max}. In the exhaust manifold, the exhaust gas flows into the first turbocharger turbine in the exhaust pressure p_5 and exhaust temperature T_5. The pressure after the last turbocharger is defined as the ambient exhaust pressure p_6. The definitions described here are illustrated in figure 2.1.

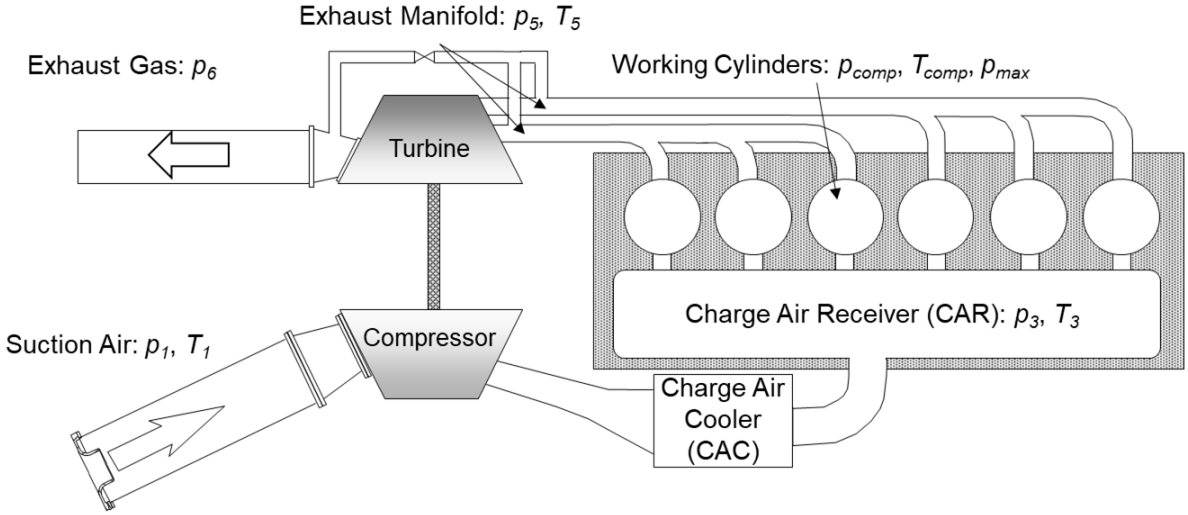

Figure 2.1. A schematic of the usual layout of a medium-speed engine, showing also the definitions for the pressure in different parts of the engine.

2.2 Compressor and turbine basics

In the comparisons between the engine concepts and the four-stroke engine, it is important to see, whether the total engine compression in the concepts is more efficient than the total compression in a four-stroke engine. Therefore, a comparison method for the efficiency of the compression need to be defined.

It is important to mention the basics of compression, to understand some of the definitions mentioned later. There are three main types of compression: isentropic compression, polytropic compression and isothermal compression. If the system is completely heat insulated, thus no heat is transferred in and out of the system, the compression is adiabatic (Cengel and Boles 2007, p. 372). An adiabatic and reversible compression is called isentropic compression (Lampinen 1997, p. 31). If the compressor is cooled so efficiently, that the temperature in the end of compression is the same as in the beginning of compression, the compression process is isothermal. Isothermal compression is the most efficient compression, isentropic compression being the least efficient. A polytropic compression process is between the isentropic and isothermal process. The different types of compression can be seen in figure 2.2. As the surface area under the curve in the isothermal process is the smallest, it consumes the least amount of energy. (Wiksten 2009, p. 104—105.)

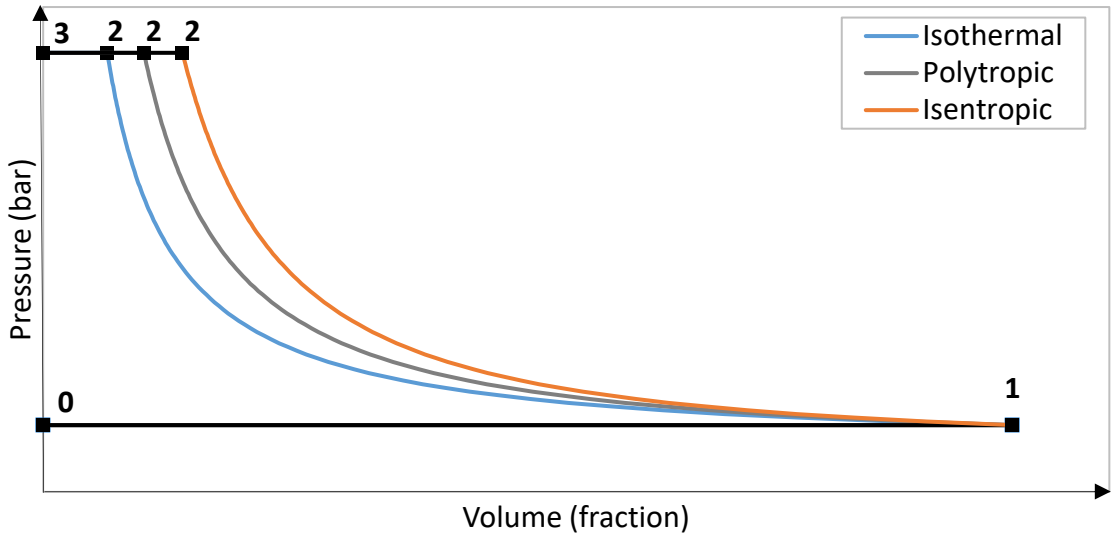

Figure 2.2. The p-V-diagram of a piston compressor with isentropic, polytropic and isothermal compression. Point 0 represents the start of the intake stroke and point 1 the start of compression. The process between point 2 and 3 is the discharge of the compressed air.

If the temperature in the beginning of compression is referred to as T_{begin}, and the temperature in the end of compression as T_{end}, then for isothermal compression $T_{end} = T_{begin}$ is true. However, according to Wiksten (2009, p. 109), the following is true for isentropic compression:

$$T_{end} = T_{begin}\left(\frac{p_{end}}{p_{begin}}\right)^{1-\frac{1}{\gamma}} \qquad 1)$$

where p_{begin} is the pressure in the beginning of the compression, p_{end} the pressure in the end of compression and γ the ratio of the specific heat in constant pressure and the specific heat in constant volume. From equation 1 the following observation can be made; the higher the pressure ratio (PR) in a single isentropic compression stage, the higher the temperature in the end of compression will be. In isentropic compression, pressure increase will always result to a temperature increase as well.

According to Wiksten (2009, p. 105), the theoretical isentropic compression work $P_{s,C}$ and isothermal compression work $P_{iT,C}$ can be calculated in two ways. If an engine's charge air production is thought of as a single compression stage, the theoretical work for charge air compression can be calculated:

$$P_{s,C} = p_1 \dot{V}_1 \frac{\gamma}{\gamma-1}\left[\left(\frac{p_3}{p_1}\right)^{\frac{\gamma-1}{\gamma}} - 1\right] = \dot{N}_C R T_1 \frac{\gamma}{\gamma-1}\left[\left(\frac{p_3}{p_1}\right)^{\frac{\gamma-1}{\gamma}} - 1\right] \quad 2)$$

$$P_{iT,C} = p_1 \dot{V}_1 \ln\left(\frac{p_3}{p_1}\right) = \dot{N}_C R T_1 \ln\left(\frac{p_3}{p_1}\right) \quad 3)$$

where p_1 is the suction air pressure, p_3 the charge air pressure and $\dot{V}_1$ the volumetric flow rate of the suction air before the first compressor, $\dot{N}_C$ is the molar mass flow rate of the charge air, R the gas constant at the inlet of the first compressor and T_1 the suction air pressure. As molar mass flow rate can be derived from the fluid mass flow rate, the equations can be rewritten using the mass flow rate of the charge air $\dot{m}_C$ and specific molar mass of air M_{air}.

$$P_{s,C} = \frac{\dot{m}_C}{M_{air}} R T_1 \frac{\gamma}{\gamma-1}\left[\left(\frac{p_3}{p_1}\right)^{\frac{\gamma-1}{\gamma}} - 1\right] \quad 4)$$

$$P_{iT,C} = \frac{\dot{m}_C}{M_{air}} R T_1 \ln\left(\frac{p_3}{p_1}\right) \quad 5)$$

The efficiency of compression depends on the process which is used as the reference. Commonly the reference process used is isentropic compression. According to Cengel and Boles (2007, p. 379), the compression isentropic efficiency $\eta_{s,T}$ is the ratio of the actual compression work P_C and the isentropic compression work $P_{s,C}$ (equation 2 and 4):

$$\eta_{s,C} = \frac{P_C}{P_{s,C}} \quad 6)$$

Wiksten (2009, p. 105) defines the ratio of the compressor outlet pressure p_{out} and the inlet pressure p_{in} as the pressure ratio, symbolised with π. The pressure ratio can be defined for a single compressor stage, or the whole charge air production.

$$\pi = \frac{p_{out}}{p_{in}} \quad 7)$$

The compression process can be moved closer to isothermal compression by dividing the compression to many stages and cooling the compressed air in between. Figure 2.3 shows the same ideal piston compressor p-V diagram as in figure 2.2, where the compression is made in four isentropic compression stages, with cooling of the compressed air in between

each stage. This type of compression can be referred to as multiple stage intercooled compression.

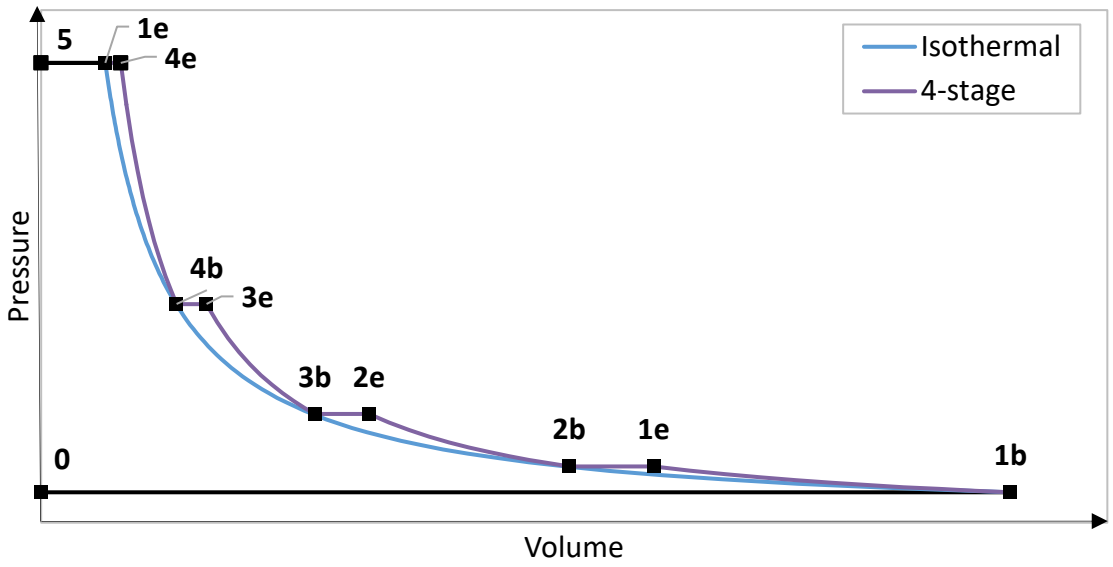

Figure 2.3. One stage of isothermal compression (blue) compared to a four-stage isentropic and intercooled compression (purple). Here the numbering indicates the compression stage, and whether the point is at the beginning (b) or the end (e) of compression.

According to Wiksten (2009, p. 111—117), the theoretical work required for a multiple stage intercooled compression can be calculated with the following equation:

$$P_{s,min} = p_1 \dot{V}_1 \frac{n\gamma}{\gamma-1}\left[\left(\frac{\pi}{\pi_{s1}} \cdot \pi_{s2} \cdot \pi_{s3} \cdots \pi_{sn-1}\right)^{\frac{\gamma-1}{n\gamma}} - 1\right] = \dot{m}_C R_1 T_1 \frac{n\gamma}{\gamma-1}\left[\left(\frac{\pi}{\pi_{s1}} \cdot \pi_{s2} \cdot \pi_{s3} \cdots \pi_{sn-1}\right)^{\frac{\gamma-1}{n\gamma}} - 1\right] \quad 8)$$

where n is the number of compression stages, π is the total compression pressure ratio and π_{sn} is the pressure ratio of a single compression stage. Furthermore, according to Wiksten (2009, p. 111—117), the equation 5 can be rewritten if the pressure ratio of all the stages is assumed to be the same. This means that the temperature rise in each stage is also the same.

$$\pi_{sn} = \sqrt[n]{\pi} \quad 9)$$

$$P_{s,min} = p_1 \dot{V}_1 \frac{n\gamma}{\gamma-1}\left[\left(\sqrt[n]{\pi}\right)^{\frac{\gamma-1}{\gamma}} - 1\right] = \dot{m}_C R_1 T_1 \frac{n\gamma}{\gamma-1}\left[\left(\sqrt[n]{\pi}\right)^{\frac{\gamma-1}{\gamma}} - 1\right] \quad 10)$$

Certain correlations are true for equations 8—10. If the number of stages n is increased, the pressure ratio of a single stage π_{sn} of the multiple stage compression decreases. According to equation 1, the temperature rise in a single isentropic stage will decrease when the pressure ratio of the stage is decreased. If the compressed air is assumed to be cooled down to ambient temperature (T_1, ~25 ºC) after each stage, the increase in the number of stages will decrease the work required for a single stage, as applies according to equations 2 and 4. Therefore,

with an increasing number of stages, the temperature rise in each compression stage will decrease. If the number of stages is approaches infinite, the temperature rise in each compression stage will approach 0, since the pressure ratio of a stage will approach 0 as well. Therefore, with the assumption that air is cooled down to ambient temperature between each stage, with an increasing number of intercooled stages, the total compression will approach isothermal compression, where the temperature during compression is constant.

The cooling of the compressed air is the key factor why a multiple stage cooled compression is more efficient than doing the same compression in a single stage. What also applies according to the equations 2 and 4 is that if the temperature in the beginning of the compression in each stage increases, also the work required for compression increases. If the compressed air is not cooled between the stages in a multiple stage compression, the total work required is the same as if the compression were made in a single stage. In this case, the next compressor will only continue the compression with an increased temperature from the ambient temperature, increasing the work required for the stage. Therefore, a multiple stage compression is more efficient than a single stage only when the compressed air is cooled in between the stages.

Figure 2.4 shows how many stages of isentropic compression are needed to get close to isothermal compression. If isothermal compression is thought of as the reference (100% work), then according to equations 2—6 and 8—10 a one-stage isentropic compression requires roughly 85 % more work. Most advantage comes already from moving from one-stage to two-stage compression; it requires only 34 % more work than fully isothermal. An additional improvement can be made by moving from two- to four-stage compression; compression requires only 15 % more work than isothermal in a four-stage compression. Only slight improvement from six-stage and onwards can be seen. To get very close to isothermal compression, 20 or more stages are required. Coming close to isothermal compression, the number of stages must be increased much more to get any significant improvement.

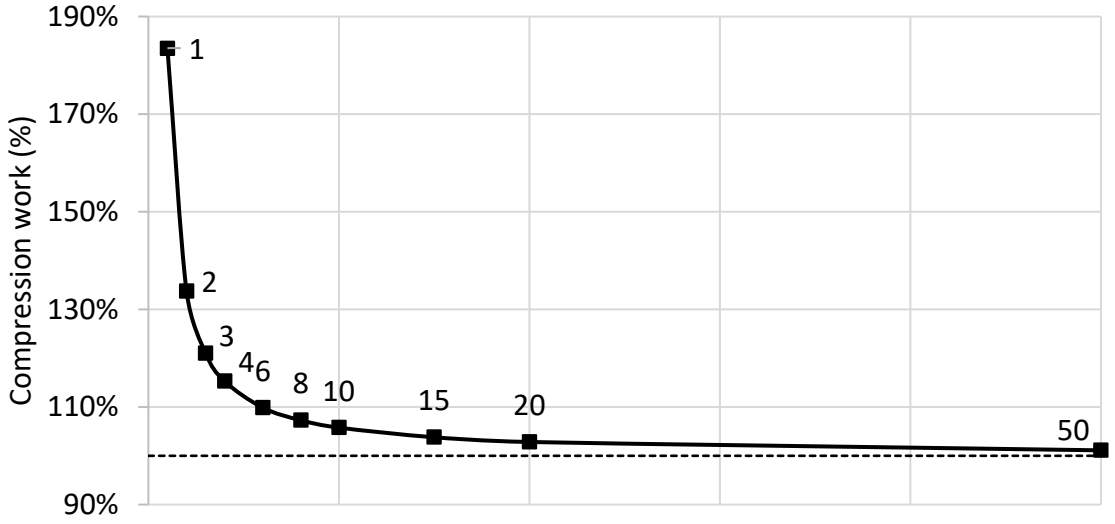

Figure 2.4. Theoretical work required for compression with different number of intercooled stages, when air is cooled to ambient temperature after each stage.

To compress charge air, the energy for the compressors must come from somewhere. In a supercharger the power to drive the compressor is taken from the engine crankshaft. In a

turbocharger, the energy of the exhaust gases is used to drive a turbine, which drives the turbocharger compressor. According to van Basshuysen and Schäfer (2004, p. 362), the theoretical isentropic power produced by a turbocharger turbine can be calculated with the following equation:

$$P_{s,T} = \dot{m}_T R_5 T_5 \frac{\gamma}{\gamma-1}\left[1 - \left(\frac{p_6}{p_5}\right)^{\frac{\gamma-1}{\gamma}}\right] \quad 11)$$

where $\dot{m}_T$ is the mass flow rate going through the turbines, R_5 the specific gas constant of the exhaust gas, T_5 the exhaust gas temperature before the first turbine, p_6 the pressure after the last turbine and p_5 the exhaust pressure before the first turbine.

The efficiency of a turbine is usually indicated as isentropic efficiency, where the reference process used is isentropic expansion (Hattar 2017). According to Cengel and Boles (2007, p. 377), the isentropic efficiency of a turbine $\eta_{s,T}$ is the ratio between the actual power produced by the turbine P_T, and the theoretical isentropic turbine power $P_{s,T}$:

$$\eta_{s,T} = \frac{P_T}{P_{s,T}} \quad 12)$$

According to van Basshuysen and Schäfer (2004, p. 362), the total efficiency of a turbocharger η_{TC} depends on the efficiency of the turbine, compressor and the mechanical efficiency of the compressor $\eta_{mech,C}$, the mechanical efficiency of the turbine $\eta_{mech,T}$. The mechanical efficiency of the turbine and compressor can be depicted as the total mechanical efficiency of the turbocharger η_{mech}. Mechanical efficiency depicts the frictional and mechanical losses between the turbine and the compressor.

$$\eta_{TC} = \eta_{s,T} \cdot \eta_{s,C} \cdot \eta_{mech,C} \cdot \eta_{mech,T} = \eta_{s,T} \cdot \eta_{s,C} \cdot \eta_{mech} \quad 13)$$

Some observations can be made from equation 11. If the ambient exhaust pressure p_6 is assumed to be roughly 1 bar (a) and the mass flow rate of the exhaust gases constant, then the power produced by a turbine, and the power that is available to drive the turbocharger compressor is dependent on the exhaust pressure p_5 and the exhaust temperature T_5. The higher the exhaust temperature and pressure, the higher will be the power produced by the turbocharger turbine. A higher exhaust pressure will produce a higher turbine power; however, it will also restrict the exhaust stroke of an internal combustion engine more. A higher pressure against the piston during the exhaust stroke will resist the piston upwards motion more. Charge air pressure can be adjusted in a turbocharged engine by adjusting the turbine entry area. It is the flow area, through which the exhaust gas flows into the turbine; it is referred to as the turbine area. By decreasing the turbine area, referred to as the turbine area, the exhaust pressure p_5 will increase, and more power will be produced by the turbine to drive the compressor. (Hattar 2018, Mollenhauer and Tschöke 2010, p. 50.)

2.3 Turbocharging efficiency

According to Heywood (1988, p. 27), turbocharging was implemented in internal combustion engines to increase their power output per a certain engine displacement, and for engine downsizing. Exhaust gas energy that would otherwise go to waste, is used to compress the intake air to decrease gas exchange losses. Additionally, leaner air-fuel ratios

can be used to decrease heat transfer losses. Intercooling or charge air cooling further improves the efficiency of a turbocharged engine. By cooling the charge air, the compressed charge air becomes denser, so that more air can be fit into the cylinder with a certain charge air pressure. Like with Miller timing, charge air cooling lowers the compression temperature, giving more margin for NOx tuning (explained in chapter 2.4). (Heywood 1988, p. 796.)

Increasing the turbocharging efficiency has been shown to increase the engine overall efficiency in four-stroke engines. Increasing the efficiency of turbocharging shows up as decreased losses of the gas exchange in four-stroke engines. With efficient turbocharging, the gas exchange can be so efficient that it does positive work to the engine cycle, instead of being a loss of work. (Lam et al. 2015.)

With an increased turbocharging efficiency, more of the exhaust gas energy will be transferred to be used by the turbocharger compressor. As an example, two cases are considered: charge air is produced by a turbocharger system with a higher total efficiency (a) and a lower total efficiency (b), as is according to equation 13 in chapter 2.2. In equations 4 and 11 of chapter 2.2, the mass flow rate through the compressor and the turbine is assumed to be constant, as well as the suction air pressure and the ambient exhaust pressure. The exhaust temperature is assumed to constant, and it is assumed that the same charge air pressure would be produced. Therefore, the power required by the turbocharger compressor will remain constant. With these assumptions, with a high turbocharging efficiency, an exhaust pressure p_{5a} will produce the required power to compress charge air to the charge air pressure p_3. With a low turbocharging efficiency (case b), the exhaust pressure p_{5b} required to create the same charge air pressure p_3 will be higher than with the higher turbocharging efficiency (case a). Therefore, $p_{5a} < p_{5b}$ applies. A higher exhaust pressure will resist the piston movement more during the exhaust stroke of the engine, and therefore increase the gas exchange losses of the engine.

Increasing the number of turbocharging stages will increase the efficiency of turbocharging. The reason is that the total compression efficiency $\eta_{s,C}$ of the turbocharging system is increased, as described in chapter 2.2. For example, if the isentropic efficiency of one compressor stage is 82 %, then the total isentropic compression efficiency of a two-stage system will be 112 %. If the assumption is made that the turbine and mechanical efficiency of the turbocharging system remains constant, then according to equation 13 the efficiency of turbocharging is increased. The increase of turbocharging efficiency comes simply through the increase of the total compression efficiency. Therefore, increasing the number of intercooled turbocharging stages will increase an internal combustion engine's efficiency.

2.4 Atkinson and Miller Cycle

James Atkinson invented his alternative engine working cycle 1846. The purpose of the Atkinson cycle is to increase engine efficiency by having a higher expansion ratio than the compression ratio. Atkinson did this by shortening the intake and compression stroke, while keeping the expansion and exhaust stroke length the same. Atkinson's cycle increases the efficiency of an internal combustion engine; however, the engine output is limited due to the shortened intake stroke. As the intake stroke is shorter, less air is trapped in a naturally aspirated Atkinson engine than in a comparable four-stroke engine. Atkinson realised his engine by using a complex crank train mechanism. The engine was more efficient than the engines of that time, however it was less robust than an engine with a conventional crank train mechanism. (Heywood 1988, p. 3—4.)

Atkinson's cycle is used in modern engines by using late or early inlet valve closing to decrease the engine effective compression ratio, while keeping the expansion ratio the same. One of the ways to realise the Atkinson cycle is the cycle invented by Ralph Miller, referred to as the Miller cycle. (Anderson et al 1998.)

The valve timing used in the Miller cycle is referred to as Miller timing. In this thesis, Miller timing refers exclusively to early inlet valve closing. Strong Miller timing refers to a very early inlet valve closing; the stronger the Miller timing, the earlier the intake valve closes. Like the Atkinson cycle, Miller timing decreases the engine effective compression ratio, while keeping the expansion ratio constant. The difference to the Atkinson cycle is that in the Miller cycle, charge air pressure is increased not to decrease the cylinder output. The charge air pressure is increased so that the same amount of air is trapped in the cylinder with the early inlet valve closing, as in a case where the inlet valve closes at bottom dead centre (BDC). (Anderson et al 1998.)

In Miller cycle, the charge air is trapped inside the cylinder, while the piston is still moving down. The piston expands the charge air inside the cylinder, decreasing its temperature. Therefore, the temperature of the charge air is lower at the beginning of compression than during the intake stroke. By decreasing the temperature in the beginning of compression, the temperature at top dead centre in the end of compression is also lower. (Anderson et al 1998.)

International regulators impose limits for Nitrogen Oxides (NOx) emitted by medium-speed engines (International Maritime Organization 2018). Adjusting the Nitrogen Oxide (NOx) emissions in an internal combustion engine can done by adjusting the combustion phasing. It can be delayed from top dead centre to decrease the pressure and temperature rise during combustion. Delaying the combustion phasing from TDC moves the combustion to a point where cylinder volume is larger. Since NOx emissions form in very high temperatures, by decreasing the overall temperature during combustion decreases the amount of NOx formed during combustion. An optimal combustion timing takes place close to top dead centre, however at this point the cylinder volume is very small and combustion results to a high pressure and temperature rise, and a high amount of NOx. The combustion timing is adjusted to get the best possible engine efficiency while staying under the imposed NOx limits (Hattar and Järvi 2018.).

Due to the decreased temperature in the end of compression, Miller timing gives extra margin for the engine NOx tuning. With a comparable compression pressure and combustion timing, Miller cycle will result to a lower level of NOx emissions compared to a non-Miller engine, with the same combustion phasing and engine efficiency. The combustion timing can therefore be advanced to increase engine efficiency, while still staying under the NOx limits. This is the most significant mechanism how Miller cycle increases engine efficiency. (Hattar and Järvi 2018.)

Another way that Miller cycle increases engine efficiency is by decreasing the compression work done by the working cylinder, while retaining the expansion ratio, like the Atkinson cycle. According to Pulkrabek (1997, p. 103—105), Miller cycle increases the indicated work generated by the engine cycle by decreasing the compression work, or in other words expanding the gases more than compressing them. In theory, Miller cycle increases the engine indicated efficiency by decreasing the compression work.

2.5 Homogeneous Charge Compression Ignition

HCCI is regarded as the ideal combustion in an internal combustion engine, combining the best parts of premixed and non-premixed combustion. In HCCI, the fuel and air are pre-mixed before compression and combustion like in a spark-ignited engine, but instead of a spark, the fuel-air mixture is ignited by the high temperature caused by compression, like in a compression ignited engine. Engines with HCCI combustion have demonstrated a high thermal efficiency, as well as low NOx and particulate matter emissions. (Stanglmaier and Roberts 1999.)

HCCI combustion has a very fast rate of heat release; when the combustion phasing is timed right it moves the working cycle of an engine operating with HCCI towards the ideal Otto cycle. The Ideal Otto cycle with its instantaneous heat release is seen as the most efficient of the theoretical internal combustion engine cycles. As the HCCI combustion is of very low temperature and lacks the flame front of the conventional premixed combustion, or the locally rich areas of the non-premixed combustion, the production of both NOx and PM is decreased. Ignition takes place all over the cylinder in the fuel-air mixture, instead of one place like in a conventional premixed combustion. The low temperature and non-luminous combustion also decreases the heat transfer losses to the cylinder wall. (Stanglmaier and Roberts 1999.)

HCCI's major challenge is related to the combustion phasing, speed and stability, which is why in four-stroke engines it has been limited to a relatively small load window at low loads. The combustion phasing is controlled by adjusting the moment when the autoignition temperature of the air-fuel mixture is reached in the cylinder during compression. This thesis discusses a certain way to control HCCI combustion phasing: through the adjustment of the charge air temperature, and the use of Exhaust Gas Recirculation (EGR). (Stanglmaier and Roberts 1999, Hyvönen 2005.)

In this method, the amount of EGR (EGR-rate) is used to control the ignition delay and combustion speed. Recirculated residual gases decrease the ignition delay of the fuel-air mixture but slow down the combustion reactions. A high relative air-fuel ratio will also slow down the combustion, keeping the pressure rise during combustion reasonable. HCCI is difficult to operate at idle load, because of a too slow combustion reaction caused by the very high relative air-fuel ratio. At high loads, the problem is reverse; at high loads, more fuel is injected, so the relative air-fuel ratio is low. Even when the EGR-rate is increased, the combustion speed is too high and results to an unreasonably high maximum cylinder pressure and heat transfer losses to the cylinder wall. Since HCCI combustion is basically the same as knocking in spark-ignited engines, the combustion noise is very loud in high load operation. (Hyvönen 2005.)

Furthermore, this way to control of the combustion phasing in HCCI is a precise balancing act. From cycle to cycle, there will be some variations in the charge air temperature, the residual gas temperature, the ignition temperature of the fuel-air mixture and the ignition delay. Therefore, even if a perfect adjustment is reached in one cycle, on the next cycle one of the characteristics might change, which will lead to the ignition timing changing. It is essential for HCCI that the charge air temperature is not too high so that the fuel-air mixture does not ignite, for example halfway into compression. (Hyvönen 2005, Axelsson 2017.)

2.6 External compression engines to increase engine efficiency

As mentioned in chapter 1.2, the process where air is compressed from the suction air pressure (p_1) up to the compression pressure (p_{comp}) is called total compression. The process which compresses the charge air from suction air pressure to the charge air pressure (p_3) is referred to as external compression. External compression is the compression completed outside of the working cylinder and is a part of the total compression. The purpose of external compression engines is to minimize the work required for the total compression by increasing the share of external compression. This part presents some theory and calculations as to why this would increase the engine overall efficiency.

The system completing the external compression is referred to as the external compressor, which can be any compressor such as a piston compressor or a turbocharger, or a combination of compressors. The system where the charge air is admitted, and where combustion and expansion take place, is referred to as the working cylinder.

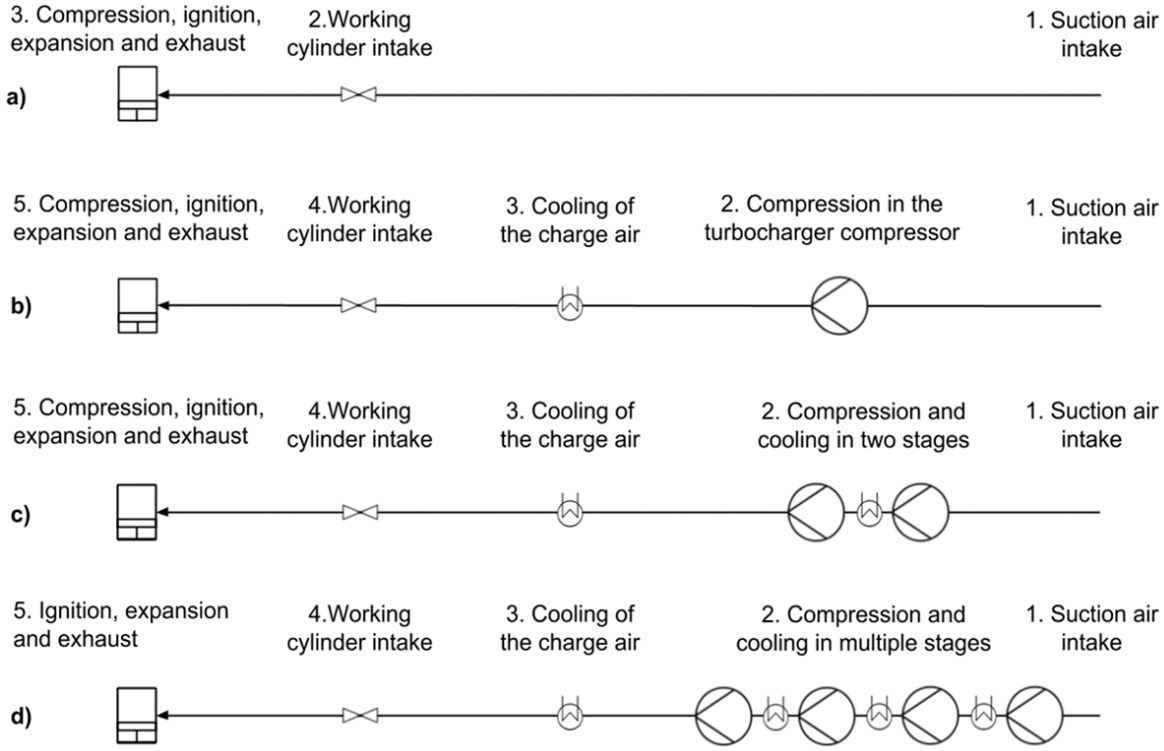

Figure 2.5. The process steps of different engines: a) a naturally aspirated engine, b) a turbocharged engine, c) a partly external compression engine and d) a fully external compression engine is illustrated here.

Figure 2.5 illustrates the different stages of the total compression process in different engines. As an example, four different kind of engines are considered in this chapter: a) a naturally aspirated engine, b) a turbocharged engine, c) a partly external compression engine and d) a fully external compression engine. In the naturally aspirated engine a), all charge air is taken in through the intake valves in suction air pressure. The charge air is compressed from the suction air pressure to the compression pressure in a single stage in the working cylinder. The total compression in the naturally aspirated engine therefore consists of a single compression stage, which takes place inside the working cylinder. In a naturally aspirated engine, there is no external compression, therefore $p_3 = p_1$.

In the turbocharged engine b), the air flows inside the turbocharger compressor in suction air pressure and exits in the charge air pressure. Here, the turbocharger compressor is the external compressor. The charge air flows through a charge air cooler and is admitted inside the working cylinder in the charge air pressure. The charge air is finally compressed from the charge air pressure to the compression pressure inside the working cylinder. Therefore, the total compression of a turbocharged engine consists of two compression stages, with a charge air cooler in between. In a turbocharged engine, part of the compression work of the working cylinder is moved outside, to the turbocharger compressor. Therefore, the turbocharged engine can also be defined as a partly external compression engine.

In the fully external compression engine d), air flows in suction air pressure in the first compressor. The charge air is compressed from the suction air pressure up to the compression pressure in the external compressors and is admitted to the working cylinder. The charge air is not compressed further, instead fuel is injected and ignited. Therefore, in a fully external compression engine, $p_3=p_{comp}$ applies: no compression is done inside the working cylinder. All compression is done externally. The total number of compression stages depends on how many compressor stages the external compression consists of. In the example of this chapter, the total compression is done in four stages (figure 2.5).

Some of the external compression engines are somewhere between the fully external compression engine, and the turbocharged engine, like the partly external compression engine c) considered here. The charge air exits the final compressor in a charge air pressure considerably higher than in the turbocharged engine. The compression ratio is considerably lower than in the turbocharged engine. The total compression consists of the compression stages of the external compression, and the compression stage inside the working cylinder. In this example, the total compression consists of three compression stages.

Figure 2.6 shows how the compression work in theory is divided in these different types of engines. With an increasing number of turbocharging stages and stronger Miller timing, more of the compression is moved outside of the working cylinder. If external compression is thought of as a spectrum, where one end is 0 % external compression and the opposite end is 100 % external compression, then the external compression engine concepts studied in this thesis and the naturally aspirated engine are in theory situated on the opposite ends of this spectrum.

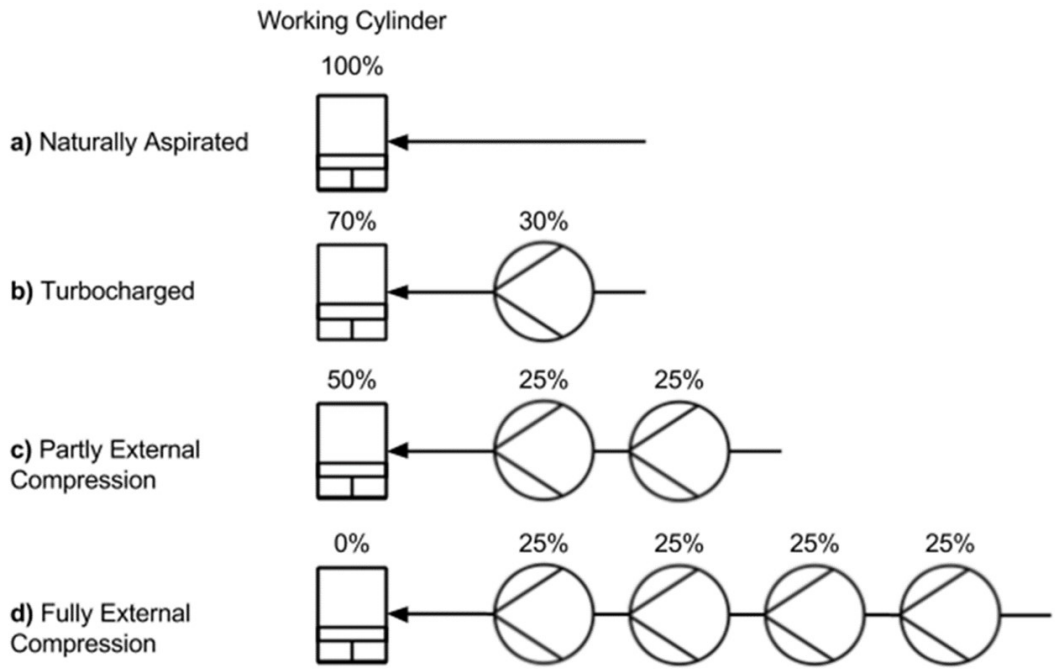

Figure 2.6. An illustration of how the compression work is in theory divided in the different kind of engines compared: a) the naturally aspirated engine, b) the turbocharged engine, c) the partially external compression engine and d) the fully external compression engine.

The theoretical compression work and turbocharging efficiency can be predicted for the four engine types. As an example, a theoretical comparison is made between the four engines considered. For this, some assumptions are made. Suction air temperature is assumed to be 25 ºC (ambient air temperature), and air is assumed to be cooled to ambient temperature in the intercoolers after each compression stage. In the single-stage turbocharged engine, charge air is compressed to 5 bar (a). In the partially external compression engine, charge air is compressed to 15 bar in two compressor stages and in the fully external compression engine, it is compressed to 20 bar (a) in four compressor stages. The compression pressure is assumed to be 200 bar in each engine.

The isentropic efficiency of the external compressors is assumed to be 82 %, and the efficiency of the compression in the working cylinder is assumed to be 100 %. To simplify the comparison, the charge air is assumed to be produced by a single turbine with an isentropic efficiency of 84 %. The mass flow of exhaust gas and charge air is assumed to be the same in each engine.

With these boundary conditions and assumptions, the theoretical compression temperature (T_{comp}), the total compression work, theoretical exhaust pressure (p_5) required for charge air production and the total turbocharging efficiency (η_{TC}) can be calculated. The compression temperature is calculated using equation 1. The reference isentropic compression work is calculated using equation 4 and the reference turbine work, and actual work and the theoretical exhaust pressure is calculated using equations 11—12. The actual work of the multiple stage cooled compression is calculated using equation 9—10. Figure 2.7 illustrates how much total compression work is required for the different engines. Table 2.1 displays the boundary conditions used and the summary of this comparison.

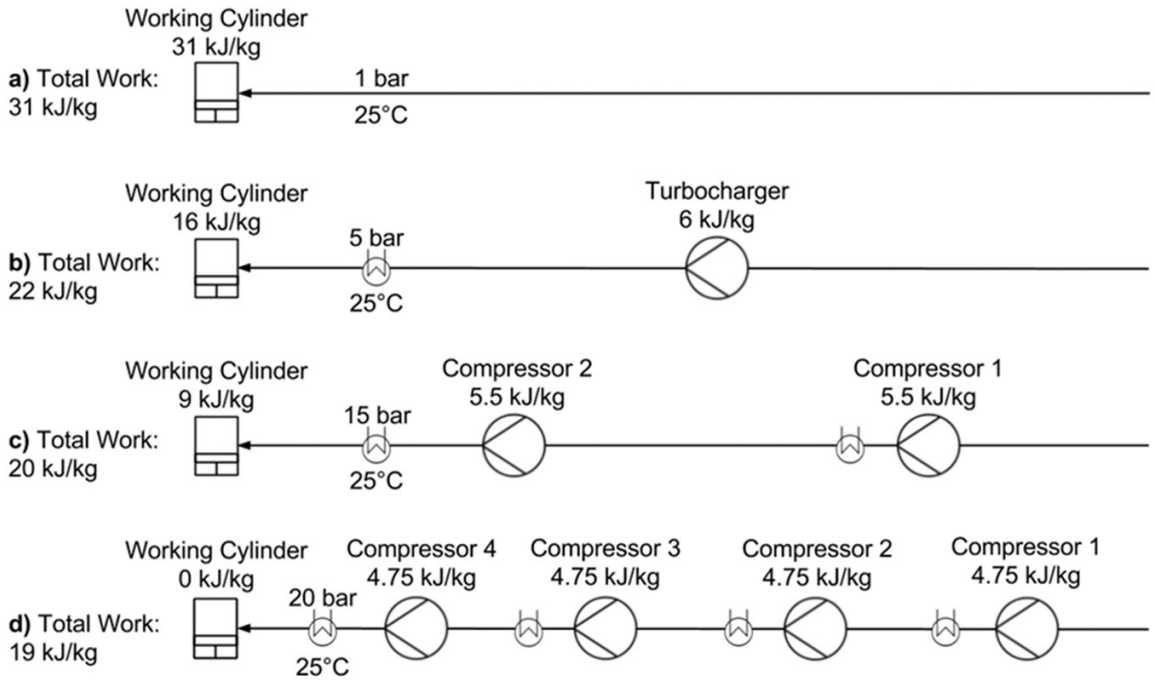

Figure 2.7. The work required for compression in a) the naturally aspirated engine, b) the turbocharged engine, c) the partly external compression engine and d) the fully external compression engine.

Even though the efficiency of the working cylinder compression is much better than the one on the external compressors, it still pays off to move compression outside the working cylinder into multiple stages. Merely moving the compression work outside of the working cylinders does not help; the key is to divide the total compression to as many stages as is possible. As the compression in the working cylinder can only amount to one compression stage, the solution is to move compression work to multiple external compression stages.

Since in theory the fully external compression engine does no compression in the working cylinder, the compression temperature is the same as the temperature of the incoming charge air. The temperature would be hundreds of degrees lower in the fully external compression engine, than in the turbocharged engine. The compression temperature would be roughly 200 ºC lower even in the partially external compression engine. In theory, this gives an immense margin to increase engine efficiency and NOx emissions by advancing the combustion timing towards TDC.

The turbocharging efficiency will be considerably better in the external compression engines than in the single-stage turbocharged engine due to the more efficient multiple stage compression. However, to compress the charge air up to the compression pressure, a considerably higher exhaust pressure is needed. In the fully external compression engine, the turbocharger turbine area would have to be decreased so that the exhaust pressure is roughly 166 bar (a), which is considerably more than in the turbocharged engine, 2.5 bar (a). Even though total compression is moved to turbochargers, the charge air production has a price.

Table 2.1. Theoretical comparison of the a) naturally aspirated engine (NA), b) the turbocharged engine (TC), the partially external compression engine (ECE) and the fully external compression engine.

Theoretical comparison					
	a) NA	**b) TC**	**c) Partially ECE**	**d) Fully ECE**	**Unit**
Boundary conditions					
p_1	1				bar (a)
p_{comp}	200				bar
T_5	800				K
p_3	1	5	15	200	bar (a)
Result					
Rate of external compression*	0	30	50	100	%
N. of total compression stages	1	2	3	4	-
Total Compression Work	31	22	20	19	kJ/kg
T_{comp}	970	560	350	25	^oC
p_5	1	2.5	5.6	166	bar (a)
η_{TC}	0	68	101	159	%
*The portion of total compression which is done externally					

External compression engines would in theory increase engine efficiency through some of the mechanisms described earlier in this chapter. Moving the total compression out of the working cylinder, and into more intercooled stages increases the turbocharging efficiency, which will increase engine efficiency.

NOx margin; if the assumption is made that air is cooled to ambient temperature before admission to the working cylinder, then the external compression engines will have a considerably lower compression temperature than a conventional engine. This gives even more margin to increase the engine efficiency in the similar way that Miller timing does. For the same reason, the external compression engines could be advantageous for HCCI. For example, in the fully external compression engine, the compression temperature is not even nearly enough to autoignite any fuel used in medium-speed engines. However, it is still more practical to heat the charge air rather than cool it.

The external compression engines would increase engine indicated work in the same way as the Atkinson and Miller cycles do; the effective compression ratio of the engine is decreased, while the expansion ratio stays the same. The compression work done by the working cylinders would decrease, but the expansion work would stay the same. In theory, this increases the engine indicated efficiency.

3 Engine concepts

This chapter describes the working principle of the engine concepts studied in this thesis, the Z-engine and the Hoos engine. To provide a background to the thesis, a literature review was done to find out, what kind of external compression engine concepts exist and how they work. Over 30 different engine concepts of three distinct types were found.

3.1 History

After reviewing all the older engine concepts, it is quite clear that external compression in internal combustion engines is not a new idea at all. Most of the ideas appearing in the engine concepts found in the literature review have already been tried by the beginning of the 20th century. Two of those engine concepts are shown in figure 3.1.

An external compressor cylinder can be found on the Stirling engine, which was developed in 1816, and Brayton's engine, developed in 1872 (Cummins 1989, p. 17—22 & 186—191). However, it should be noted that the Stirling engine is an external combustion engine, not an internal combustion engine. All the other concepts considered in this chapter are internal combustion engines. External expander cylinders were found in the engines that were called compound engines (Mollenhauer and Tschöke 2010, p. 3). External expander cylinders were found together with external compression in engine concepts already in 1910 (US 961059 1910).

First engines that were called split-cycle engines were patented by Webb and Casaday in the beginning of the 20th century. These engines have a working cylinder for combustion and expansion and a compressor cylinder for intake and compression, with the pistons connected to a common crankshaft. (US 1062999 A 1913, US 1372216 1921.)

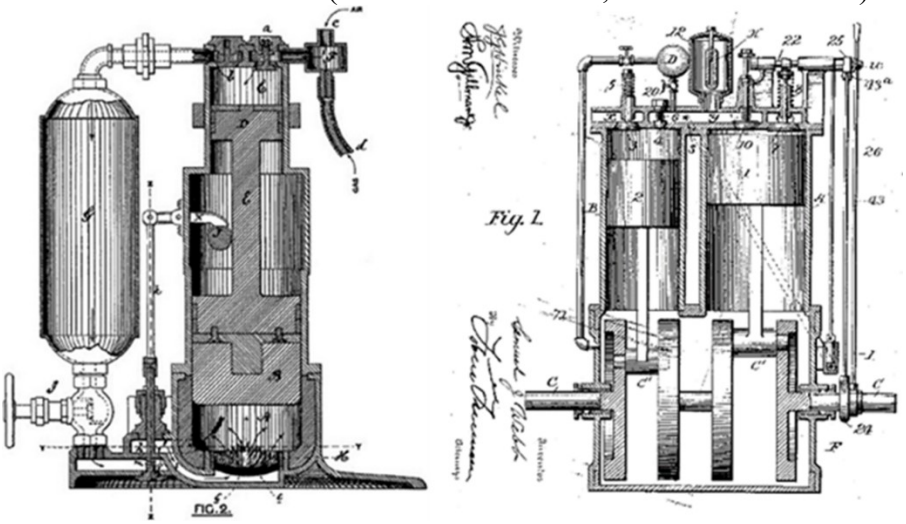

Figure 3.1. Two historical concepts, on the left Brayton's Ready Motor (1872) and on the right Webb's engine (1913). (Brayton Ready Motor 2016, US 1062999 A 1913).

3.2 The Z-engine

The Z-engine concept was developed by Timo Janhunen (M. Sc.) in 2001. The Z-engine mixes aspects of four-stroke and two-stroke engines in its gas exchange cycle, which is an alternative type of two-stroke engine cycle.

In a conventional two-stroke engine, gas exchange is done with so called scavenging, where the air flowing into the cylinder pushes the exhaust gases out. In a four-stroke engine, the upwards moving piston pushes the exhaust gases out of the exhaust valves. After the exhaust stroke the piston moves down, and the charge air flows in the cylinder from the intake valves. The gas exchange therefore takes a whole revolution in the four-stroke engine, and combustion takes place only once per two revolutions. The working cycle of the Z-engine is two-stroke, meaning that combustion takes place once per revolution. However, instead of exhaust scavenging, the gas exchange is done like in the four-stroke engine.

In the Z-engine, the expansion stroke goes like in a four-stroke engine. The exhaust stroke starts slightly before bottom dead centre, but it ends approximately at 70 degrees of crank angle (ºCA) before top dead centre, which is slightly after halfway of the stroke. Because the exhaust stroke is incomplete, some residual gases will always remain in the cylinder. The intake valve opens slightly before the exhaust valve closes. The intake period is very short; the intake valve closes around 40 ºCA before top dead centre, the duration of the intake period being roughly 30 ºCA. During the intake period, highly pressurized charge air (8—25 bar (a)) flows into the cylinder and mixes with the residual gases that are present. The charge air flows in the cylinder while the piston is moving up: therefore, a very high charge air pressure is required. The intake valve closure is followed by a final short compression period, ignition and combustion. This gas exchange cycle is referred to as the Z gas exchange, and it is illustrated in figure 3.2. (Janhunen and Nyyssönen 2017, Tiainen et al. 2003.)

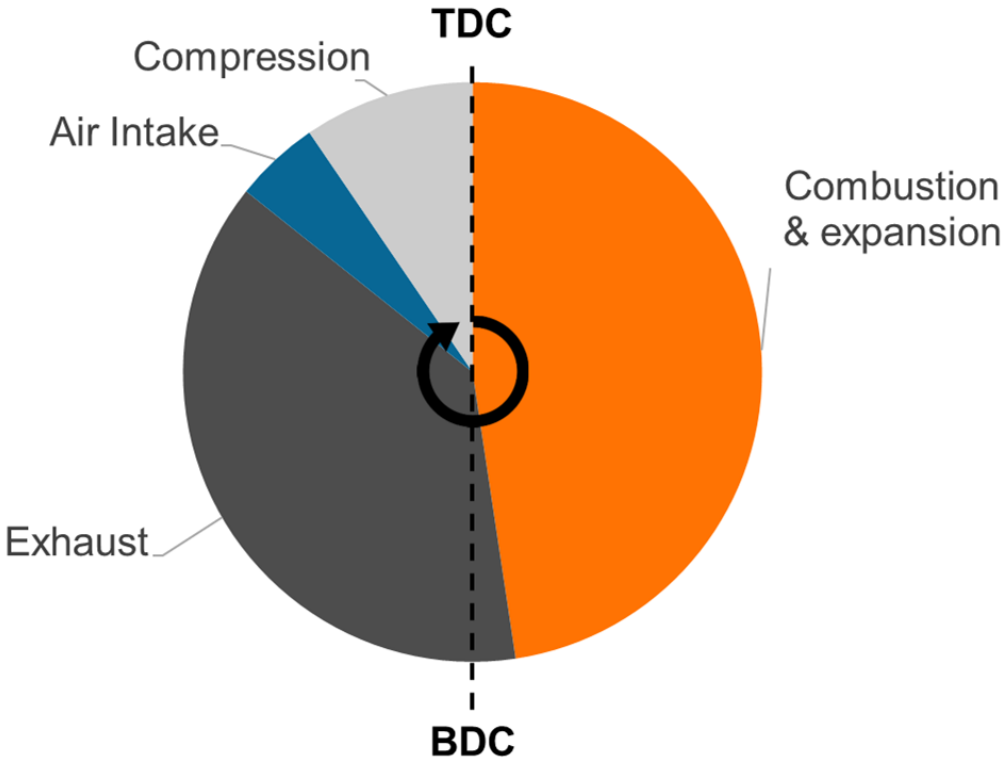

Figure 3.2. The working cycle of the Z-engine. Here TDC indicates top dead centre, and BDC bottom dead centre.

The total engine compression is partially external in the Z-engine. To have adequate airflow into the cylinders during the short intake period, the charge air pressure must be considerably higher than in a conventional engine. The charge air is compressed in the first stage in a

turbocharger compressor, which acts as a pre-compressor. After the turbocharger compressor, the charge air is cooled in an intercooler, and compressed in the second stage in a crankshaft-driven piston compressor. The charge air is cooled a second time after the piston compressor, after which it flows into the working cylinders. The final part of the compression is done in the working cylinder, where the charge air is mixed with the residual gases. A schematic of the concept is shown in figure 3.3. (Tiainen et al. 2003).

A feasibility study for the Z-engine was done at the Helsinki University of Technology in 2003 (Tiainen et al. 2003). A prototype valvetrain was designed and built (Grönlund 2003, Grönlund and Larmi 2004). The valve train (VT) prototype was run for several hours in the test bench. The prototype of the working cylinders followed soon and was tested for 2 years beginning in 2005 (Janhunen and Nyyssönen 2017). Many patents are issued for the Z-engine.

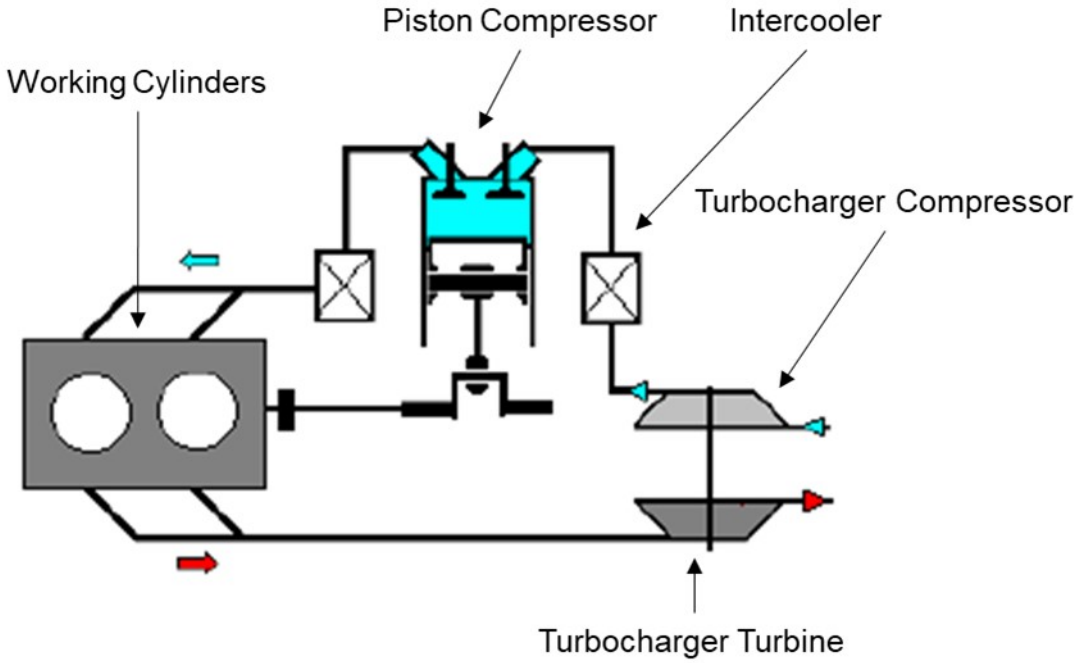

Figure 3.3. Schematic of the Z-engine (after Kuleshov et al. 2015).

3.3 The Hoos engine

An engine concept named the New Generation Combustion Engine was developed by Mr. Frank Hoos (2015). The engine concept shall be referred to as the Hoos engine. The Hoos engine is a fully external compression engine concept, meaning that compression is done exclusively outside the working cylinder. The Hoos engine working cylinder uses a two-stroke gas exchange cycle without exhaust gas scavenging, very similar to the Z gas exchange.

The important difference from the Z gas exchange is that in the Hoos engine, the intake period comes after top dead centre, while in the Z gas exchange it takes place before top dead centre. This means that in the Hoos engine, the exhaust stroke is complete, and the intake period shortens the expansion stroke instead. In the Hoos engine, the intake valve opens around top dead centre, slightly before the exhaust valve closes. The intake period is roughly the same duration, 30 ºCA. After the intake valve opens, hot highly pressurized air flows in the cylinder. The hot air expanding to the cylinder generates work during the intake

period. After the intake valve closes, fuel is injected, and more work is generated from the combustion and expansion. The gas exchange is illustrated in figure 3.4, and a schematic of the engine is shown in figure 3.5. (Hoos 2015.)

Because all compression is done externally, the charge air pressure in the Hoos engine must be even higher than in the Z-engine, roughly 100 bar (a). Instead of using a piston compressor, the external compression is completed in four-stage turbocharging system. The concept is depicted as utilising a single turbine, which powers four compressor stages. After each compressor stage, except the last one, the charge air is cooled in an intercooler. After the fourth compressor stage, the charge air is heated in a recuperator by the hot exhaust gases. The charge air is heated so that it generates work to the downwards moving piston during the intake period. Exhaust gas from the cylinders flows first into the recuperator, where it transfers part of its heat to the charge air. After the recuperator, the exhaust gas flows into the turbine, generating work to drive the compressors. The developer predicts an 80% thermal efficiency for his engine, however no other studies have been made for the concept. The concept is protected by a number of Mr. Hoos' patents (US 2017/0045230 A1 2017). (Hoos 2015.)

The Z-engine and the Hoos concepts are very similar engine concepts. A significant part of the total engine compression is done externally, either by a series of turbochargers or a combination of a turbocharger and a piston compressor. Both concepts use a two-stroke cycle without exhaust gas scavenging, with certain differences in valve timing.

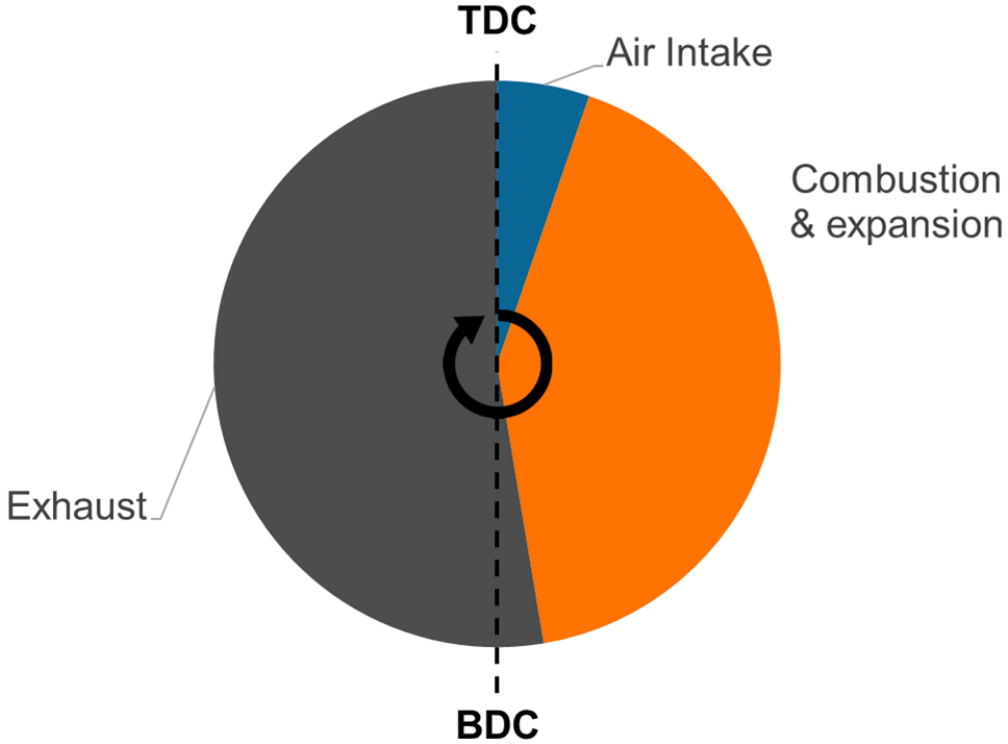

Figure 3.4. The gas exchange cycle suggested for the Hoos engine.

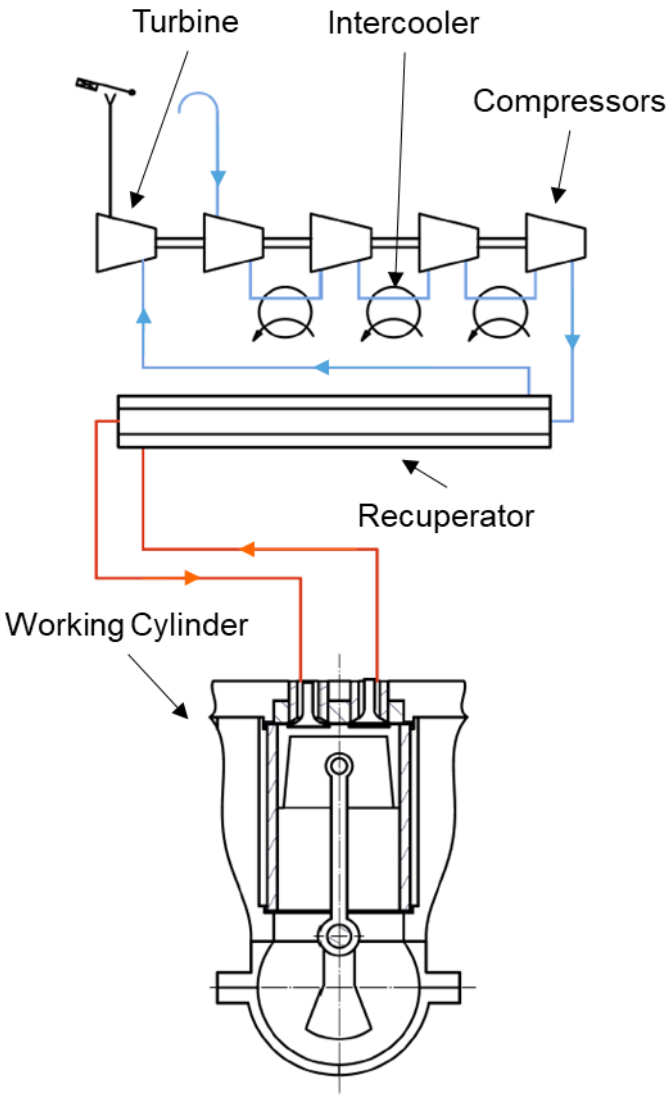

Figure 3.5. Schematic of the Hoos engine (after Hoos 2015).

3.4 Engine concepts review

In this literature review, over 30 external compression engine concepts were found. They were divided into three groups: the split-cycle engines, split cycle engines with isothermal compression and the multi-stage compression and expansion engines.

3.4.1 Split-cycle engines

A large part of the concepts, including the Z-engine, belong to the first group of the concepts, the split-cycle engines. The name comes from the split four-stroke cycle, also referred to as the split-cycle. It is basically a general term for a working cycle, which is like the ones used in the Z-engine and the Hoos engine. In the split four-stroke cycle, the four-stroke cycle is divided into two systems: the power and exhaust strokes are completed in the working cylinder, and the intake and compression strokes are done by an external compressor, which is in most cases a piston compressor. Selected split-cycle concepts are shown in figure 3.6. (Philips et al. 2011.)

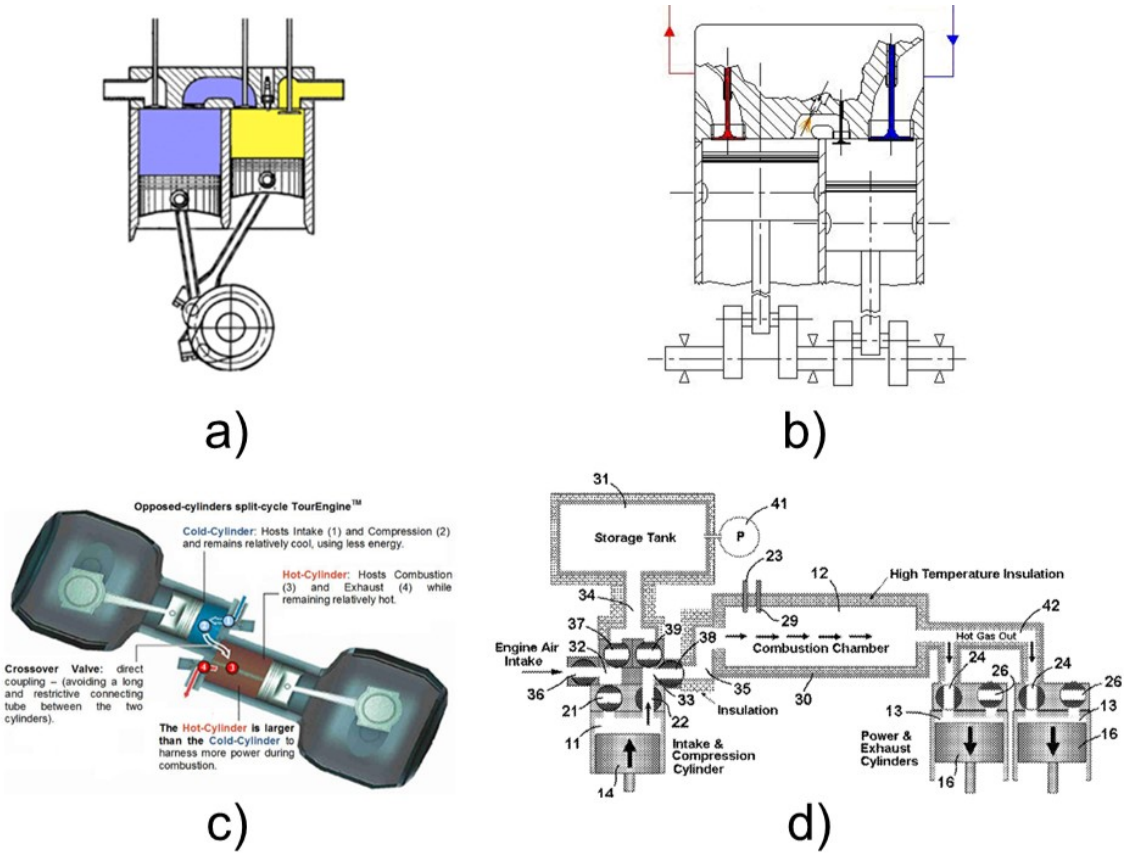

Figure 3.6. Split-cycle engine concepts, where a) is the Scuderi split-cycle engine, b) the Homogeneous Charge Progressive Combustion concept, c) the Tour engine and d) the Zajac engine (Kuleshov et al. 2015, Musu et al. 2010, The Tour Engine 2017, US 2011/0303185 A1 2011).

The working cylinder cycle is a two-stroke cycle very similar to which is used in the Hoos engine and Z-engine concepts. Instead of exhaust gas scavenging, exhaust gas is pushed out by the piston. The intake period is either before or after top dead centre. Like the Z and Hoos engine concepts, the intake period is very short, approximately 20—40 ºCA, and the charge air is compressed to a very high pressure. A very fast-acting valve train is needed, like the one designed for the Z-engine. A valve train like this needs pneumatic or hydraulic actuators or pneumatic valve springs. On the Z-engine, the prototype intake valves were made of titanium to withstand the forces during the intake period. This will make the intake valve train much more expensive than normally. (Grönlund and Larmi 2004, Philips et al. 2011.)

The concepts are divided to ones that have the intake period before top dead centre and the ones that have it after top dead centre of the working cylinder. When intake period is after top dead centre, the exhaust stroke can be complete, but the time for expansion is limited by the intake phase. When the intake period is before top dead centre, expansion stroke is complete, but the exhaust stroke is limited, always leaving some residual gases in the cylinder before the start of combustion. Therefore, the place of the intake period will always be a compromise.

Unlike in the conventional two-stroke or four-stroke engines, there is no cooler period during the cycle in a split-cycle engine's working cylinder. Conventionally, the cylinder is either flushed with cool air, or the hot exhaust gases pushed out by the working cylinder. In split-

cycle engines, the working cylinders are constantly working with hot compressed air and hot exhaust gases. It is assumable that the heat load of the working cylinder would be higher than in the conventional cycles.

3.4.2 Split-cycle engines with isothermal compression

The second group of the concepts are the split-cycle engines with isothermal compression. The purpose of these concepts is high thermal efficiency; every developer promises at least a 60% efficiency. The working cylinder gas exchange cycle is like the one in the split-cycle engines. Two isothermal compression engine concepts were found in addition to the Hoos engine: the Isoengine and the Cryopower engine. The two concepts can be seen in figure 3.7.

In these engine concepts, the purpose is to complete compression isothermally, which is the most efficient type of compression. Isothermal compression is realised in the Isoengine and Cryopower concepts by injecting a coolant (water or liquid nitrogen) in the external piston compressor. The Hoos engine does this by implementing four intercooled turbocharger stages. (Wiksten 2009, Coney et al. 2003, Gurr et al. 2016, Hoos 2015.)

Each concept utilises a heat exchanger (recuperator) that uses the exhaust gases from the working cylinders to heat up the charge air. In the Hoos engine, in addition to provide a temperature high enough for autoignition, the purpose of it is to minimize the heat transfer losses by bringing the charge air temperature as close to the cylinder wall temperature as possible. In the Isoengine and Cryopower concepts, the idea to use exhaust heat recovery comes from the recuperated Brayton cycle (gas turbines). Along the principles of Carnot, recuperation increases the temperature where heat is added to the system, which in theory increases thermal efficiency. (Coney et al. 2004, Gurr et al. 2016, Hoos 2015).

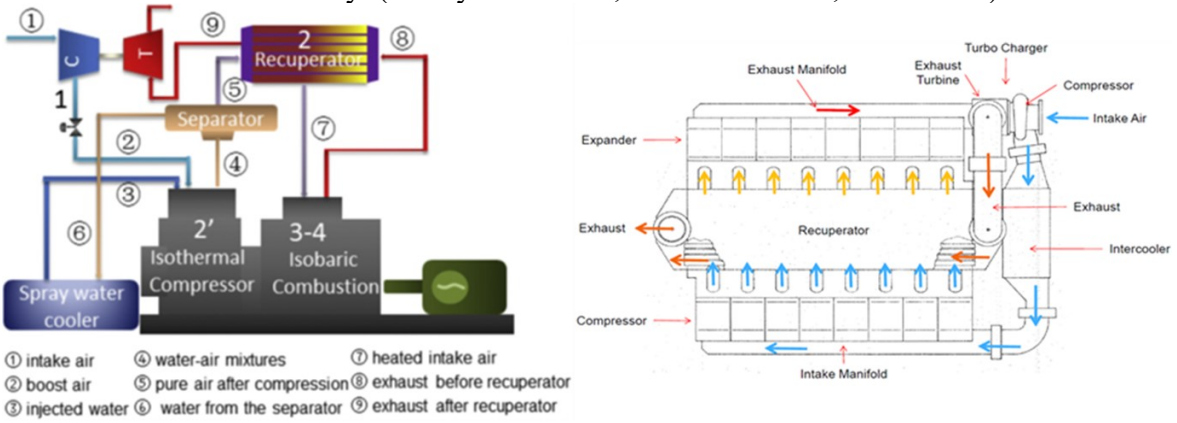

Figure 3.7. The isothermal engine concepts, the Isoengine on the left and the Cryopower engine on the right (Coney et al. 2004, Gurr et al. 2016).

3.4.3 Multi-stage compression and expansion engines

The third group of the engine concepts are the multi-stage compression and expansion engines. In addition to external compression, also part of the expansion is done externally in these concepts. The working cylinder cycle is familiar from the split-cycle engines, with one concept making an exception. There is a compressor, the working cylinder and an external expander. This means that there is a lot of transfer stages in these engine concepts. In addition to having efficient compression, the idea in these concepts is increasing the expansion ratio, which increases the efficiency of the internal combustion engine; the gas can be expanded more, creating more work (Heywood 1988 p. 185). Another improvement in the concepts is

to decrease the working cylinder heat transfer losses by minimizing the combustion chamber surface area, as expansion and compression are completed externally. Four concepts were found in this group, and two of them can be seen in figure 3.8. (Clarke 2009, US 3688749 1972, Zima and Ficht 2010, US 5325824 1994, Lam et al. 2015.)

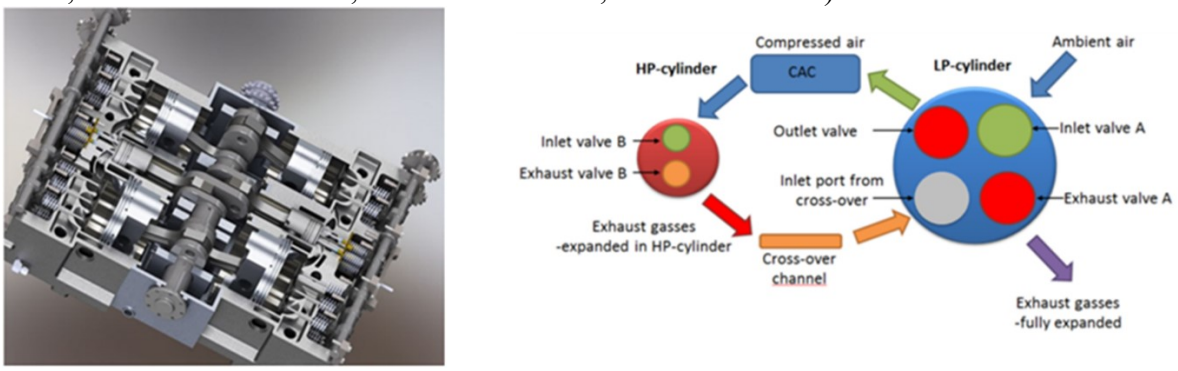

Figure 3.8. The Compact Compression Ignition on the left and the Dual Compression Expansion Engine on the right. (Motiv Engines 2012, Lam et al. 2015.)

3.5 Summary of the concepts review

The fundamental working principle of the concepts found in this review is the same. Everyone has basically invented the "same wheel" with new details. In each concept, except one, the working cylinder cycle is the same two-stroke cycle with poppet valve gas exchange, as in the Z-engine and the Hoos engine concepts. External compression is made in either a piston compressor or a series of turbochargers, or a combination of both. Even a part of the expansion is moved outside of the working cylinder in some concepts. The Z-engine stands out as a very extensively studied concept. The Hoos engine stands out as the only concept, which implements more than two compression stages.

Every concept makes use of the very short intake period, like in the Z and Hoos engine concepts. This means that a very fast-acting valve train, like the one designed by Grönlund and Larmi (2004), is required. Unlike in the conventional two- and four-stroke engine cycles, there is no cool period in the working cycle of these engine concepts. This raises the question, what will the cylinder heat load of these type of engines be?

The trend in the medium-speed market is to go towards stronger Miller timing, or in other words earlier intake valve closure. Two-stage turbocharging has enabled this, as stronger Miller timing requires the increase of the charge air pressure to keep the power level constant. Stronger Miller timing is moving more of the compression work outside of the working cylinder, to the turbocharger. Shorter intake valve opening duration and higher charge air pressure is moving the four-stroke engine towards the external compression engines. The external compression engines are basically engines with extreme Miller timing. According to a benchmark study made for Wärtsilä by an external company, the trend in the industry is towards stronger Miller timing, which also indicates an increase in charge air pressure level. Therefore, the direction in the market is in any case towards more external compression. (External Company 2015.)

4 Method

This chapter introduces the method used for the sensitivity analysis, optimization and the comparison of the engine concepts. The simulation method and the simulation models will be described.

4.1 GT-Power

For the studies of this Master's thesis, GT-Power from Gamma Technologies Inc. is used. GT-Power is a one-dimensional engine performance simulation software. GT-Power can be used for steady state and transient simulations. It can be used to simulate the conventional four- and two-stroke engines as well as some unconventional concepts such as the ones studied in this Master's thesis. In this study, the comparisons are done with steady-state simulations. GT-Power can evaluate all the engine performance characteristics such as power and fuel consumption. The tool can accurately predict in-cylinder flow, combustion, heat transfer and flow characteristics in the intake and exhaust ducts. Engine components such as turbochargers, charge air coolers and exhaust systems can be modelled. (Gamma Technologies 2017.)

For the flow in the intake and exhaust pipelines, GT-Power uses the Navier-Stokes equations. The pipe systems are discretised into many smaller volumes, which are connected by boundaries. Simulations are solved one engine cycle at a time. The cycles are divided to time steps, usually ranging from 0.5—1 ºCA. For each time step, scalar and vector quantities, such as pressure and mass flow rate are solved for each volume and boundary. The first simulation cycle is started with initial values that are imposed by the user. Initial values for pressure, temperature and flow composition are defined for the engine components. As the simulation runs, new initial values for the scalar and vector quantities for the next cycle. The simulation is continued for so many cycles until steady-state is achieved; once the scalar and vector quantities do not change or change only slightly from cycle to cycle. (Gamma Technologies 2017.)

4.2 Included features from the Z-engine and the Hoos engine

By the definition of the developer, the Hoos engine uses a gas exchange where the intake period takes place after top dead centre, unlike in the Z-engine. The concept survey found that most of the external compression engine concepts use a gas exchange cycle like in the Hoos engine. However, the gas exchange cycle in the Z-engine, where the intake period is takes place before top dead centre, is the only one which is properly tested and proved to be working. So that the workload of the thesis does not get unnecessary large, the gas exchange suggested for the Hoos engine was left out of this study. Both concepts will be simulated using the Z gas exchange cycle. The effect of the Hoos engine's recuperator will not be studied with simulations. Therefore, the full Hoos engine, as defined by the developer, will not be studied in this thesis. The only feature included from the Hoos engine is the four-stage turbocharging setup.

The variant simulated is a four-stage turbocharged external compression engine using the Z gas exchange cycle. Since the idea of four-stage turbocharging is taken from the Hoos engine, the engine concept that is simulated along with the Z-engine shall be referred to as the Hoos Variant. The Z-engine will be simulated as is defined by the developer. Throughout the whole thesis, the engine concepts simulated are the Z-engine and the Hoos Variant. For simplicity, from now on they will be referred to as the concepts, or the engine concepts.

4.3 Engine models

Even though the GT-Power two-stroke engine mode is meant for modelling conventional two-stroke engines with exhaust gas scavenging, it is quite straightforward to create the Z gas exchange cycle. Instead of modelling scavenging ports and scavenging channels, the model is simply fitted with intake and exhaust valves with their respective profiles, like a in a four-stroke engine model.

For the sensitivity analysis, a simple model was built to represent both engine concepts. This model is referred to as the simple model. The model was made as simple as possible: a one-cylinder model with one exhaust valve and one intake valve. Intake and exhaust pressures are produced by "EndEnvironment" elements, which are indefinitely large tanks with an imposed constant pressure. The simple model makes it faster to run large sweeps with many parameters.

The Z-engine full model was done according to the idea of the developer; however, the Hoos Variant model was done differently. As explained earlier, the recuperator and the gas exchange cycle of the Hoos engine were left out of the model. The charge air production is a bit different; instead of one turbine and four compressors, the model was done with four turbines and four compressors to represent a four-stage turbocharging setup.

As the reference engine the Wärtsilä 20 (W20) is used. The reference GT-Power model used is a model used at Wärtsilä, with certain modifications done for the sake of this study. They are explained 4.4.4. The W20 is a one-stage turbocharged and intercooled compression ignition engine using the Miller cycle. (Wärtsilä 2017.)

An additional reference model was built: the W20 using the four-stage turbocharging setup of the Hoos Variant engine. If the assumption is made that the Hoos Variant engine will be more fuel efficient than the W20 due to its four-stage turbocharging setup, it is sensible to test how good the W20 would be with the same configuration. The four-stage W20 model will be referred to as the W20 four-stage or W20 FS. Otherwise, W20 or Wärtsilä 20 refers to the standard (one-stage turbocharged) W20.

Some components of the engines are referred to later in the thesis. The full concept models, and the reference model are illustrated in figures 4.1—4.3. For all the engines, the coolers between the compressor stages are referred to as intercoolers (IC), and the final air cooler before the working cylinders is referred to as the charge air cooler (CAC). On the Z-engine, the piston compressor (PC) is referred to, as well as the turbocharger (TC) turbine and compressor (Figure 4.1). On the Hoos Variant engine, unless otherwise mentioned, the turbine 4 (T4), which is the first turbine after the working cylinders, is referred to. The numbering of the other turbines and compressors is shown in figure 4.2.

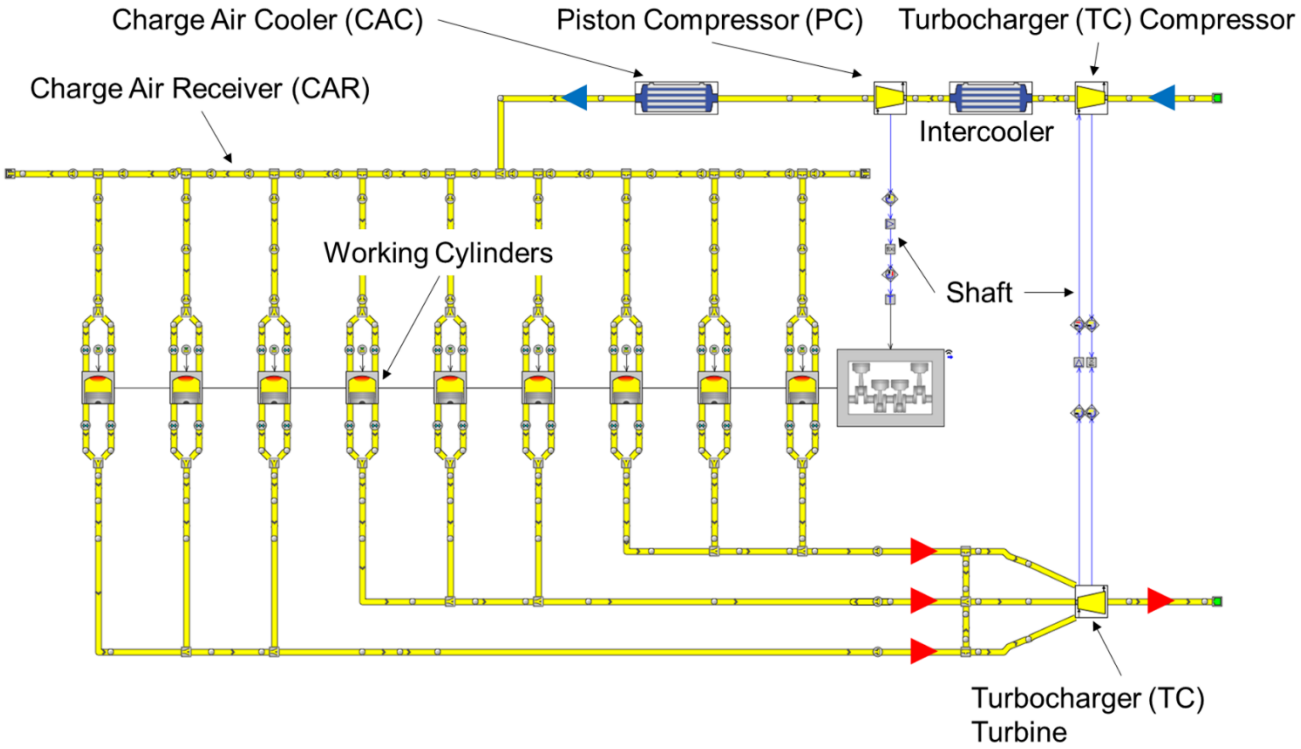

Figure 4.1. The Z-engine GT-Power model. Air flow is depicted with blue arrows, and exhaust gas with red arrows.

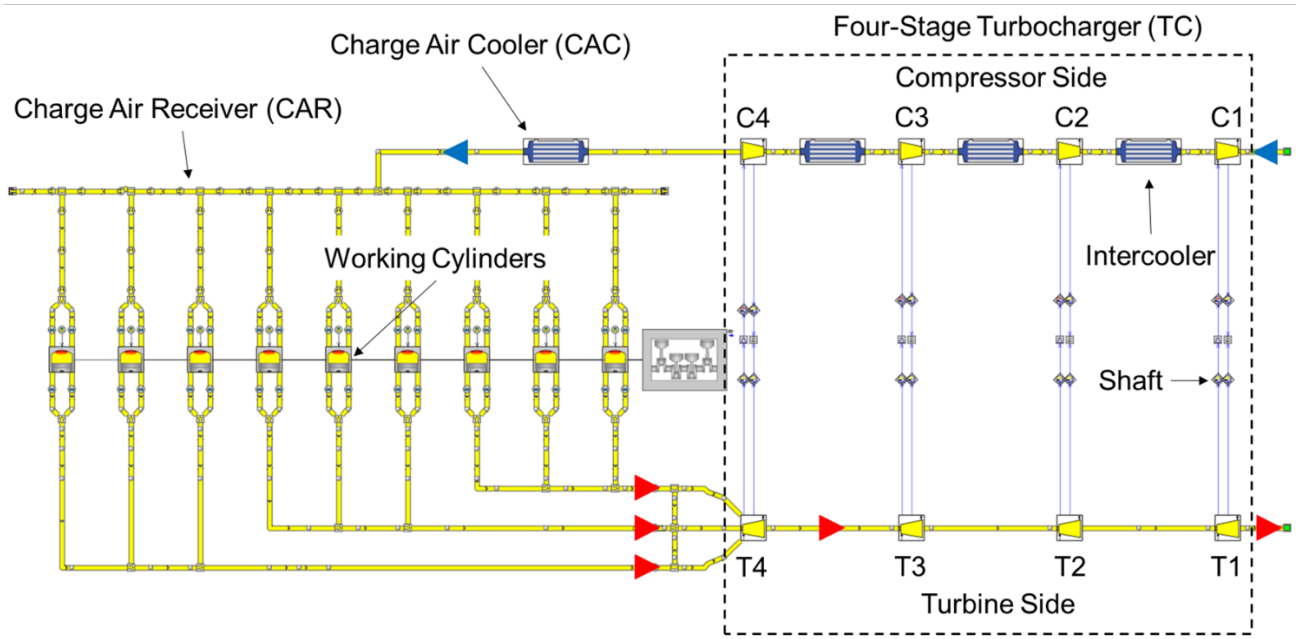

Figure 4.2. The Hoos Variant engine GT-Power model. Air flow is depicted with blue arrows, and exhaust gas with red arrows.

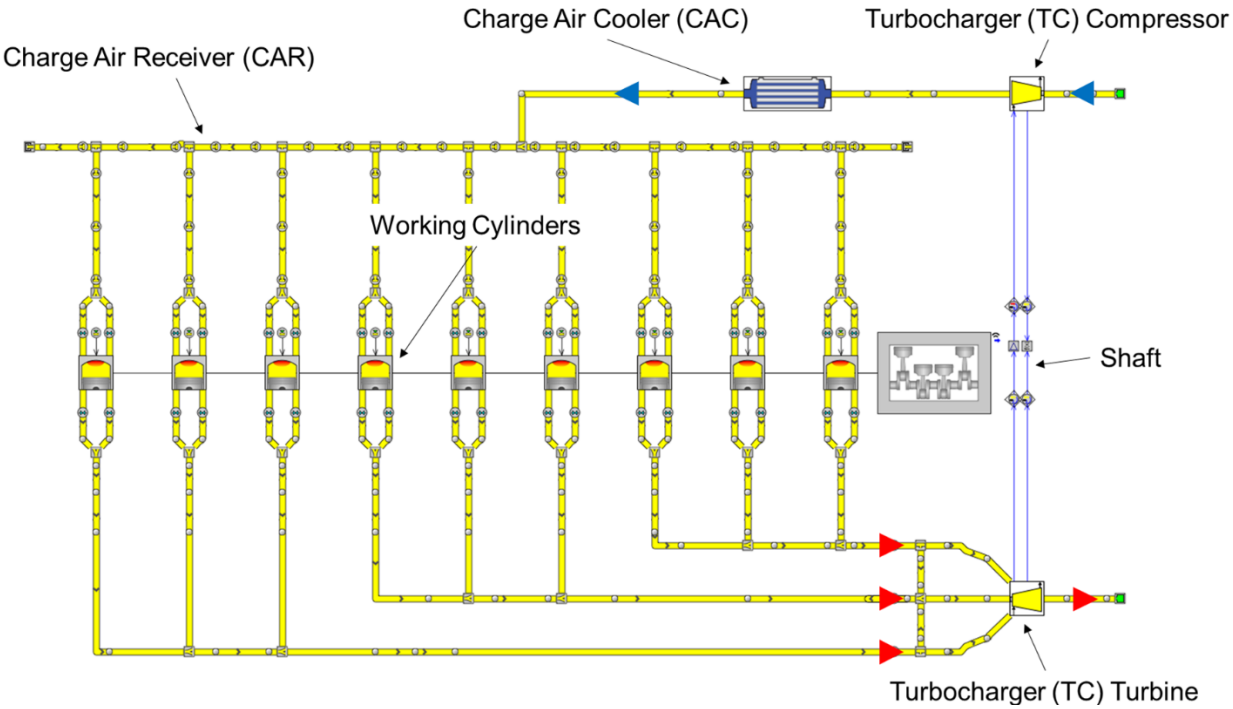

Figure 4.3. The W20 (W9L20) reference model. Air flow is depicted with blue, and exhaust gas with red.

4.4 Model parameters

I order to get a sensible comparison between the engine concepts and the reference engine, common parameters are defined. A summary of the boundary conditions and simulation parameters is shown in table 4.1. These will be referred to as the standard boundary conditions. The comparisons are done with the W20 cylinder geometry and with the full cylinder output of the W20. As both concepts are two-stroke engines, a brake mean effective pressure (BMEP) of 13.65 bar produces the 200-kW cylinder output of the W20. All models use a load controller, which sets the injected fuel amount to reach the desired load.

4.4.1 Heat release

The heat release object used in the comparisons and the sensitivity analysis is a heat release profile derived from W20 engine measurements. Since the engine concepts are run with a BMEP half of what the W20 runs at, the heat release profile used in the concepts is that of the W20 50% load. For the W20, the 100% load heat release profile will be used, which is somewhat longer than the heat release profile at half load. Injection timing and combustion phasing are kept constant.

4.4.2 Friction

If the assumption is made that the concepts would be built and run with W20 components, then the friction losses can be assumed to be the same. One concern regarding the friction is, that the concepts operate with a different maximum cylinder pressure than the W20. According to a Master's Thesis study done at Wärtsilä, cylinder pressure has little significance to the friction losses of a medium-speed engine. Therefore, for the purposes of this thesis the friction losses are assumed to be constant, regardless of the maximum cylinder pressure. A mechanical efficiency of 88% was assumed for the W20, which corresponds to a friction loss of 230 kW. The friction loss is assumed to include the losses of auxiliaries such as fuel and water pumps. (Master's Thesis 2018.)

During the sensitivity analysis and the concept optimization, a Chenn-Flynn friction model was used with the parameters from the reference W20 model. The model calculates the engine Friction Mean Effective Pressure (FMEP) with the Chenn-Flynn equation. In its simplest form, the equation consists of a constant FMEP part, a mean piston speed part and a maximum cylinder pressure part. The constant part of FMEP is set by the user, and the impact of mean piston speed and maximum cylinder pressure can be weighted by user-set multipliers. Therefore, the friction losses are not constant in the sensitivity analysis and optimization. The simulations that are presented in chapters 5 and 6 are done with the Chenn-Flynn model, while the simulations presented in chapter 7 are done with a constant friction (230kW). (Gamma Technologies 2017.)

4.4.3 Flow components and piping

This part concerns the full engine models (9-cylinder in-line, modelled charge air production). The concepts have a significantly different charge air production layout than the W20 engine, which is single-stage turbocharged. The charge air receiver, intercoolers, charge air coolers, intake and exhaust ports and the exhaust manifold are recycled from the reference W20 model. The intake port and runner lengths will most likely be different for the Z-engine and Hoos Variant models, as these will be optimized. The surface roughness and pipe thermal properties will be kept constant. The intercoolers and the charge air coolers are multiple pipe elements with a set wall temperature. The wall temperature is imposed so that the charge air is cooled to the desired temperature in the cooler.

To save on simulation time, some simplifications were made to the full concept models for the concepts' optimization. The simulations presented in chapter 6 are done with these simplified full engine models. The optimization matrices were done with one exhaust and intake valve per cylinder, and a simplified intake and exhaust side geometry. The detailed full models and simplified full models provide near identical simulation results. However, since the detailed full models take considerably more simulation time, it was acceptable to optimize the concepts with the simplified full models.

4.4.4 Compressors and turbines

The piston compressors and the turbochargers are modelled with simple compressor and turbine elements. GT-Power simple turbine and compressor models do not use compressor maps, instead efficiency and input power are imposed. Rotating speed and turbine shaft is not modelled either. Turbines input the power they produce to the turbocharger compressors. A damping factor models the inertia of the turbocharger shaft. The piston compressor input power is imposed to the crankshaft of the Z-engine as an auxiliary load.

Suitable values for turbine, compressor, piston compressor and mechanical efficiency are assumed based on rules of thumb at Wärtsilä and values found in literature (as described in equation 13, chapter 2.2) (Isaksson 2017, Hattar 2017, Campbell 2014). It was decided, that using complete compressor models with maps would bring no extra value to the study; it would only bring extra work in form of turbo-matching. The same applies for the piston compressor. It is possible to create a detailed model of the piston compressor in GT-Power; however, this was also expected to bring no extra value to the study. Therefore, the same compressor model is used for the piston compressor as for the turbocharger compressors, the only difference between the turbocharger compressor and the piston compressor being their efficiency.

Some modifications needed to be done to the reference model to get a fair comparison. As the concept models use simple turbine and compressor elements, the reference model turbocharger was also converted to use these elements. Due to the modifications done, the results given by the reference model are slightly changed. This is acceptable since it is more important to have a comparison between the four-stroke engine and the concepts with the same boundary conditions, rather than produce results that correspond exactly to a real engine. Values that are given for the W20 in this Master's thesis are not therefore corresponding to actual W20 performance values.

4.4.5 Cylinder heat transfer and heat load

To compare the heat transfer and heat load characteristics of the engine, a cylinder wall temperature solver "EngCylTWallSoln" is used. This wall temperature solver uses a simple finite element structure to calculate the heat conduction to the cylinder walls. GT-Power creates the finite element structure of the cylinder wall, piston, cylinder head and the valves based on measurements input by the user. Characteristics such as coolant water temperature and mass flow are given by the user. Coolant flow characteristics are kept constant in all models, to be able to compare the heat load of the cylinders. Based on the heat transfer, the solver calculates the temperature in different parts of the cylinder wall, piston, head and the intake and exhaust valves. The results this model gives are by no means accurate but should give a good indication of the difference between the concepts. (Gamma Technologies 2017.)

The cylinder wall temperature solver was used only in the final comparison simulations presented in chapter 7. For the sensitivity analysis and optimization simulations, which are presented in chapters 5 and 6, a standard GT-Power element was used (Gamma Technologies 2017). This element calculates the cylinder heat transfer losses using the Woschni equation. This was used for the same reason as the simple engine model and the intake and exhaust geometry simplifications: to decrease the required simulation time for long simulation runs.

4.4.6 Intake valve opening timing

Intake valve opening timing (IVO), or alternatively intake valve timing is referred to as the moment when the intake valve opens over zero millimetres of lift, in degrees relative to the firing top dead centre. As an example, -60 ºCA aTDC means that the intake valve opens -60 degrees of crank angle after top dead centre, or in other words 60 degrees before top dead centre.

Since the Z gas exchange works so that the intake valve opens right after the exhaust valve closes, a way to adjust the intake valve opening timing had to be made. Simply keeping the exhaust valve opening duration constant and adjusting the opening timing would not work; with an early intake valve opening timing, also the exhaust valve would open too soon, for example in the middle of the expansion stroke. Therefore, the exhaust valve opening timing would remain constant in all optimizations and variations, and instead the opening duration on the maximum lift would be adjusted. It is adjusted so that the exhaust valve dwells at the maximum lift, the later the intake valve opening timing is. The method is illustrated in figure 4.4.

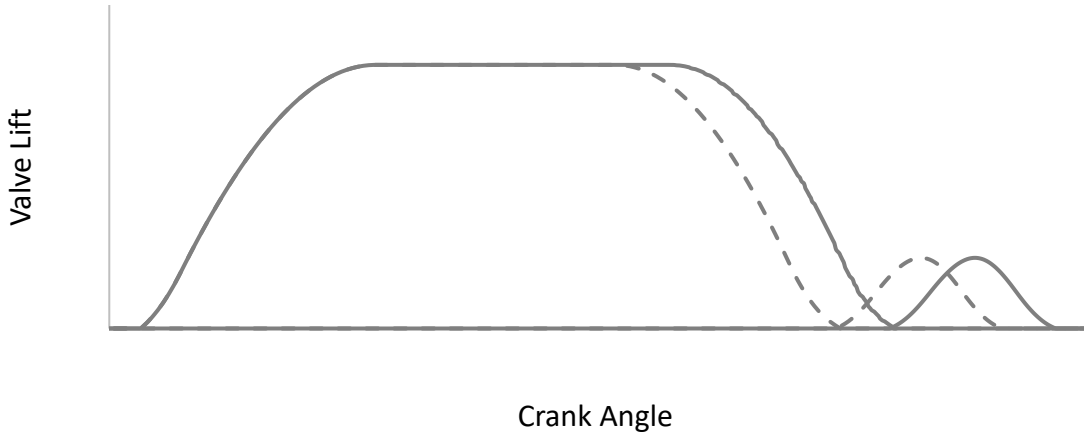

Figure 4.4. Method to adjust the exhaust valve opening duration, when intake valve opening timing is delayed by 10 ºCA. The profile on the left is the exhaust valve profile and the smaller profile on the right is the intake valve profile.

4.4.7 Cam lift profiles

For the concepts, five different intake cam lift profiles of different actuation speed are used. The profiles include, from the slowest to the fastest: a W20 production engine profile, an experimental cam profile for a two-stage turbocharged engine, the cam profile designed for the Z-engine, a faster version of the Z-engine profile and the step cam lift profile (Grönlund 2003). The profiles will be referred to as the W20-cam, 2-stage-cam, Z-cam, the fast Z-cam and the step cam. The profiles are shown in figure 4.5.

The W20 cam and the 2-stage cam are far too long to be used in the concepts, so they were scaled down to a much shorter length using the GT-Suite application VTDesign, maintaining a similar acceleration curve. This way also the maximum lift provided by the profiles decreases in proportion. The Z-cam was provided from the Master's thesis of Grönlund (2003). The fast Z-cam was simply made by upscaling the Z-cam lift in the VTDesign-application.

The W20-cam represents a cam profile that could be realised with existing Wärtsilä solutions. The Z-cam represents a profile which is realisable with additional development work. The fast Z-cam and the step cam represent ideal cam lift profiles.

The step cam profile is used in the sensitivity analysis simply because the opening duration and lift is simple to adjust. All cam profiles are compared in a part of the sensitivity analysis. The Z-cam is used for the full concept model optimization and the final comparisons, since it is regarded as the fastest cam profile that can be realised in practice. On the W20 engine, the standard Miller cam profile will be used. Regardless of the cam profile, the W20 Miller profile valve coefficients are used on the intake valves.

For the exhaust valves, the same cam profile and valve lift coefficients are used in in the concepts and the W20. The exhaust cam profile is like in a normal engine also in the Z-engine prototype and was not seen as a limiting factor.

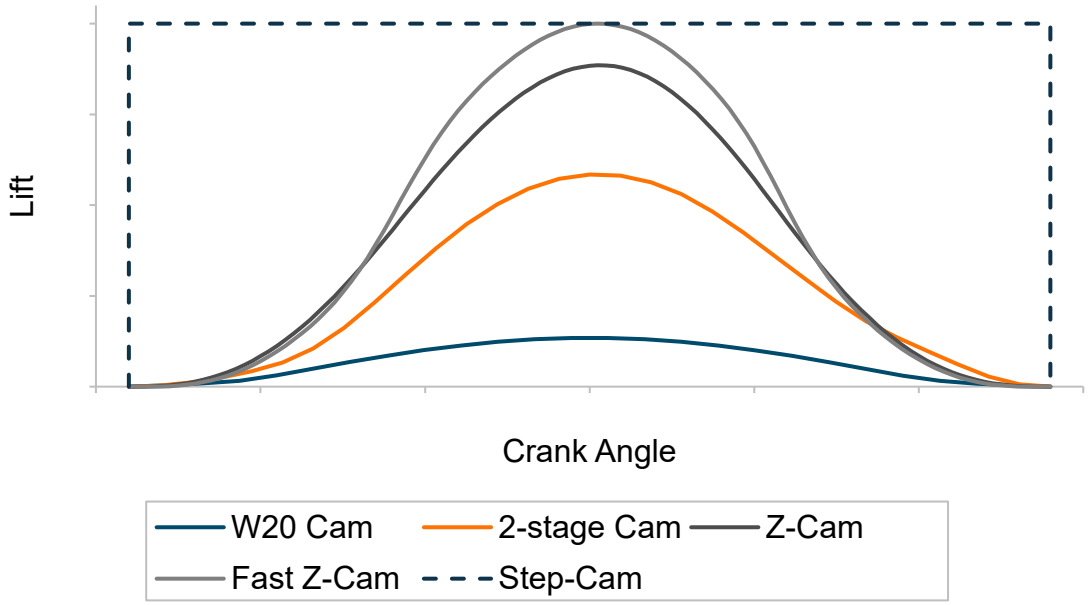

Figure 4.5. The cam profiles used for the concepts.

The method used for adjusting the cam opening duration and lift at the same time is presented in figure 4.6. With such a low maximum lift for the Z-cam, it was assumed that if the cam opening duration is increased, the maximum lift of the cam profile is also increased. This way, with a certain cam acceleration the cam profile has time to lift the valve to a higher lift when the opening duration is increased. This method was used in the cam profile comparisons of the sensitivity analysis as well as in the full model optimizations.

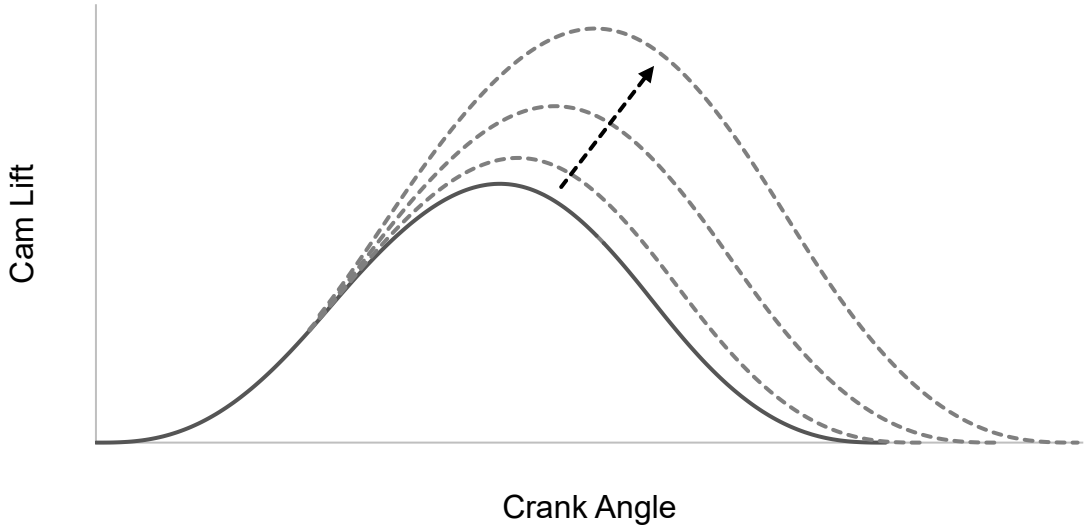

Figure 4.6. The method to adjust valve lift and opening duration with the realistic cam profiles.

Table 4.1. The standard boundary conditions used in the comparison.

Standard Boundary Conditions				
	Concepts	**W20**	**W20 4-stage**	**Unit**
Engine				
Bore	200			mm
Stroke	280			mm
Engine speed	1000			r/min
Cylinder Configuration	9-cylinder in-line			
BMEP	13.65	27.3		bar
Cyl. output	200			kW
Heat Release	W20 50% load	W20 100% load		
Friction losses	230			kW
Cyl. Wall T	Solver (EngCylTWallSoln)			
T aft. CAC	45			^{o}C
CAC wall T	baseline			^{o}C
p. drop in CAC	constant			%
Ambient T	25			^{o}C
Charge Air Production & Gas exchange				
p_3	optimized	baseline		
Turbine efficiency $\eta_{s,T}$	84			%
TC compressor efficiency $\eta_{s,C}$	82			%
PC efficiency $\eta_{s,PC}$ (Z only)	85			%
Mechanical efficiency* η_{mech}	98			%
Intake cam	Z-cam	Miller		
Simulation				
Max. timestep duration	0.5			^{o}CA
Max. n. of cycles	1500			-

*The mechanical efficiency depicts the loss from the turbocharger turbine shaft to the compressor, and the loss from the crankshaft to the piston compressor in the Z-engine. Turbine, PC and compressor efficiencies are presented as isentropic efficiency.

5 Sensitivity analysis

This chapter presents the results of the sensitivity analysis. At this phase, it was not important to optimize the different parameters, but rather learn, what should be optimized and how. The sensitivity analysis was also a way to learn, how the Z gas exchange works. The sensitivity analysis was done using ideal gas calculations and one-cylinder engine model simulations.

5.1 Introduction

Before the sensitivity analysis simulations, simple ideal gas calculations were done using Microsoft Excel. This study was done to see, what charge air pressure is required in theory for a certain intake valve opening timing and with certain parameters such as relative air-fuel ratio and exhaust pressure.

For the sensitivity analysis simulations, the one-cylinder simple engine model was used. This means that in the sensitivity analysis simulations, the charge air production, meaning the turbines and compressors, are not modelled. The most suitable way to conduct the analysis was to make intake valve opening timing variations. It was apparent that intake valve opening timing determines how long the intake valve can be open and what is the residual gas percentage at the start of combustion. Unless otherwise mentioned, the step intake cam lift profile is used. Comparisons are done with constant air-fuel ratio, unless otherwise mentioned. This way, the work needed for charge air production can be ignored. Air-fuel ratio is adjusted by controlling the intake valve opening duration.

Altogether, the parameters tested for engine sensitivity are the pressure difference over the cylinder, intake valve opening timing and duration, intake cam lift and profile, intake port length and engine speed.

5.2 Charge air pressure predictions

This analysis was done to see, what charge air pressure is required for certain operating points of the concepts. The method and assumptions made is described in chapter appendix 1. The required charge air pressure is heavily impacted by the target air-fuel ratio, intake valve opening timing and the exhaust pressure. This study is a very theoretical one but provides an insight to how and why the charge air pressure requirement changes so significantly with intake valve opening timing and exhaust pressure.

Figure 5.1 shows the charge air pressure that is required at two air-fuel ratios. This shows the difficulty with the Z gas exchange process; air is inducted while the piston is moving up. With later intake valve opening timing, the required charge air pressure starts increasing exponentially as the cylinder volume decreases. It can be expected that the intake valve opening timing will be a compromise; the charge air pressure will be the limiting factor. There will be a maximum charge air pressure that can be produced efficiently with these engine concepts. This also suggests, that there might be an optimal or maximum air-fuel ratio. In figure 5.1, going from λ=1.2 to λ=2 requires at least 30—60% higher charge air pressure depending on the intake valve opening timing.

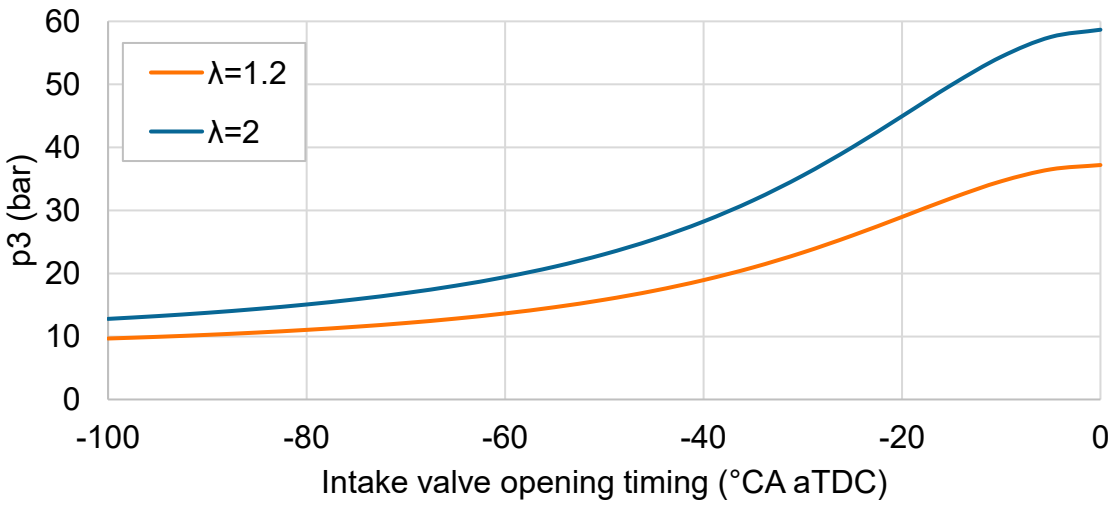

Figure 5.1. Required charge air pressure to run the concepts at two λ levels. Here p_3 is the charge air pressure, and λ the relative air-fuel ratio.

Figure 5.2 shows, how charge air pressure develops with changing intake valve opening timing and different exhaust pressure levels. Two things can be clearly seen from here: with increasing exhaust pressure and later intake valve opening timing, charge air pressure must be increased to get the air in. Therefore, the change in pressure over the cylinder, referred to as the delta p, is important rather than only the charge air pressure.

Intake Valve Timing (°CA aTDC) \ Exhaust pressure (bar)	1	2.5	5	7.5	10	12.5	15	17.5	20	22.5	25	27.5	30
-100	8.8	10.3	12.8	15.3	17.8	20.3	22.8	25.3	27.8	30.3	32.8	35.3	37.8
-95	9.2	10.7	13.2	15.7	18.2	20.7	23.2	25.7	28.2	30.7	33.2	35.7	38.2
-90	9.8	11.3	13.8	16.3	18.8	21.3	23.8	26.3	28.8	31.3	33.8	36.3	38.8
-85	10.4	11.9	14.4	16.9	19.4	21.9	24.4	26.9	29.4	31.9	34.4	36.9	39.4
-80	11.1	12.6	15.1	17.6	20.1	22.6	25.1	27.6	30.1	32.6	35.1	37.6	40.1
-75	11.9	13.4	15.9	18.4	20.9	23.4	25.9	28.4	30.9	33.4	35.9	38.4	40.9
-70	12.9	14.4	16.9	19.4	21.9	24.4	26.9	29.4	31.9	34.4	36.9	39.4	41.9
-65	14.0	15.5	18.0	20.5	23.0	25.5	28.0	30.5	33.0	35.5	38.0	40.5	43.0
-60	15.4	16.9	19.4	21.9	24.4	26.9	29.4	31.9	34.4	36.9	39.4	41.9	44.4
-55	17.1	18.6	21.1	23.6	26.1	28.6	31.1	33.6	36.1	38.6	41.1	43.6	46.1
-50	19.0	20.5	23.0	25.5	28.0	30.5	33.0	35.5	38.0	40.5	43.0	45.5	48.0
-45	21.4	22.9	25.4	27.9	30.4	32.9	35.4	37.9	40.4	42.9	45.4	47.9	50.4
-40	24.2	25.7	28.2	30.7	33.2	35.7	38.2	40.7	43.2	45.7	48.2	50.7	53.2
-35	27.6	29.1	31.6	34.1	36.6	39.1	41.6	44.1	46.6	49.1	51.6	54.1	56.6
-30	31.5	33.0	35.5	38.0	40.5	43.0	45.5	48.0	50.5	53.0	55.5	58.0	60.5
-25	36.0	37.5	40.0	42.5	45.0	47.5	50.0	52.5	55.0	57.5	60.0	62.5	65.0
-20	40.9	42.4	44.9	47.4	49.9	52.4	54.9	57.4	59.9	62.4	64.9	67.4	69.9
-15	45.9	47.4	49.9	52.4	54.9	57.4	59.9	62.4	64.9	67.4	69.9	72.4	74.9
-10	50.4	51.9	54.4	56.9	59.4	61.9	64.4	66.9	69.4	71.9	74.4	76.9	79.4
-5	53.5	55.0	57.5	60.0	62.5	65.0	67.5	70.0	72.5	75.0	77.5	80.0	82.5
0	54.7	56.2	58.7	61.2	63.7	66.2	68.7	71.2	73.7	76.2	78.7	81.2	83.7

Figure 5.2. Required charge air pressure for the Z gas exchange process with different intake valve opening timing and exhaust pressure, with the engine running at full load and.

5.3 Intake valve opening timing

Some points about intake valve opening timing should be noted first: generally, later timing performs better up to a point. As an example, brake specific fuel consumption is plotted against intake valve opening timing, swept from -100 to -20 ºaTDC, in figure 5.3.

Later intake valve opening timing allows the exhaust valve to be open longer, leaving less residual gases in the cylinder. With a constant air-fuel ratio, independent of the charge air pressure, the residual gas percentage decreases linearly with later intake valve opening timing. Like the residual gases, BSFC improves linearly with later timing until the optimum point. As the timing is delayed, cylinder efficiency increases; in addition to the decreasing residual gas percentage, compression work done by the working cylinder is decreased.

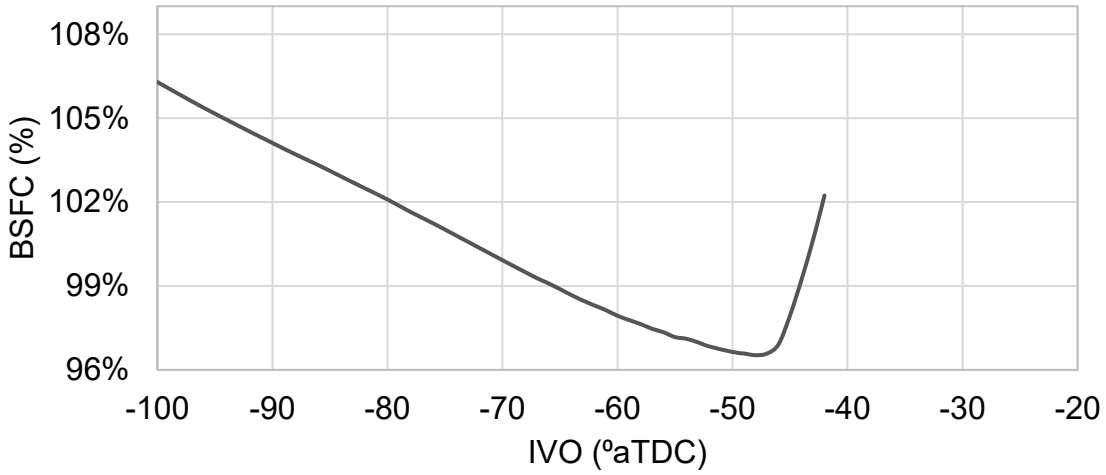

Figure 5.3. Brake specific fuel consumption with changing intake valve opening timing, with constant delta p.

The margin at the optimum BSFC point is narrow; delaying the intake valve opening timing even a few degrees from the optimum increases fuel consumption significantly. Close to the optimal point, intake valve opening duration must be increasingly longer to get the target air-fuel ratio. Some degrees after the optimal point, increasing the opening duration does not help; the engine cannot reach load and air-fuel ratio anymore. The upwards moving piston will push the charge air out of the cylinder. After this point, the cylinder volume during the intake period starts to be so small that trapping the desired air mass is impossible without increasing charge air pressure. This is demonstrated in figure 5.4.

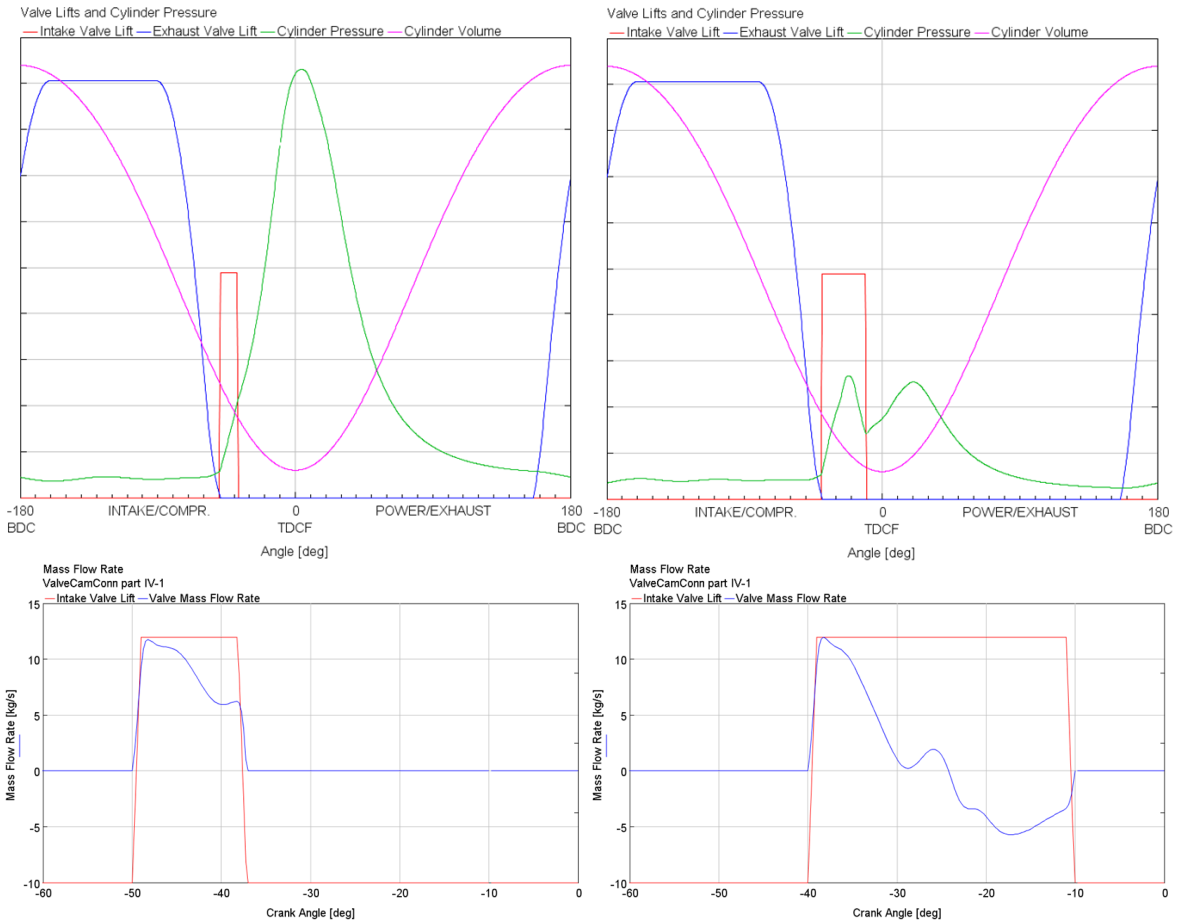

Figure 5.4. Here, data is plotted for two cases with the same charge air pressure: on the right side, intake valve opens at -40 ºaTDC, and on the left side at -50 ºaTDC. The upper plots show cylinder pressure (green), cylinder volume (pink) and intake (red) and exhaust (blue) valve lifts plotted against crank angle. The lower plots show the intake valve mass flow (blue) and intake valve lift (red) develops against crank angle.

5.4 Pressure difference over the cylinder

As seen in the analysis in chapters 5.2 and 5.3, what ultimately determines the amount of air in the cylinder is the pressure difference over the cylinder (delta p) and the intake valve opening timing. In this comparison, the intake valve opening timing was swept from -100 to -20 ºaTDC with the different delta p levels. The delta p was swept by keeping the exhaust pressure constant and sweeping the charge air pressure from 15 bar (a) to 30 bar (a).

Engine fuel consumption against the intake valve opening timing is plotted for the different delta p levels in figure 5.5. Air-fuel ratio and intake valve opening duration development with intake timing is shown in figure 5.6. The plots presented here include the points where the engine reached the target load, points where the engine does not reach load anymore were not included.

Up until a point, the gas exchange benefits from a higher delta p. The usable timing window is broader with higher delta p level. With higher delta p, obviously the intake valve can be kept open for a shorter amount of time. What can be noticed on the earlier timings is that higher delta p is worse. With a lower delta p, the intake valve must be kept open longer. Intake valve closure comes later, and the working cylinder does less compression work. If

the assumption is made that the intake valve opening duration stays constant, like in this simulation study, then a later intake valve opening timing will also move the intake valve closing timing later. A later intake valve closing will decrease the effective compression ratio of the engine. With a constant charge air pressure and exhaust pressure, this will decrease the amount of compression work done by the working cylinder.

As could be expected, the intake valve opening timing will be a compromise. Later timing increases the engine efficiency, as the compression work done by the working cylinder is decreased. As is demonstrated in this comparison, later timings cannot be achieved without increasing the delta p. In a real engine, at some point, the efficiency increase will be overtaken by the increased work required for higher charge air pressure. However, in this simulation setup the efficiency keeps increasing, because the charge air pressure production is not modelled.

From figure 5.5 the following observation can be made; brake specific fuel consumption at the optimum BSFC point is not improved after a certain point when increasing the charge air pressure. The best BSFC in this comparison comes with a charge air pressure of 22.5 bar, even though the charge air pressure was increased until 30 bar.

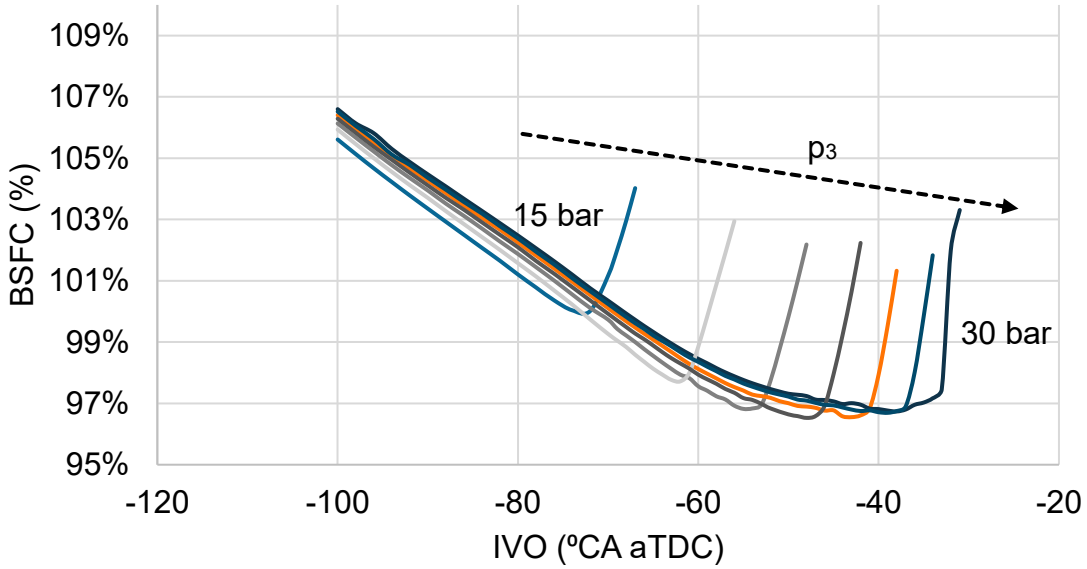

Figure 5.5. Brake specific fuel consumption with different intake valve opening timings and different charge air pressure levels.

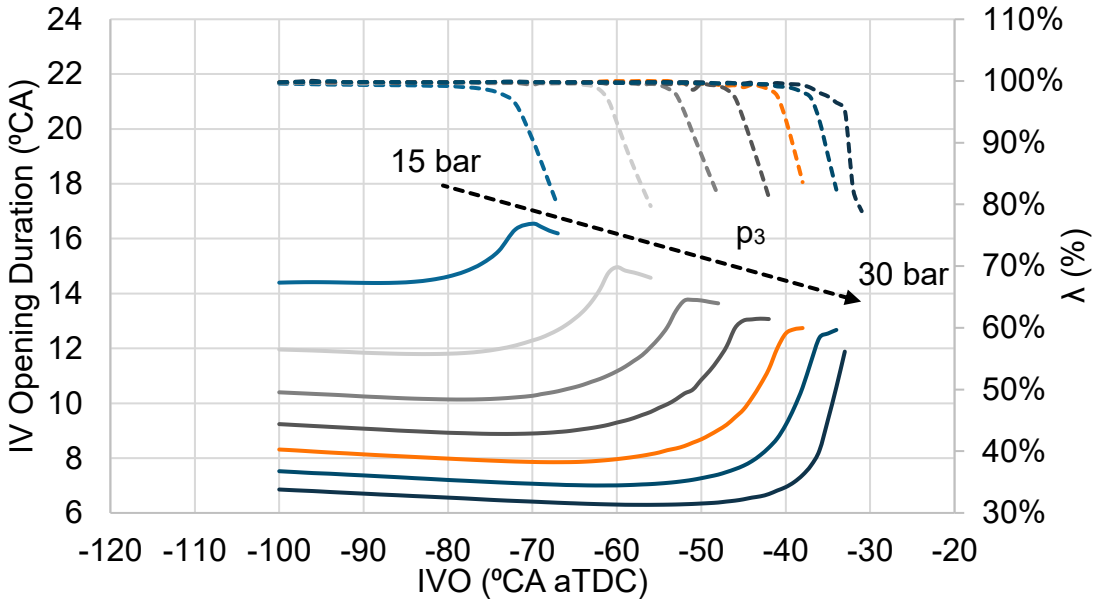

Figure 5.6. Air-fuel ratio and intake valve opening duration development in the study. Here p_3 indicates charge air pressure.

5.5 Cam lift and cam profile

The delta p comparison showed that the Z gas exchange is very sensitive to changes in air flow in the intake valves. To study the effect of the valve lift and profile, the intake valve opening timing sweep was done with different cam lift heights. In addition, the cam profiles described in 4.4.7 are compared.

The step lift profile is a theoretical, very ideal lift profile, and it was used in the first comparisons because of its adjustability. In this part, more realistic cam profiles are compared: the W20 cam, 2-stage cam, Z-cam and the Fast Z-cam. This comparison is done to see, if the Z gas exchange could even be realised with valve train actuation speeds that are used in Wärtsilä engines.

In the cam lift comparison, the step profile cam lift was reduced from the baseline 6mm to 1mm. Decreasing cam lift has the same effect as decreasing the cylinder delta p. This is demonstrated in figure 5.7. With lower lift, the available air flow inside the cylinder is limited. The optimum point shifts to an earlier timing point, and the available timing window is narrower. With a valve lift under 1.5mm, it is impossible to get the target load at any of the timing points used.

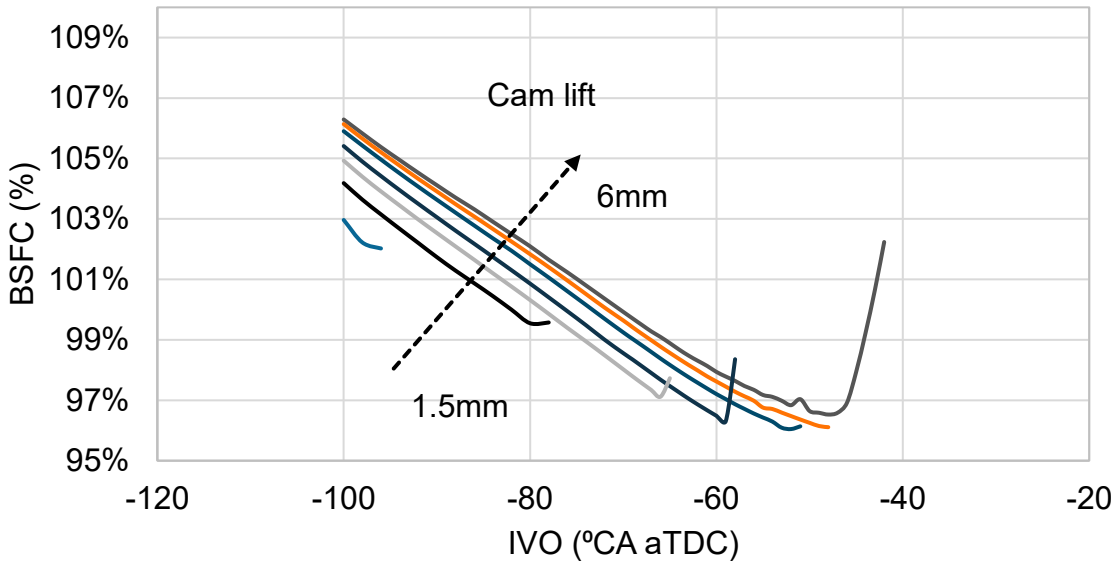

Figure 5.7. Brake specific fuel consumption against IVO timing, with different cam lift heights.

The results of the cam profile comparison can be seen in figure 5.8. As could be expected, the fastest cam profile, fast Z-cam, performed the best. After that follows the Z-cam and the 2-stage-cam. The performance of the W20-cam is very poor: only the very earliest timing points are usable. With the Z-cam, one can go as late as -60 ºaTDC with intake timing, which is still much earlier than what is possible with the step cam profile. What is interesting that the scaled down 2-stage cam does not come too much behind the Z-cam.

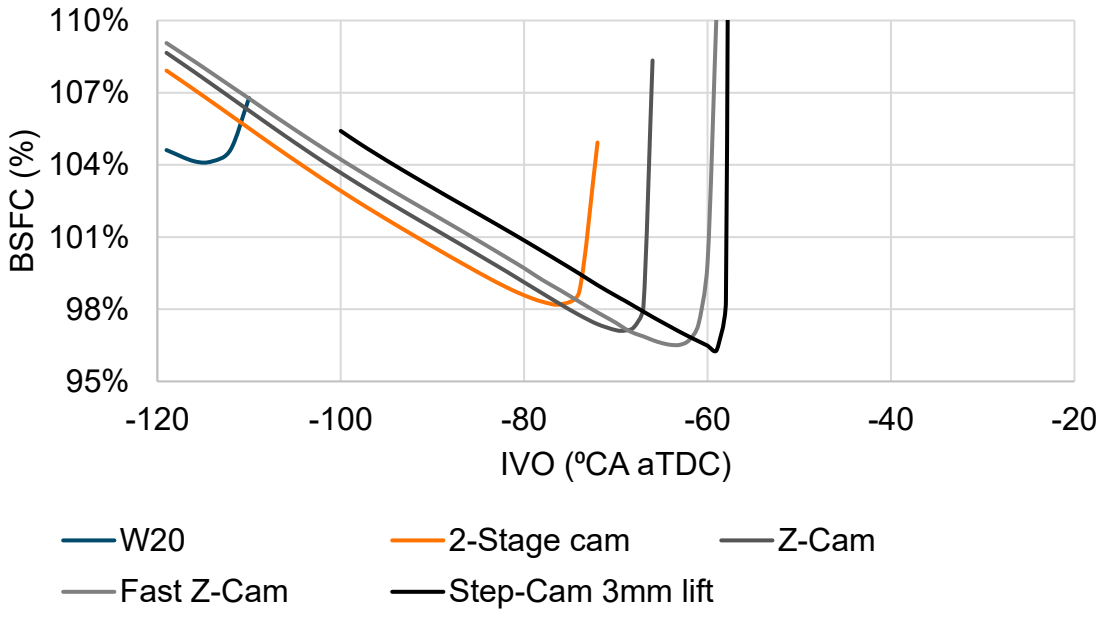

Figure 5.8. Brake specific fuel consumption in different IVO timing points with the various cam profiles. For comparison, the step-cam with 3mm cam lift is also included.

The realistic cam profiles do not perform nearly as well as the ideal step-cam profile. As the realistic cam profiles are slower to lift and come down, they take more time to get the same amount of air in as the step-cam. Therefore, intake period must be earlier to have an adequate

time for the intake period. Conventional valve train actuation speeds used in Wärtsilä engines are not even nearly enough for the Z-engine and Hoos Variants concepts. To realise the gas exchange, faster cam profiles like the 2-stage-cam and Z-cam are needed.

5.6 Intake port length and engine speed

Zenkin and Kuleshov (2014) demonstrated, that the intake port length has a big effect on the operation of the Z-engine. Their studies showed, that if one moves even 100mm from the optimum intake port length, the volumetric efficiency of the engine can be 70 % worse due to wrong phasing and length of the intake pressure pulses.

In the first comparison, the intake port length was simply swept at one operating point; the optimum BSFC point with charge air pressure of 22.5 bar (a), from chapter 5.4 was chosen. The valve timing and duration were set constant, and the air-fuel ratio control was turned off. The intake port length was swept from 20mm to 2000mm in roughly 2mm steps to get a good accuracy. The results from the sweeps look almost identical to the results of Zenkin and Kuleshov (2014). The volumetric efficiency of the engine is best with very short intake ports (20—210mm). Volumetric efficiency goes quickly worse with longer port lengths. Figure 5.9 shows the development of volumetric efficiency in the operating point used in this sweep.

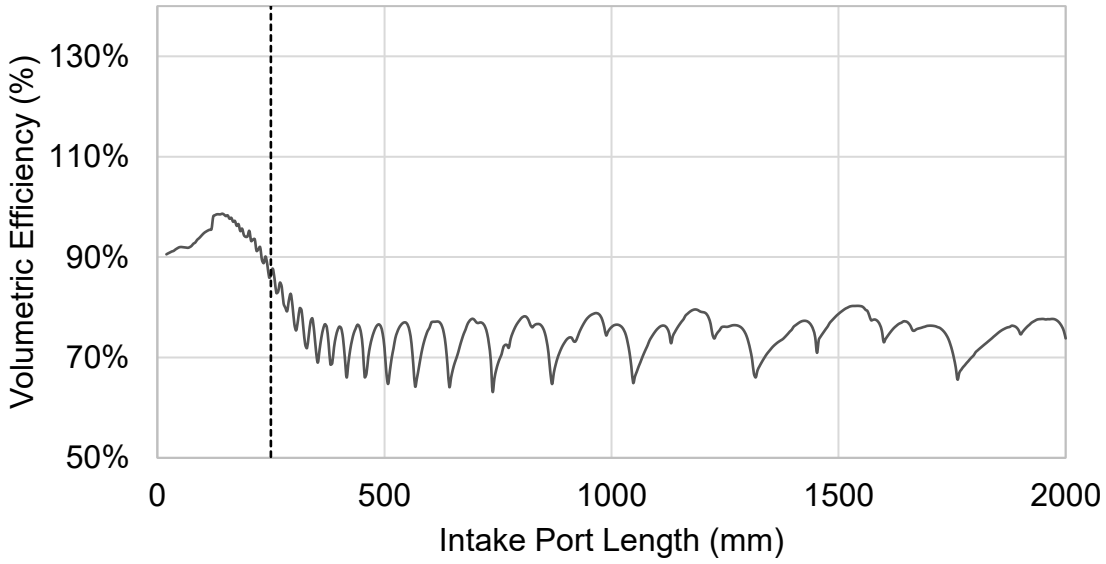

Figure 5.9. The volumetric efficiency with different intake port lengths in the optimum operating point of 22.5 bar (a) charge air pressure. The sectioned line represents the baseline intake port length that was used in the previous simulations.

If one goes 100 mm longer from the optimum point, the difference is drastic: the engine reaches the desired load, but the relative air-fuel ratio is at worst 20 % lower. The wave-like pattern how the volumetric efficiency develops is worth noting: with the longer port lengths, a difference of few centimetres in intake port length can mean a 10 % decrease in air-fuel ratio and a 20 g/kWh increase in fuel consumption.

With short intake port length, the intake pulse frequency is so high, that during the intake period, two or more intake pulses reach the valve. When the first intake pulse starts to decrease, shortly after a second one comes and pushes more air inside the cylinder. After the

optimum point, the intake pulse length starts to increase so that only one pulse can be used during the intake period. After that, the most important factor is the phase of the intake pulse. Changing the intake port length changes the phase at which the intake pressure pulse is when the intake valve is opened. Therefore, volumetric efficiency develops in this wave-pattern.

In the subsequent intake port length sweeps, the swept port length sweep range was narrowed down. The minimum port length was chosen as the practical minimum intake port length on the W20. With this intake port length, the charge air receiver would be directly attached to the cylinder head. With this limitation, the optimum point in figure 5.9 is not usable, as it comes at a port length shorter that would be practically possible. Maximum port length was chosen as an even length, after which no considerable improvement can be seen.

In the next comparison, the intake port length was optimized for the different timing points with the 22.5 bar (a) charge air pressure case. This means, that the intake port length was swept separately in each intake valve opening timing point. Therefore, at each timing point, the optimum intake port length is slightly different. Figure 5.10 shows the effect of the intake port length optimization on brake specific fuel consumption.

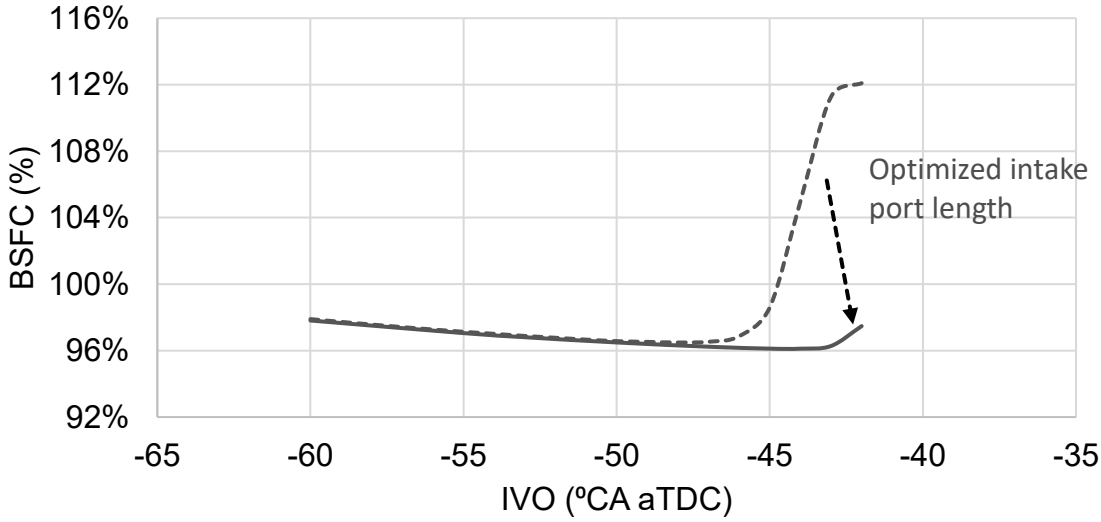

Figure 5.10. The effect of optimizing the intake port length to brake specific fuel consumption in different timing points.

The result of the optimization is clear. Optimizing the intake port length allows to move the optimum point, in this case from -48 ºCA aTDC to -43 ºCA aTDC. The fuel consumption was improved from the previous optimum point by 0.8 g/kWh, and residual gas amount dropped by 1.2%. Most importantly, optimizing the intake port gave an additional 5 ºCA margin in the intake valve opening timing.

Figure 5.11 shows brake specific fuel consumption with different intake port lengths, for the various intake valve opening timing points. The plots are cut from a point where air-fuel ratio and load targets are no longer reached. When intake valve opening timing is delayed, the engine becomes more and more sensitive to intake port length. With the earliest timing -60 ºCA, the BSFC level is higher, but stays steady with a wide window of intake port lengths. Air-fuel ratio and load can be kept throughout the whole intake port range. As intake valve opening timing is delayed, the usable window is narrower, even though the fuel consumption at the best point gets better.

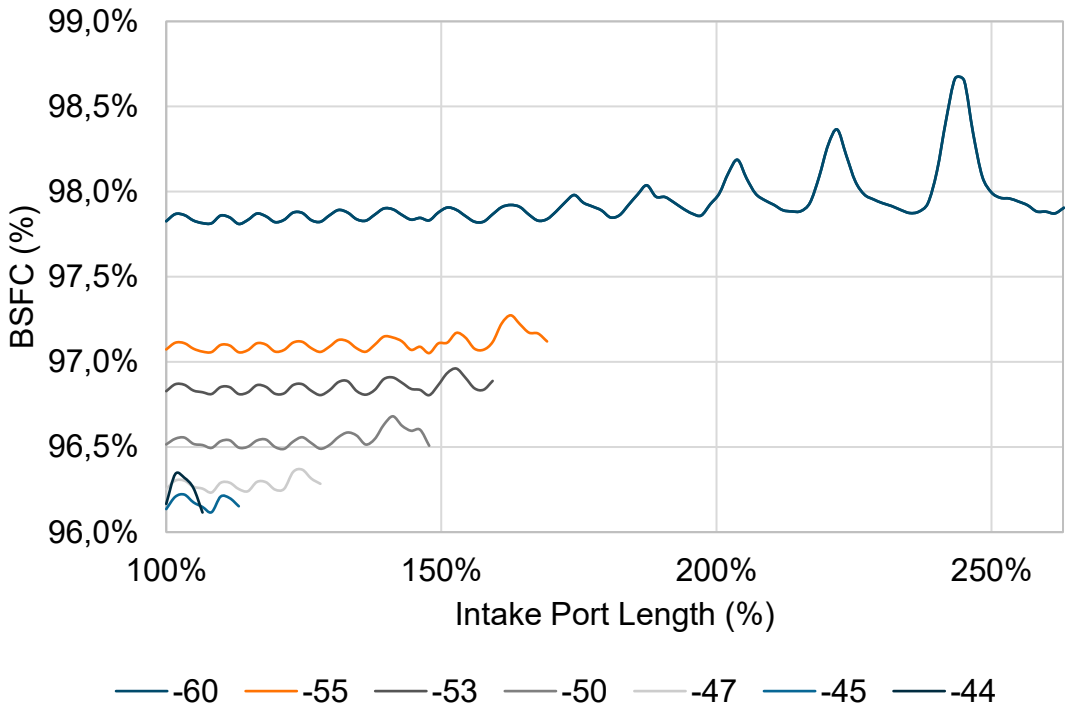

Figure 5.11. Fuel consumption in different timing points against intake port length. Only the points where air-fuel ratio is constant are showed.

Since the intake pressure pulses have such a significant effect, there is a need to test how the engine reacts to changing operating speed as well. If intake valve opening duration is kept constant (in degrees), increasing engine speed will decrease the time to get air in, and vice versa. It will also have an effect to the intake pressure pulses as the frequency at which intake valve is opened cycle-to-cycle changes. A simple sweep was made: the engine speed was swept ±10% around the baseline 1000 r/min. The comparison was done with a constant BMEP to have roughly the same fuel amount in the cylinder. Air-fuel ratio will not be constant: for this sweep's purposes the cost for charge air comparison can be ignored. This sweep is done to see, how engine speed changes air intake and the intake pulses. For comparison, the same sweep was made with the W20 model.

Brake specific fuel consumption with changing engine speed are shown in figure 5.12. As can be expected, trapped air mass increases and fuel consumption decreases with decreasing engine speed. The general trend is noticeably stronger in the Z gas exchange compared to the W20. With the Z gas exchange, a wave pattern can be noticed in the brake specific fuel consumption like in the intake port length sweeps. Engine speed changes the intake pulse phasing which is why at some points more air is trapped regardless of a higher engine speed, and vice versa. Therefore, the concepts are more sensitive to engine speed than the W20. This is because they are so sensitive to the frequency and phasing of intake pressure pulses.

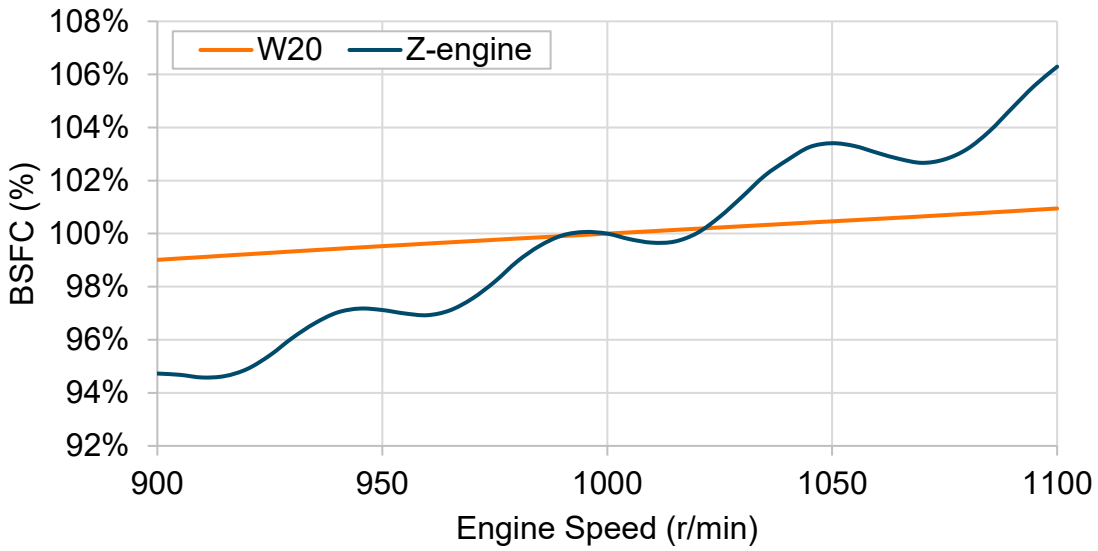

Figure 5.12. Brake specific fuel consumption with changing engine speed.

5.7 Summary of the sensitivity analysis

One of the objectives of this thesis was to study the sensitivity of the engine concepts to different operating and design parameters. In this sensitivity analysis the effect of parameters such as intake valve opening timing, delta p, intake cam lift and profile, intake port length and engine speed was studied.

With the Z gas exchange, the best intake valve opening timing is the latest possible one. Later intake valve opening timing decreases the residual gas percentage in the cylinder. Later intake valve opening timing is however a compromise; the later the intake period is, the higher delta p is required. With a constant exhaust pressure, charge air pressure must be growingly increased to trap the required amount of air for combustion in the cylinder. With a constant delta p, the optimum intake period timing comes at the limit; even at a couple degrees later timing the engine does not work.

The most efficient external compression engine gas exchange would have an instant intake period at top dead centre. With this kind of timing, both the exhaust and expansion strokes would be complete, and residual gas percent would be near zero. This means that at a relatively low air-fuel ratio, a delta p of over 30 bar would be required. If air-fuel ratio is to be increased by 70% to levels more corresponding with medium-speed engines, the delta p required increases to roughly 50 bar.

Intake valve lift and profile have a similar effect to the gas exchange as delta p. For the Z gas exchange, the fastest cam profile possible is the best; the fastest profile here means the profile which produces the highest valve lift in the shortest amount of time. A faster cam lift profile enables to use a later intake period timing. However, if the delta p over the cylinder is not enough, even the most aggressive cam profile does not help. Comparison between the different cam profiles showed, that cam actuation speeds used in Wärtsilä engines are not enough for the Z gas exchange. Faster profiles like the Z-cam cam are required. This finding is related to the third research question of this thesis: can the concepts be realised with existing Wärtsilä solutions (chapter 1.3)? It seems that if the intake cam lift profiles are considered, then it is not possible.

The intake period is so short in the Z gas exchange that the intake pressure pulse phasing and frequency have a significant effect to the flow through the intake valves, therefore changing the intake port length has a considerable effect. A very short intake port length, was seen to be the optimum. The optimum intake port length is so small, that in a W20-size engine, the charge air receiver would have to be almost directly attached to the cylinder head. With a short intake port length, two pressure pulses can be used during the intake period, and phasing is less significant. With a long port, the intake pulse phasing becomes more significant. With a considerably longer intake port length, the intake pressure pulse is too long to trap the required amount of air in the cylinder. The gas exchange is sensitive to the intake port length only at later intake valve opening timings, however if the intake port length is not in the right ballpark, the engine does not reach the desired load. The gas exchange was found to be more sensitive to engine speed variation than the W20 for the same reason.

Optimizing the intake port length around the optimum timing point gave an additional 6 ºCA of intake timing margin, and a slight improvement in brake specific fuel consumption. Optimized intake port length is a requirement to operate the engine at the latest possible IV timing.

The Z gas exchange is indeed quite sensitive to changes in engine operating parameters, such as charge air pressure, intake valve opening timing, intake port length and engine speed. This study provided useful insight for the optimization of the full concept models, which will be described in the next chapter.

6 Concepts optimization

To have as fair as possible a comparison with the W20, the concepts are optimized to the best extent that is possible in the scope of this thesis. This chapter describes the method and results of the concepts' optimization.

6.1 Introduction

The simulations presented in this chapter are done with the simplified full (multi-cylinder) engine models, described in chapter 4.3. The lessons learned in the sensitivity analysis (chapter 5) are applied here in simulations, where also the charge air production is modelled. Therefore, the effect of the turbochargers and the piston compressor on the Z-engine is considered. For the Z-engine, a suitable balance between the turbocharger and the piston compressor was determined. For the Hoos Variant engine, a suitable turbine area for the turbochargers was determined.

The optimization was done using the Design of Experiment function in GT-Power. This allows to make a matrix sweep of various parameters. For the Z-engine, the parameters in the matrix include intake valve opening timing and duration, piston compressor input power and turbocharger turbine flow area. For the Hoos Variant engine, the matrix includes intake valve opening timing and duration, and the turbine area of the first stage turbine (Turbine 4). A matrix with wide window of parameters and low accuracy is run first to see the approximate best area of fuel consumption. After that more accurate matrix can be run.

After finding an optimum BSFC point for the concepts in the first matrices with the parameters, the intake port length is varied in this operating point to optimize the effect of the intake pressure pulse phasing and length, like in chapter 5.6.

It is interesting to find out, what the relative air-fuel ratio at the optimum BSFC point for the concepts will be, as well as the maximum achievable air-fuel ratio. The relative air-fuel ratio λ is an important design point, since it is mostly a compromise between smoke or soot emissions, which form in rich air-fuel ratios and nitrogen oxides, which form in lean air-fuel ratios (Mollenhauer and Tschöke 2010, p. 69). According to Mollenhauer and Tschöke (2010, p. 17), medium-speed four-stroke engines run commonly at λ=2.2. Based on the results of the optimization the concepts cannot reach this air-fuel ratio at all.

To increase air-fuel ratio, charge air pressure must be increased, by decreasing the turbine area or increasing the input power to the piston compressor. Higher air-fuel ratio is also easier to achieve with earlier valve timing and a longer intake period. However, with the Z-engine and the Hoos Variant, this usually results to the maximum cylinder pressure increasing unreasonably; this phenomena is explained later in the chapter.

Maximum cylinder pressure is another important design feature of the medium-speed engines. Maximum cylinder pressure in medium-speed engines range around 200 bar (Mollenhauer and Tschöke 2010, p. 581—582.). Increasing the maximum pressure means that the engine must be built sturdier, therefore it was not sensible to choose an optimum point where the maximum cylinder pressure is considerably over 200 bar. According to this optimization, the concepts run best with maximum cylinder pressures well below 200 bar.

6.2 Hoos Variant turbine flow area

In the beginning of the Hoos Variant optimizations, the biggest question mark was, how to optimize the four-stage turbocharger. The turbine area on each turbine was to be tuned so that each compressor has the same pressure ratio. This can be explained with the theory described in chapter 2.1. In an unbalanced four-stage system, one compression stage might have a temperature rise and a pressure ratio much higher than the other stages. This stage will do most of the compression work, the others doing only a small part, and move the compression process of the whole system towards one-stage compression. Controllers were implemented so that the pressure ratio of each compression stage would be the same. As the turbine area of rest of the turbines is imposed based on the one in the first turbine, the flow area of the first turbine was used as a tuning parameter. When referring to the turbine area in this chapter (6.2), specifically the Turbine 4 (described in chapter 4.3) area is referred to.

Figure 6.1 shows how brake specific fuel consumption develops in one of the optimization matrices with different turbine flow area of the first turbine (Turbine 4) and intake valve opening timing, the intake valve duration remaining constant. The following figures (6.2 and 6.3) and the figures in appendix 2 present the rest of the results of this optimization matrix.

The optimum BSFC point is a compromise of friction losses and indicated efficiency. The best indicated efficiency comes with a small turbine area and an early valve timing. This produces a high peak cylinder pressure and high friction losses. The optimum BSFC point comes at a somewhat later valve timing and larger turbine area, where friction losses do not overcome the advantage in indicated efficiency. In the optimization matrix presented here, BSFC is best at IVO timing of -68.6 ºCA aTDC. However, BSFC stays within 1 g/kWh in a relatively large IVO timing window (from -77 to -57 ºCA aTDC).

The Hoos Variant is not overly sensitive to the turbine area. Fuel consumption is within 1 g/kWh within a wide window of turbine area (80—115 %). Within this window, maximum cylinder pressure changes by roughly 60 bar, which is a big difference. The relative air-fuel ratio changes between 1.2—1.4. Regardless of the IVO timing, best BSFC is achieved with a turbine area of 32.2 cm^2.

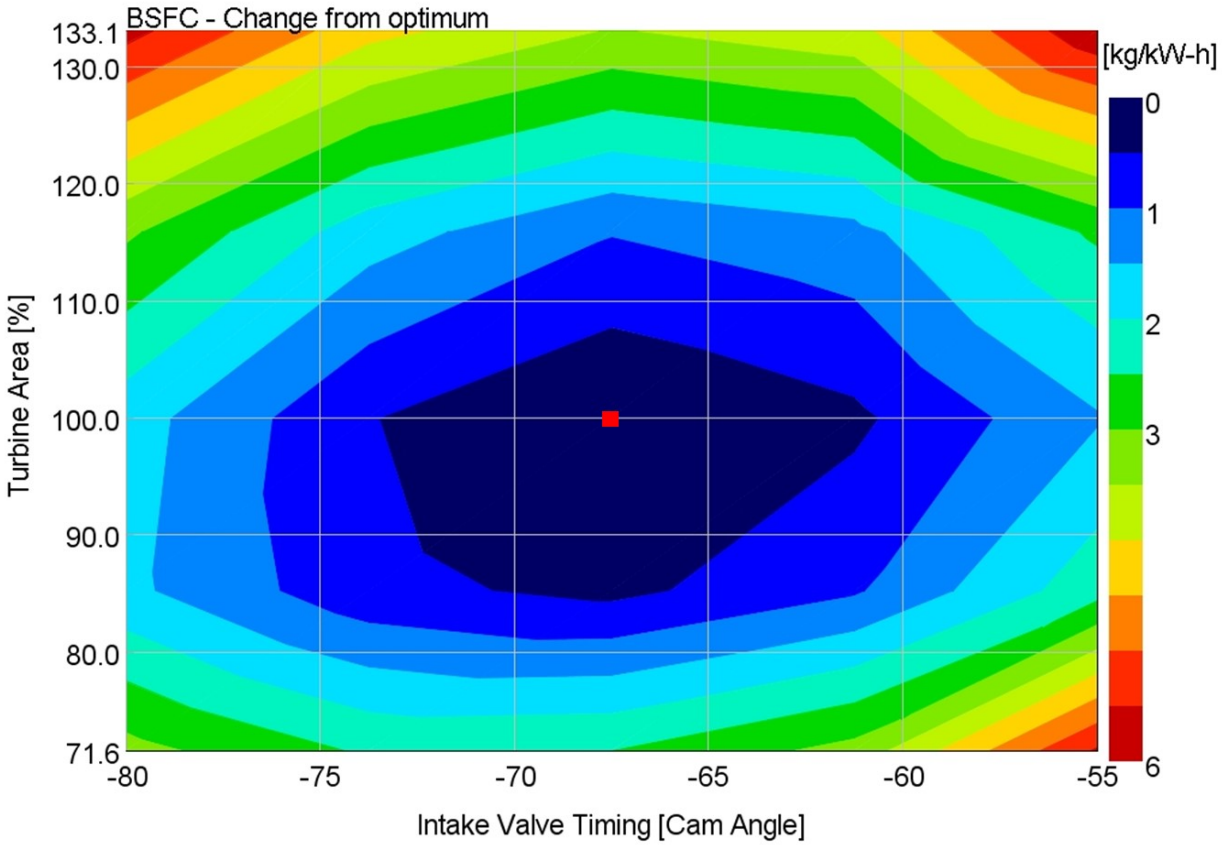

Figure 6.1. Brake specific fuel consumption development in one of the Hoos Variant optimization matrices. The turbine area of the turbine 4 in percentage is the vertical axis, and IVO timing on the horizontal axis. The optimum point is highlighted in red.

Figure 6.2 shows how air-fuel ratio develops in the optimization matrix. By decreasing the turbine area by 60 %, air-fuel ratio can be increased by roughly 40%. Advancing valve timing from -55ºCA to -80ºCA has less effect on air-fuel ratio, resulting in an additional 20% increase. The turbine area is more dominant here.

The exhaust pressure is mainly dependent on the turbine area. A smaller turbine area produces a higher exhaust pressure and charge air pressure, which increases the air-fuel ratio as well. However, charge air pressure and air-fuel ratio are dependent also on the intake valve opening timing. With earlier intake valve opening timing, the air-fuel ratio is higher since the cylinder volume is larger (more air can be trapped). Higher air-fuel ratio means that the air mass flow rate through the engine is increased. The work done by the turbines and compressors stays constant regardless of the intake valve opening timing. This means that when the mass flow rate through the compressors increases, with a constant work produced by the turbines, the total pressure ratio of the compressors decrease, resulting in a lower charge air pressure.

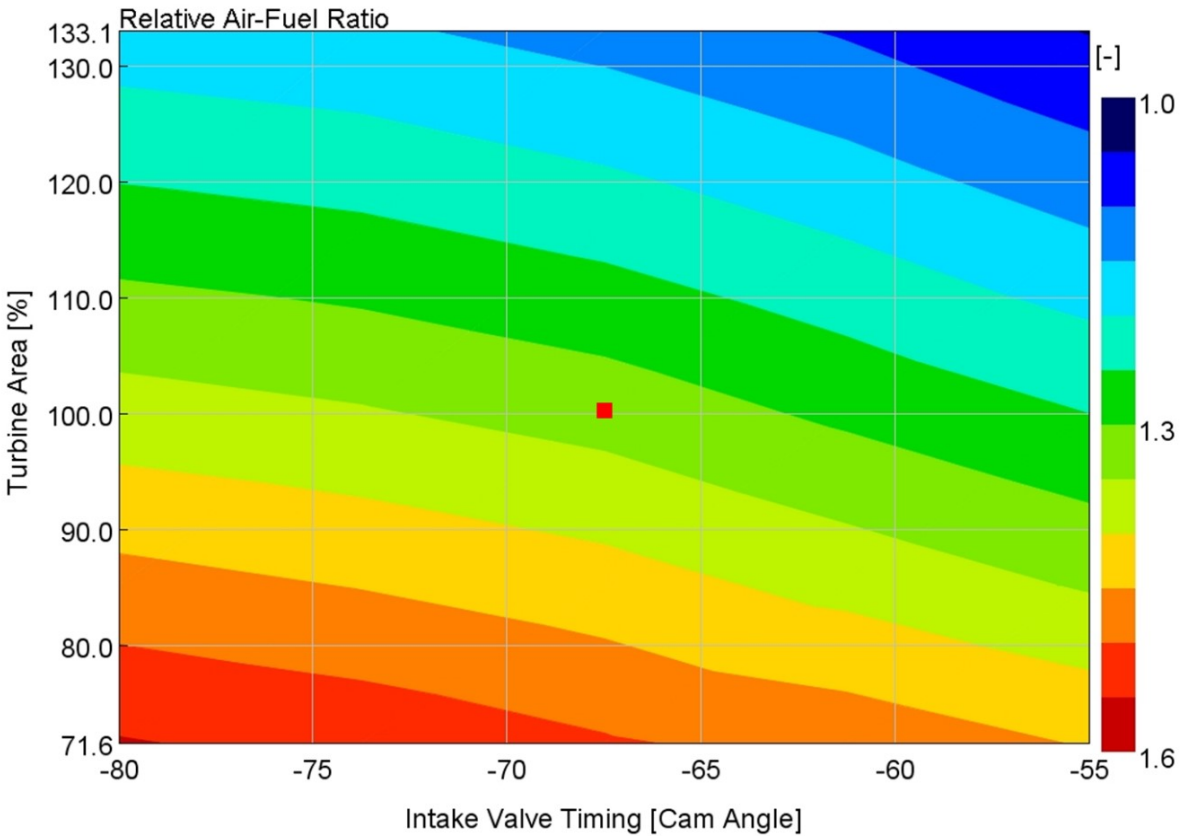

Figure 6.2. Air-fuel ratio development in the Hoos Variant engine optimization matrix. The optimum BSFC point is highlighted in red.

What is interesting is that residual gas percent in the cylinder increases along with increasing air-fuel ratio and engine air flow rate. Without the increase in residual gas percent, air-fuel ratio would increase even more. With the latest valve timing and largest turbine area, residual gas percent is roughly 30%, however with the most extreme parameters it increases to 55%. In this matrix, exhaust pressure is only dependent on the turbine area, while intake valve opening timing has also an effect to the residual gas percent.

Figure 6.3 shows how maximum cylinder pressure develops in the optimization run. Maximum cylinder pressure develops in the same way as the air-fuel ratio. Valve timing and turbine area have a significant effect to the maximum cylinder pressure, intake valve opening timing being more dominant. In this run, the variance in maximum cylinder pressure is wide; moving to the most aggressive parameters from the optimum increases maximum pressure by 100 bar. Intake valve opening timing is more dominant in affecting the maximum cylinder pressure; advancing timing from the latest to the earliest point increases maximum pressure by almost 100 bar. Due to the friction model used in the model, friction losses increase in the same pattern as maximum pressure.

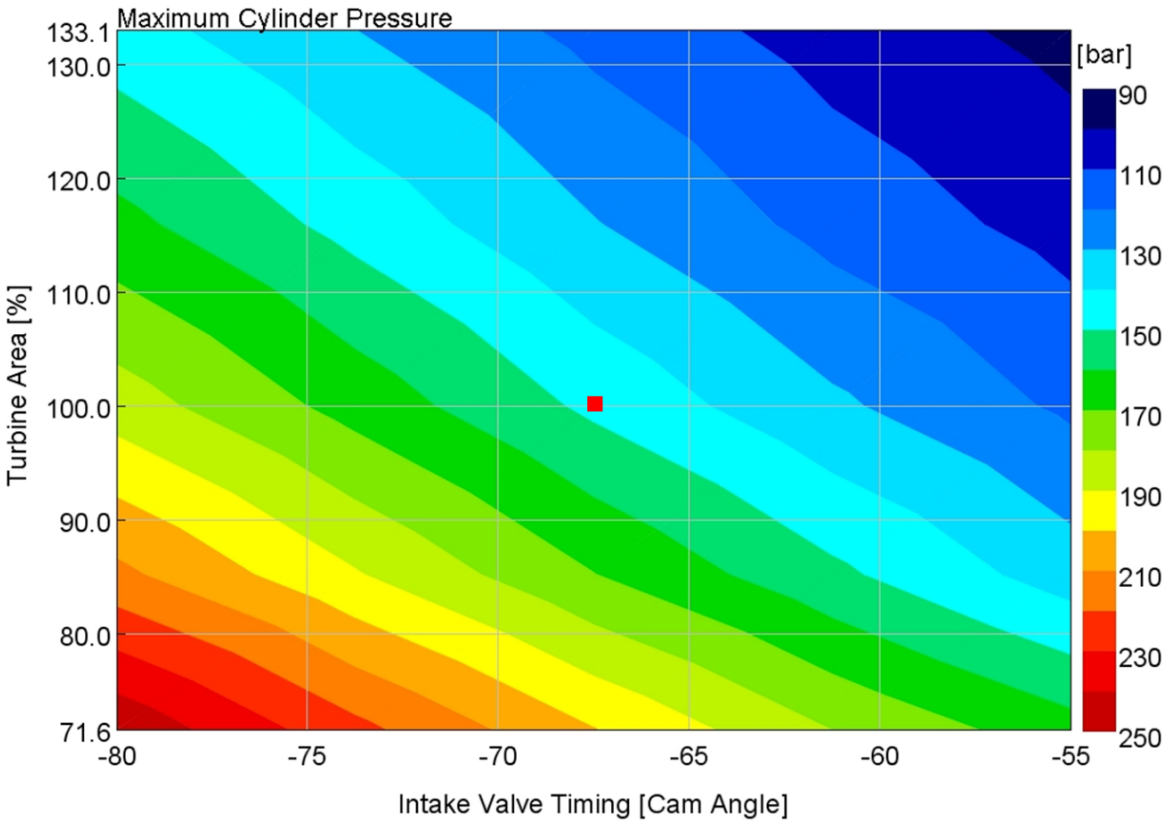

Figure 6.3. Variance in maximum cylinder pressure with different IVO timing and turbine area in the Hoos Variant engine. The optimum BSFC point is highlighted in red.

The optimum IVO timing point (-68.6 ºCA aTDC, 32.2 cm^2) was optimized further in terms of intake port length. This further optimized point was chosen to be used in the final comparisons presented in chapter 7. In the optimum BSFC point, air-fuel ratio and maximum cylinder pressure are far less than generally in medium-speed engines. Average residual gas percentage in the cylinders is 43%.

6.3 Z-engine compressor balance

The Z-engine optimization was more work intensive, as in addition to the intake valve opening timing and intake period length, the balance between the input power to the piston compressor and the turbine area was to be determined. The optimized point found for the Z-engine differs somewhat from the one found for the Hoos Variant engine, which is due to the different charge air production method.

Figure 6.4 shows brake specific fuel consumption in one of the Z-engine optimization matrices. The following figures 6.5 and 6.6, and the figures in appendix 3 present the rest of the results of this optimization matrix. At the best point, BSFC is roughly 10 g/kWh higher than in the Hoos Variant engine. The best fuel consumption comes with a turbine area of 49 cm^2, which is considerably (~50%) larger than in the Hoos Variant, and compressor input power of 150 kW. However, the engine is not sensitive at all to the turbine area and compressor input power: fuel consumption stays within 1 g/kWh in a very wide range (±25% turbine area, 100—220kW PC input power).

With the optimum combination, most of the charge air pressure is produced by the turbocharger rather than the piston compressor. At the optimum point of figure 6.4, the pressure ratio of the turbocharger is 7.5 and the piston compressor is 1.9. This is an interesting result, since it is an opposite result than what is suggested for the concept; the developer of the Z-engine suggests that the piston compressor would do most of the charge air production on the engine, the turbocharger acting merely as a helper compressor. However, in the latest simulations of the concept, the pressure ratios of the turbocharger and the piston compressor were roughly the same (Kuleshov et al. 2015).

It should be noted, that the maximum pressure ratio achievable with a one-stage turbocharger is roughly 6, albeit with a considerably lowered efficiency. To reach pressure ratios of 6 and beyond, like in the optimized point, at least a two-stage turbocharger setup is required. The line after which pressure ratio of the turbocharger compressor is over 6, is displayed in figure 6.4 in red. (Mollenhauer and Tschöke 2010, p. 52.)

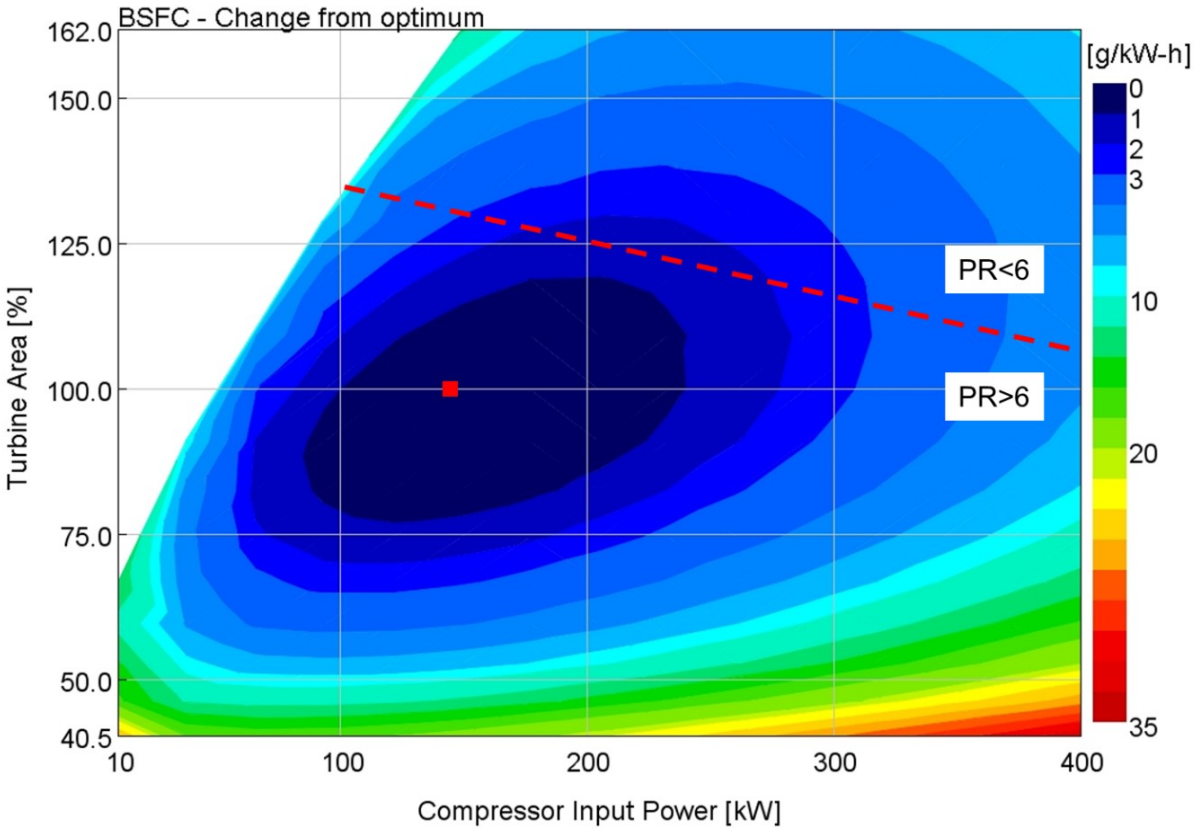

Figure 6.4. Brake specific fuel consumption in the Z-engine optimization matrix. Fuel consumption is presented as an increase over the optimum. The optimum BSFC point is highlighted with red. The vertical axis is the turbocharger turbine flow area in percentage, and the horizontal axis the piston compressor input power. The red line indicates the boundary after which the pressure ratio (PR) of the turbocharger compressor increases above 6.

The correlations for maximum cylinder pressure and air fuel ratio are the same as found with the Hoos Variant engine. Figures 6.5 and 6.6 show how air-fuel ratio and maximum cylinder pressure develop in the Z-engine. It is easier to increase the air-fuel ratio in the Z-engine since it can be done by simply increasing the input power to the piston compressor, which does not increase the exhaust pressure. This increases the engine fuel consumption but

increases charge air production so that air-fuel ratio can be increased up to 1.95, which is as considerably higher level than what is possible with the Hoos Variant engine. Decreasing the turbine area is less effective in increasing air-fuel ratio.

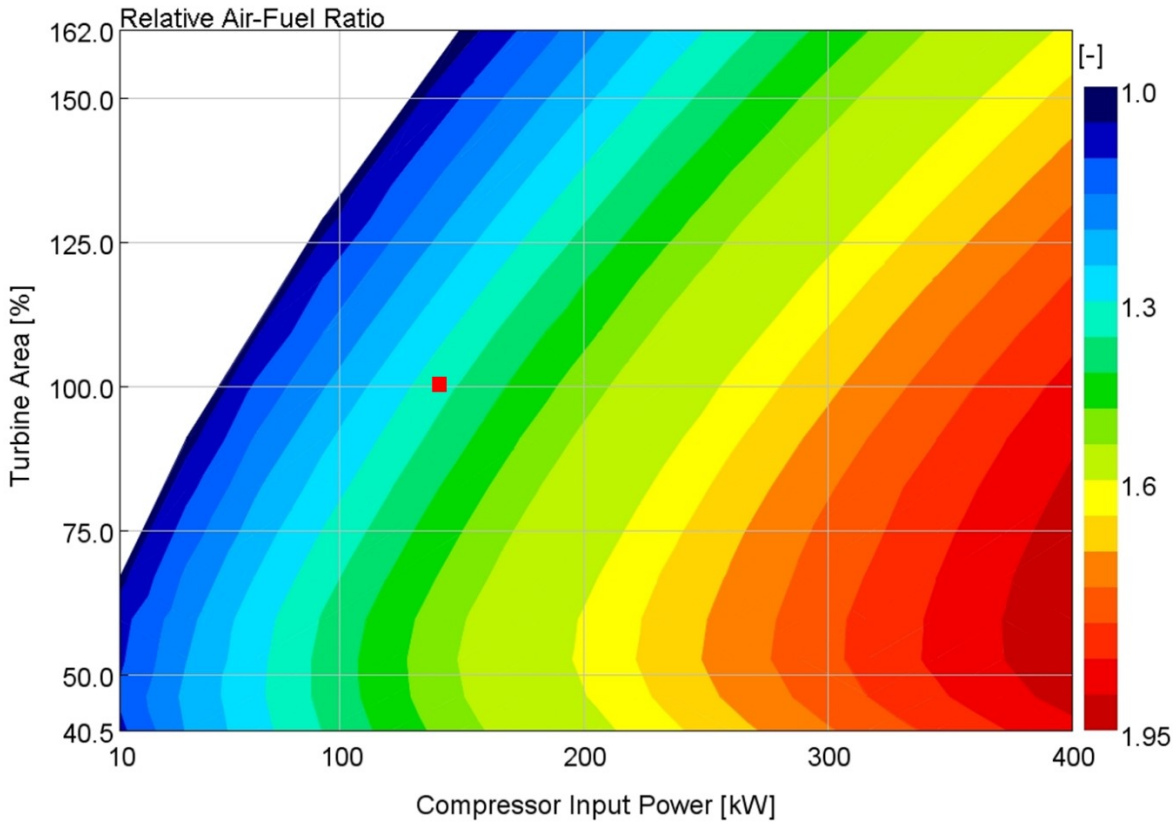

Figure 6.5. Air-fuel ratio development on the Z-engine. The optimum BSFC point is highlighted with red.

On the Z-engine, the cylinder maximum pressure "runs away" when the turbine area is too small, and the piston compressor input power is too high. Maximum cylinder pressure increases by 255 bar from the optimum with the most aggressive parameters. It is not sensible to run the engine in this area.

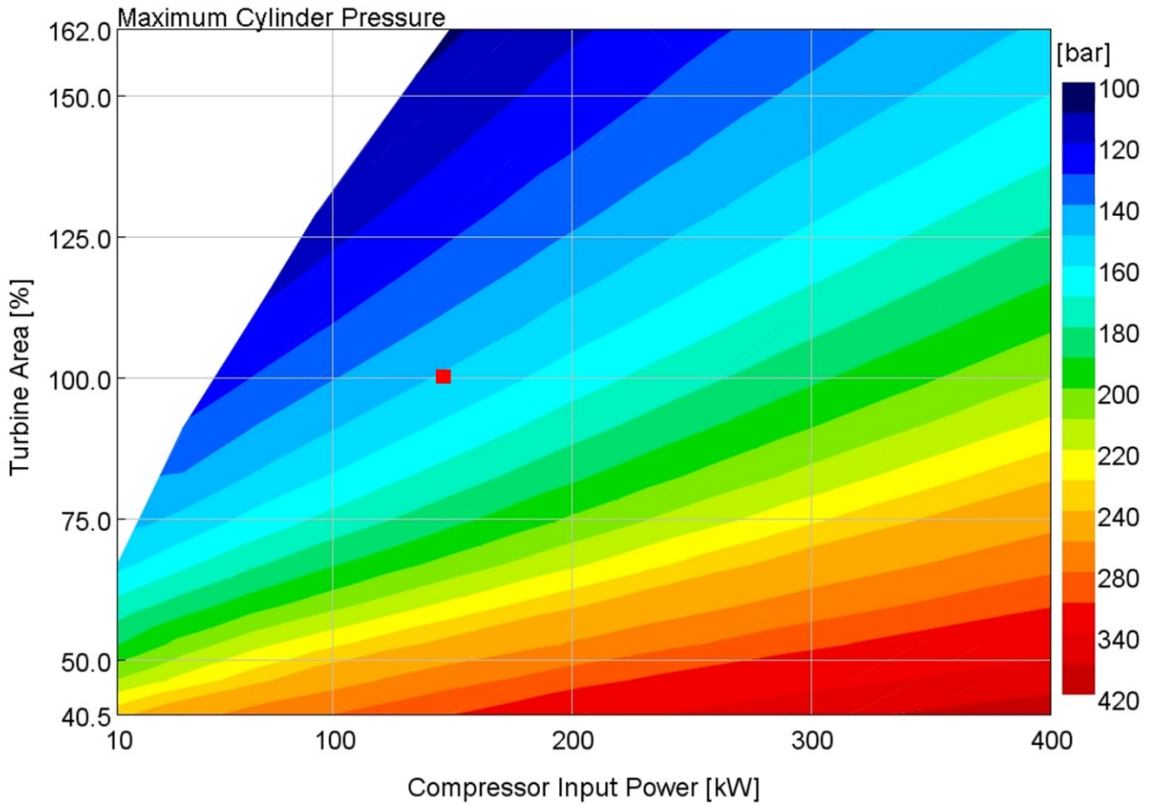

Figure 6.6. Maximum pressure on the Z-engine. The optimum BSFC point is highlighted with red.

Like with the Hoos Variant engine, the kind of compressor-turbocharger balance shown figures 6.4—6.6 work for a range of IVO timing points. Due to time constraints, it was not possible to find as accurate optimum timing point for the Z-engine as for the Hoos Variant. However, like in the Hoos Variant, IVO timing has no considerable effect to BSFC, if the balance between the piston compressor and the turbocharger is correct. BSFC seems to be best at the IVO timing point of -80ºCA aTDC, which is a much earlier timing point than on the Hoos Variant engine. Like with the Hoos Variant, this point was optimized further in terms of intake port length.

The optimum point is similar with the Hoos Variant engine: it comes with a similar air-fuel ratio and maximum pressure. Residual gas percent is lower than on the Hoos Variant optimum point, 39%, even though a much earlier valve timing is used. In the Z-engine, the turbine area is much larger due to the piston compressor helping with the charge air production. The differences between the optimum points are described more in chapter 7.

6.4 Increasing the air-fuel ratio

The biggest question when optimizing the concepts was: why is it impossible to increase the air-fuel ratio on the concepts? It is partly the cause of the Z gas exchange cycle, and a part of the reason are thermodynamics. The first thought is that the air fuel ratio could be increased by simply increasing the charge air pressure: in the Hoos Variant engine, by decreasing the turbine area and in the Z-engine by increasing the input power to the piston compressor. To study the reasons behind this, some simple parameter sweeps were made on the concepts. On the Hoos Variant, the turbine 4 area was decreased until the engine no longer works. On the Z-engine, the piston compressor input power was varied.

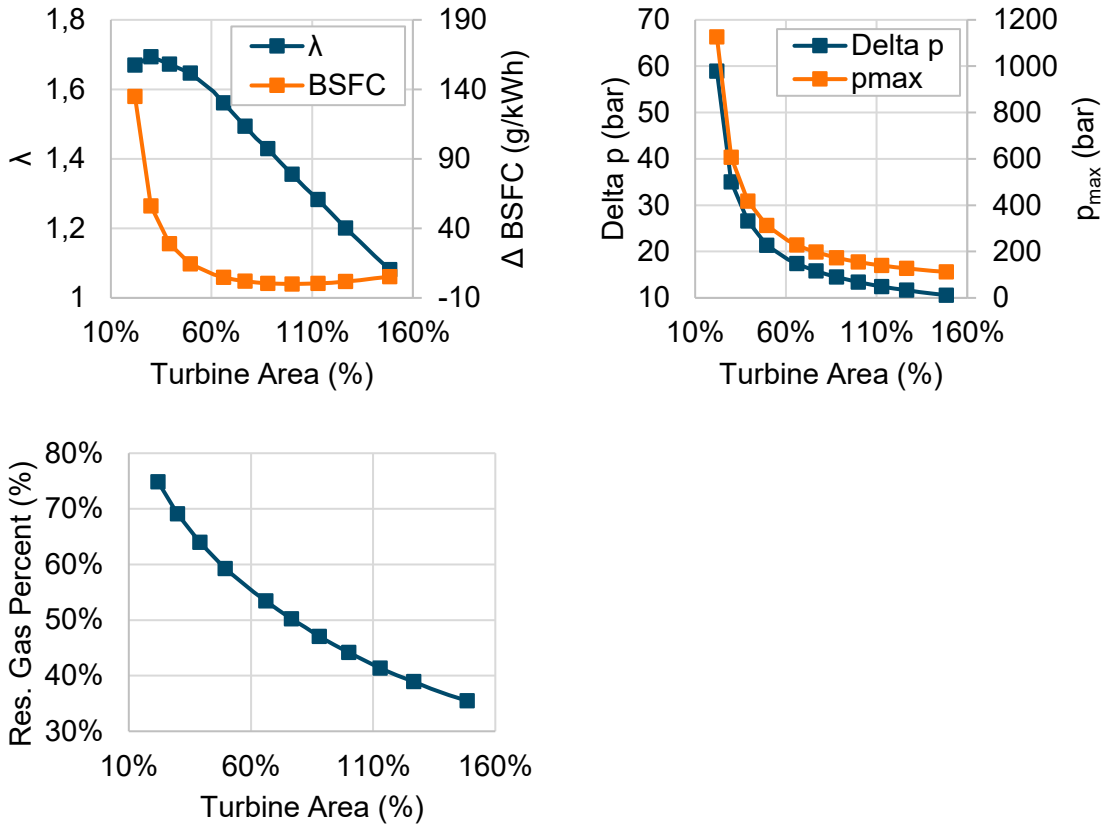

Figure 6.7. Results of the turbine area variation of the Hoos Variant, turbine 4 area as the horizontal axis in percentage.

The results of the Hoos Variant engine turbine area variation are presented in figure 6.7. The relative air-fuel ratio can indeed be increased up to 1.7, when the turbine area is decreased. This increases the delta p over the cylinder considerably. With a turbine area smaller than 20% of the baseline, the engine does not work anymore, since the restriction is too much. Coming close to the lower limit of the turbine area, maximum cylinder pressure rises unreasonably; more and more fuel must be injected to overcome the resistance of the exhaust pressure. At the smallest operable turbine area, 20% of the baseline, the charge air pressure is 105 bar (a) and the exhaust pressure 43 bar (a). Increasing the charge air pressure and delta p is therefore not a problem.

Even though charge air pressure is increased, also the exhaust pressure increases. With the smallest operable turbine area, 75% of the cylinder mass at start of combustion are residual gases. If the turbine area is decreased from this minimum area, the exhaust pressure becomes too high so that the exhaust stroke does not work anymore. With such a small turbine area, exhaust gas starts to flow back into the cylinder at the end of the exhaust stroke.

It is easier to increase air-fuel ratio on the Z-engine, where the input power of the piston compressor can simply be increased. Rather than restricting the exhaust flow, more fuel is simply injected to produce the extra work required by the compressor. The best brake specific fuel consumption on the Z-engine comes with a quite low compressor input power, whereas the indicated fuel consumption keeps on improving with a higher compressor power. Figure 6.8 shows the results of the compressor power variation done on the Z-engine.

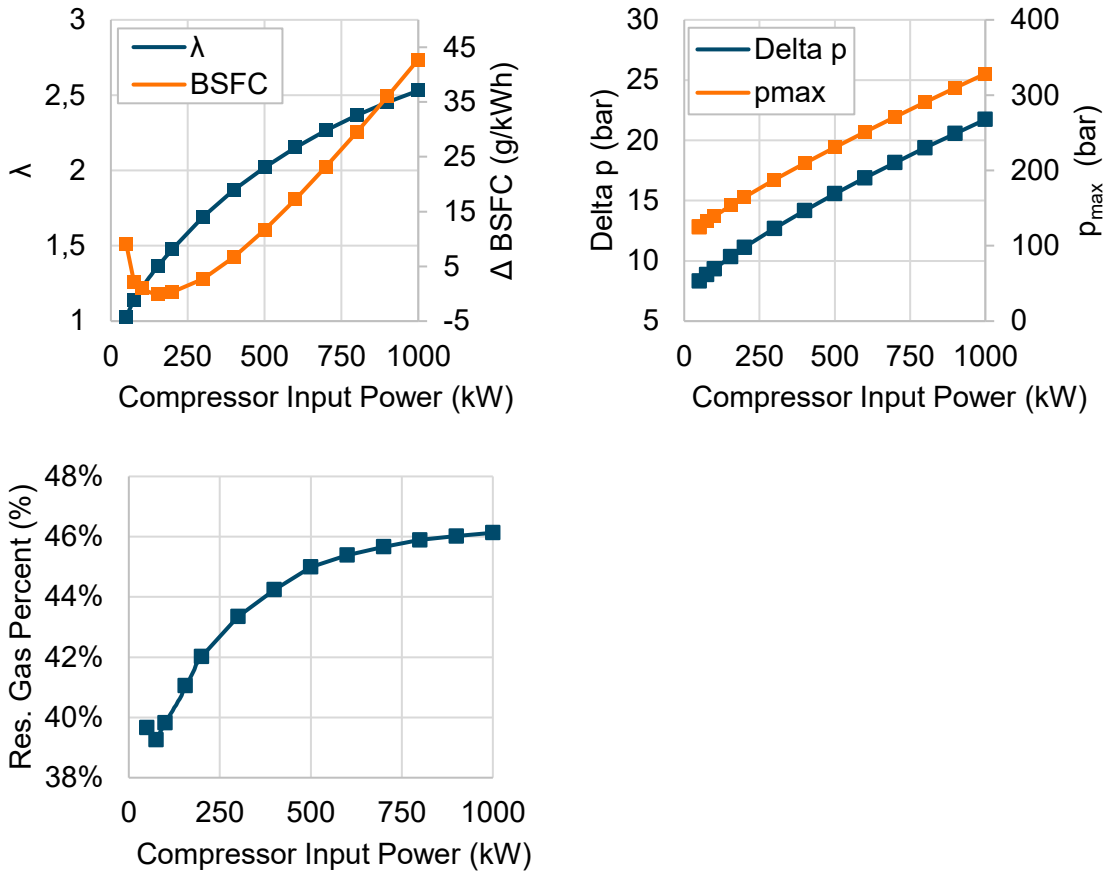

Figure 6.8. The results of the compressor input power variation. The change in specific fuel consumption is presented as brake specific. The horizontal axis is the input power to the Z-engine piston compressor.

Air-fuel ratio can be the increased up to 3 on the Z-engine, however the gain in engine indicated efficiency is not enough to overcome the increased piston compressor work and friction losses. Unlike with the Hoos Variant, increasing the compressor input power does not increase the residual gas percent so that the gas exchange does not work anymore. The input power can in theory be increased indefinitely.

Even though charge air pressure can be easily increased in the concepts, it still does not increase air-fuel ratio, or engine efficiency up to the medium-speed engine trend. After a certain point, the cost for charge air production is too much. Either the turbine restricts exhaust flow too much, or the piston compressor consumes too much work. If the concepts' air-fuel ratio cannot be increased with a higher charge air pressure, then how?

The efficiency of the turbines and compressors have a big impact. A variation of the turbocharger and piston compressor efficiency was made on the concepts and the W20 engine. The sweep was done so that the charge air pressure stays constant. The sweep showed that the concepts are significantly more sensitive to turbocharging efficiency than the W20, the Hoos Variant engine being slightly more sensitive out of the concepts. Brake specific fuel consumption in relation to turbocharging efficiency can be seen in figure 6.9.

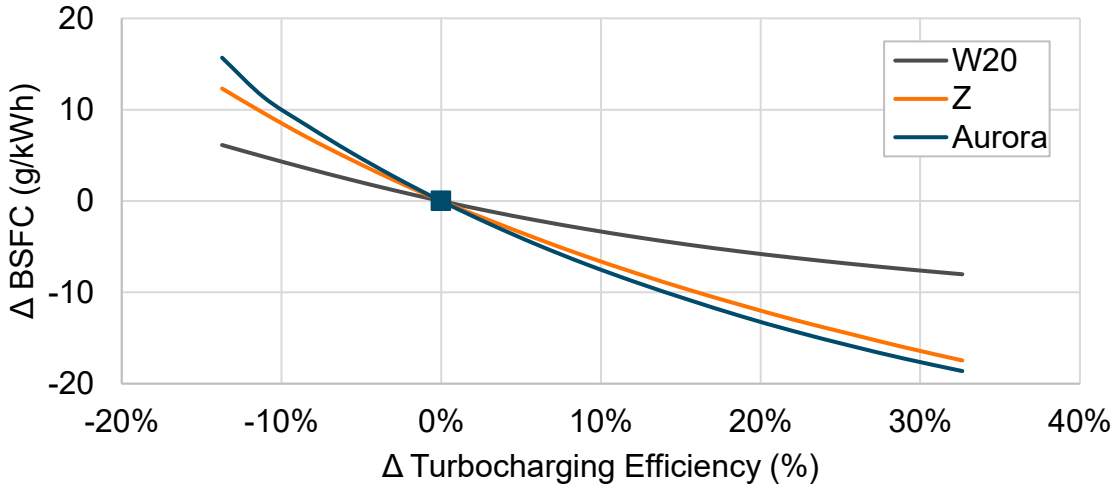

Figure 6.9. Change in brake specific fuel consumption in the engine concepts and the W20, where the baseline point is highlighted. The change from the baseline turbocharging efficiency in percent-units is used as the horizontal axis.

In the Hoos Variant engine the share of external compression out of the total compression work is the largest of the three. This is the reason why it is also the most sensitive to the efficiency of the external compression. In the Hoos Variant, a 19 g/kWh improvement in fuel consumption can be seen when increasing the turbocharging efficiency by 30 %. In the W20 the improvement is only 8 g/kWh, which is less than half. The Z-engine is slightly less sensitive to the turbocharging efficiency than the Hoos Variant.

However, when looking at air-fuel ratio, the result is slightly different. While in the Z-engine it was easier to increase the air-fuel ratio by simply increasing the input power to the piston compressor, increasing the turbocharging efficiency has a much better effect on the Hoos Variant engine. While the Z-engine sees an improvement of roughly 10%, air-fuel ratio is increased by 30—40 % in the Hoos Variant.

6.5 Summary of the optimization

This chapter described one of the intermediate objects of the thesis: optimization of the full concept models. The concepts were optimized to the best extent to have as fair as possible a comparison against the W20 engine. The concepts were optimized in terms of brake specific fuel consumption, however some limitations like cylinder maximum pressure were kept in mind. Additional studies were made to find out how air-fuel ratio and specific fuel consumption can be influenced.

The Hoos Variant engine was optimized by finding a good balancing for the turbochargers. In the beginning of the simulations, it was noticed that the best way to balance the turbochargers is to operate so, that each compressor would have close to same pressure ratio. The Hoos Variant engine was optimized then by determining an optimum turbine flow area for the first turbine in the exhaust duct, the turbine 4. Controllers would then impose the correct turbine area for the rest of the turbines. It was found that the Hoos Variant concept is not very sensitive to changes in the turbine area. Around the optimum point, the area can be changed 17.5 % in both directions, and the engine brake specific fuel consumption stays within 1 g/kWh from the optimum value.

The best balance for the Z-engine was found by determining a correct combination of the piston compressor input power and the turbocharger turbine flow area. A surprising result was that with the parameters used for this simulation, the best balance is when the turbocharger does most of the compression, and the piston compressor acts as a “helper” compressor. This is opposite to what the developer suggests for the engine. However, in the optimum operating area of the Z-engine, the pressure ratio of the turbocharger compressor is well over 6, which is the highest practically attainable pressure ratio for a one-stage turbocharger. This means that in practice, a two-stage setup should be used in the Z-engine.

Due to the high amount of residual gases, the relative air-fuel ratio remains low in the concepts. The relative air-fuel ratio in the optimum point is roughly 1.3—1.4, which is significantly less than the industry standard, ~2.2. The air-fuel ratio can be increased, however always with a cost. It is easy to increase the air-fuel ratio in the Z-engine, however the power required by the piston compressor increases unreasonably, and the overall efficiency keeps getting worse. It is impossible to increase the relative air-fuel ratio above 1.8 in the Hoos Variant engine by simply decreasing the turbine area.

In the optimum points, the maximum cylinder pressure is somewhere between 145—160 bar, which leaves a lot of marginal compared to the industry standard. Medium-speed engines run already with maximum pressures of over 200 bar. This means that the concepts could be built with significantly cheaper cranktrain components. Alternatively, there is a lot of margin to increase the maximum pressure, for example by shortening the heat release. Increasing the maximum pressure is usually related to increased engine efficiency (Mollenhauer and Tschöke 2010, p. 581—582).

7 Comparison

This chapter presents the comparison between the concepts and the W20 in various engine performance aspects, such as brake specific fuel consumption, total compression efficiency and heat load. The potential and drawbacks of the concepts are discussed in the end.

7.1 Engine performance

According to the GT-Power simulations, the result is that both concepts are less fuel efficient than the W20 engine with the standard boundary conditions. Table 7.1 shows the most important engine performance characteristics for the Hoos Variant engine, the Z-engine, the W20 and the four-stage turbocharged W20. The energy flow distribution in the Hoos Variant engine, Z-engine and the W20 is broken down in the Sankey diagrams in appendix 4.

Table 7.1. The most important performance numbers of the engines summarised. Here W20 FS indicates the four-stage turbocharged W20 engine.

Final Comparison, Standard Boundary Conditions					
	Hoos Variant	**Z-engine**	**Wärtsilä 20**	**W20 FS**	**Unit**
Cyl. output	200				kW
BMEP	13.65		27.3		bar
IMEP	15.4	16.6	30.8		bar
BSFC	196.5	205.7	193.8	190.3	g/kWh
ISFC	174.2	169.7	171.4	168.7	g/kWh
CMEP[1)]	0	-1.2	0		bar
p_3	20.1	13.5	baseline		bar (a)
p_5	5.4	3.8	baseline	<<baseline	bar (a)
λ	1.32	1.42	~2.2[2)]	>2.2[2)]	-
T_{comp}	1135	1040	baseline		°C
p_{max}	158	146	~200[2)]		bar
Res. gases	43	35	~0		%

1) CMEP depicts the work derived from the crankshaft that is required to run the piston compressor on the Z-engine.
2) As a reference values for the maximum cylinder pressure and air-fuel ratio, medium-speed typical values are assumed for the W20.

The Hoos Variant engine is the better of the two concepts, achieving a best brake specific fuel consumption of 196.5 g/kWh, however it has still roughly 3 g/kWh worse fuel consumption than the W20. The Z-engine is considerably worse than the W20 with a fuel consumption of 205.7 g/kWh. Moving to a four-stage turbocharging in the W20 gives a 3 g/kWh improvement in consumption.

The loss of the piston compressor in the Z-engine does not look significant at first glance but makes a big difference. Even though it has an edge in indicated efficiency over the Hoos Variant and the W20, the power loss to the compressor overcomes it so that the Z-engine has the highest brake specific fuel consumption of the four. Another interesting point is that the Z-engine must run with a somewhat higher IMEP than the Hoos Variant, to have enough power for the piston compressor. The next chapters go into more detail about the concepts' performance aspects, and to why the concepts have a higher fuel consumption than the W20.

7.2 Total compression efficiency and gas exchange work

It is interesting to find out, whether the total compression in the Z-engine and the Hoos Variant is more efficient than in the W20. In theory, as was described in chapter 2.6, the total compression work should be considerably lower in the concepts.

In the concepts, the residual gases that are present during the compression are also compressed together with the charge air in the working cylinder. In this chapter 7.1, the compression work done only to the charge air is considered. For the Z-engine and the Hoos Variant, determining the compression work done in the working cylinders is complicated, since the compression work done to the residual gases would have to be deducted. The compression work done inside the working cylinder was therefore calculated theoretically, according to the equations in chapter 2.2. The working cylinder compression work is calculated with the assumption that all engines compress the charge air to the same compression pressure, even though this is not the case in the simulations. This assumption is done only for the purposes of this comparison. Since it is difficult to determine the isentropic compression efficiency of the working cylinder using GT-Power data, the compression in the working cylinders is assumed to be done with a 100% isentropic efficiency. The external compression work comes by default from the GT-Power simulation results.

Figure 7.1 shows how much compression work is done in the engines, and how the compression work is divided between the working cylinder and the external compressors in each engine. Table 7.2 summarizes the total and external compression efficiency in the engines. The Hoos Variant does the least amount of compression work out of all the engines, while the W20 engine does the largest amount of compression work. Similarly, the isentropic efficiency of the total compression process is best in the Hoos Variant, and worst in the W20. Same applies for the external compression; the Hoos Variant is the most efficient, and the W20 the least efficient.

As the theory in chapter 2 predicts, the difference in total compression efficiency and total compression work is simply due to the number of compression stages. In the Hoos Variant, the total compression process consists of five compression stages. The total compression is three-stage in the Z-engine, and two-stage in the W20. The Hoos Variant total compression work is significantly less than the total compression work of the W20. The difference between the total compression work of the Z-engine and the W20 is roughly as big as the

difference between the Z-engine and the Hoos Variant. However, for the same improvement in total compression work, the Hoos Variant needs two more compression stages than the Z-engine.

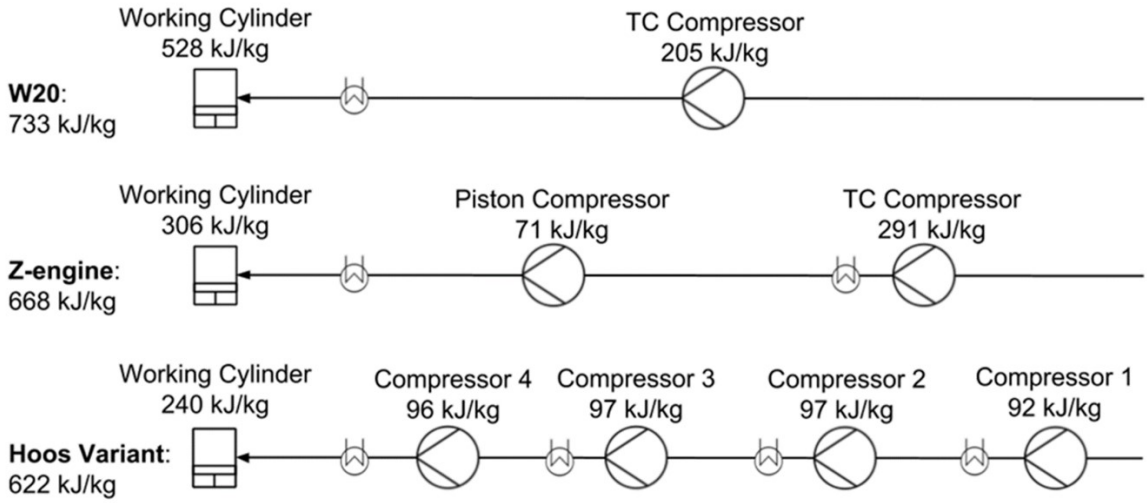

Figure 7.1. This schematic illustrates how much compression work is done in each engine, and how the compression work is divided between the working cylinders and the external compressors.

Table 7.2. Isentropic compression efficiency of the external compression and the total compression in the engines, when the charge air pressure is compressed in the same compression pressure in all engines.

	Hoos Variant	Z-engine	Wärtsilä 20	Unit
External Compression	108	91	82	%
Total Compression	150	140	127	%

An interesting finding is that even though charge air is compressed to a much higher pressure in the concepts than in the W20, a significant part of the total compression work is still done in the working cylinders. 39% of the total compression work is done in the working cylinder in the Hoos Variant. The rest of the compression work is divided equally to the four turbocharger compressors, with each compressor having a pressure ratio of roughly 2.17. The amount of external compression is high in comparison to the W20, where 72% of the total compression work is done inside the working cylinders.

In the Z-engine, 46% of the total compression work is done inside the working cylinders. A significant part of the external compression is done by the turbocharger compressor, the piston compressor acting as a helper compressor. The pressure ratio of the turbocharger is 7.76, and the pressure ratio of the piston compressor 1.83.

Due to the two-stroke cycle, and the timing of the intake period, the gas exchange is always a loss in the concepts. During the intake period, the piston is moving up, and the charge air is flowing inside the cylinder; the cylinder volume is decreasing, and the pressure is increasing. Therefore, the piston is doing work during the intake period as if it would compress a gas. In the W20, at least with the parameters used for this simulation, the gas

exchange does positive work to the cycle, instead of consuming it, which is a key difference. Even though the external compression is more efficient in the concepts, due to the nature of the Z gas exchange, the gas exchange will always be a loss in the concepts, unlike in the W20.

7.3 Heat transfer losses and heat load

There is a significant difference in the in-cylinder gas and component temperatures and the heat transfer losses between the concepts and the W20. The Hoos Variant engine has the highest amount of heat transfer losses in relation to the input fuel energy; 10% of the fuel energy goes to the cylinder walls as heat losses. The Z-engine is a bit better, where 9% of the fuel energy goes to heat transfer losses.

Both concepts operate with a considerable amount of residual gases during compression, combustion and expansion; almost half of the trapped cylinder mass is hot residual gases in the Hoos Variant. In the Z-engine, the residual gases constitute roughly 35% of the total cylinder trapped mass. Since the concepts also operate with a significantly lower relative air-fuel ratio than the W20, the temperature of the residual gases is considerably higher. With a low relative air-fuel ratio, the combustion air temperature will increase more during combustion. Due to the large amount of very high-temperature residual gases and a low relative air-fuel ratio, the gas temperature both during combustion and gas exchange is very high compared to the W20.

A unique feature of the Z gas exchange is that when the intake valve is opened, relatively cool charge air flows in the cylinder and mixes with the hot residual gases. This results to a sudden drop of roughly 250ºC during the intake period. As an example, figure 7.2 shows how the temperature develops in the Z-engine before combustion.

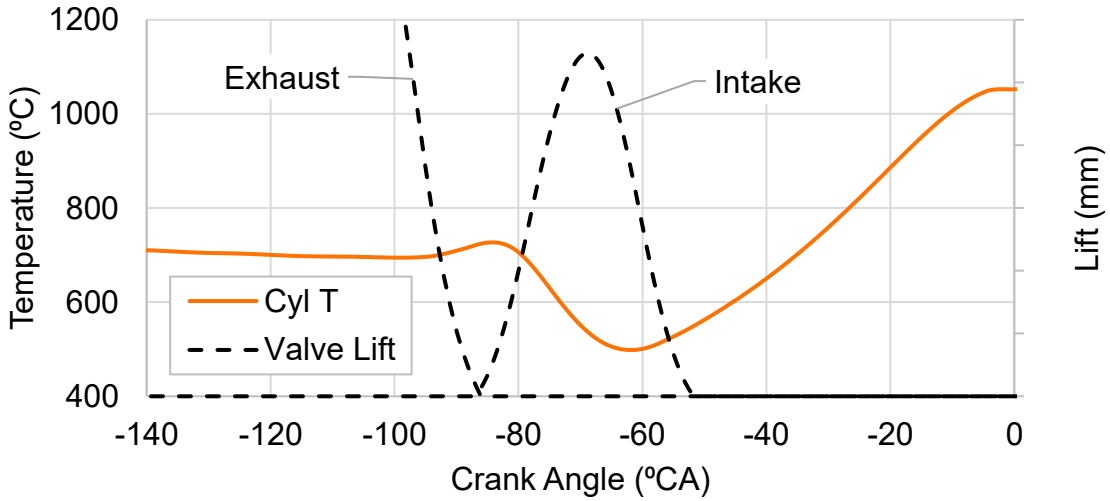

Figure 7.2. The in-cylinder (Cyl T) temperature in the Z-engine, before top dead centre of firing. The exhaust and intake valve lifts are illustrated by the dashed line.

Even though the in-flowing charge air cools the cylinder temperature by roughly 250ºC, the temperature in the end of compression is still significantly higher in the concepts than in the W20. The compression temperature in the Hoos Variant engine is 1135ºC, and somewhat lower in the Z-engine, 1040ºC. The Hoos Variant engine has a considerably higher amount of residual gases in the cylinder than the Z-engine, which explains the higher overall

temperature. Figure 7.3 compares the temperature in the engines; in the W20 during the compression stroke and in the concepts during the exhaust stroke and the intake and compression period.

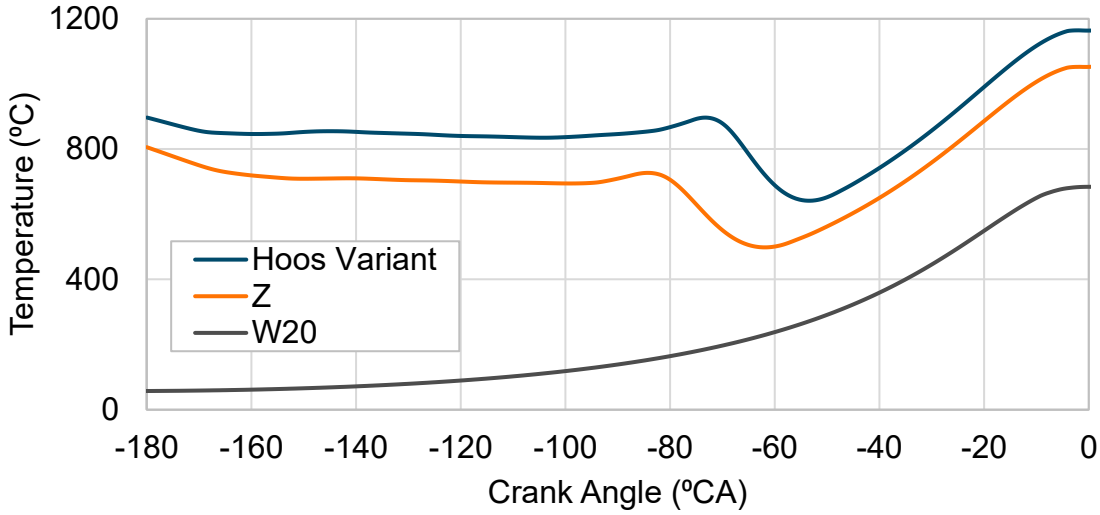

Figure 7.3. In-cylinder temperature before firing top dead centre in engines. Worth noting is that the temperature after the expansion (at 180 ºCA before TDC firing) is considerably high in the concepts.

As can be expected based on the heat transfer losses and in-cylinder temperature, the simulations predict that the heat load of the in-cylinder components is significantly higher in the concepts than in the W20 engine. During operation, the temperature of the components inside the cylinder is 300—450ºC higher in the concepts than in the W20. Like explained before, the Z gas exchange lacks a cool period. In a four-stroke engine the gas exchange takes a complete revolution, during which the working cylinder has time to cool down and is flushed with fresh air. In addition to a missing cool period, the concepts run with a high amount of extremely high-temperature residual gases.

Figure 7.4 shows the temperature distribution in the pistons. According to the simulations, the piston top of the concepts is 300—400ºC hotter during operation than in the W20. The maximum piston temperature is around 330ºC higher in the Z-engine. The Hoos Variant engine runs even hotter, where the maximum piston temperature is 400ºC higher than in the W20. The piston temperatures in the concepts are so high that steel starts to glow red. (Chapman 1972.)

The same goes for the rest of the in-cylinder components. The rest of the results can be seen in appendix 5. The cylinder head is roughly 200—300ºC hotter in the engine concepts. While the cylinder head is relatively cool around the intake valves in the W20, in the concepts also the surrounding of the intake valves is hot. The area around the intake valves is almost as hot as the one around exhaust valves in the concepts. Like with the piston, also the cylinder head is the hottest in the Hoos Variant engine. The exhaust valves are at roughly 470ºC higher temperature in the concepts than in the W20.

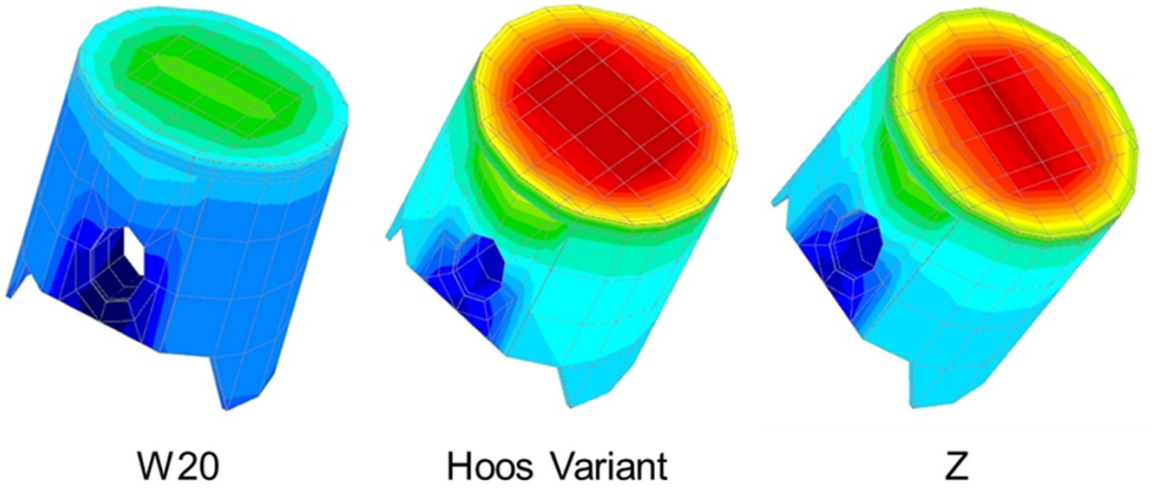

Figure 7.4. The heat load in the engines, with the same temperature scale.

7.4 Discussion

This part presents some additional comparisons between the concepts and the W20, as well as hypothetical discussion of the concepts' potential and bottlenecks.

7.4.1 Maximum pressure margin

Since the concepts run at maximum cylinder pressures much lower than the industry standard (200 bar) in their optimized points, there is some margin to increase it, for example with a fast premixed heat release. Generally, a faster heat release increases an internal combustion engine's thermal efficiency. With a fast premixed heat release, like HCCI, and a maximum pressure close to 200 bar, the Hoos Variant engine has a brake specific fuel consumption of 186.2 g/kWh and the Z-engine 191.9 g/kWh, this time both performing significantly better than the W20 with the same boundary conditions. With the premixed heat release, the Hoos Variant engine is even better than the four-stage W20 by roughly 3 g/kWh, however the Z-engine is still 2 g/kWh worse.

Here is the most significant advantage of the concepts. Because of the unique two-stroke cycle, and compression that is done mostly externally, the concepts can be run with the same cylinder output as the W20, but with a significantly lower IMEP and maximum cylinder pressure. If the boundary conditions were set so that cylinder output and maximum cylinder pressure are constant, the concepts will have a significantly better fuel efficiency than the W20.

7.4.2 Ideal boundary conditions

With the standard boundary conditions, the concepts perform worse than the W20. However, will the concepts outperform the W20 if the boundary conditions were ideal? To find out the answer, an additional comparison was done with ideal boundary conditions (Ideal IC + VT). Charge air is assumed to be completely cooled to ambient temperature in all intercoolers and the charge air cooler. Furthermore, the intake valve lift is increased so that it can be assumed to be ideal, not restricting the in-cylinder flow.

The results are presented in table 7.3. If the intercoolers and the intake cam lift profiles are assumed to be ideal, the concepts get a little closer to the W20, however the Hoos Variant

engine still falls behind the W20. The difference is not great anymore, only 1 g/kWh. Even in this case, the Z-engine is still the worst, and the four-stage W20 the best.

Table 7.3. Brake specific fuel consumption in the engines with ideal boundary conditions.

	Hoos Variant	Z-engine	Wärtsilä 20	W20 FS	Unit
Ideal IC + VT	193.7	202.4	192.6	188.7	g/kWh

7.4.3 Potential for HCCI

Chapter 2.5 described how HCCI can be controlled, and the major challenges with HCCI operation. In theory, both concepts would have some advantageous features for the use of HCCI. If assumed that a maximum of 13.65 bar BMEP load could be operated on the W20 with HCCI, the same IMEP could be operated on the concepts but producing full cylinder power with all the benefits of HCCI.

The concepts operate constantly with residual gases in the cylinder, however it can be expected that the control of the residual gas percentage is not straightforward. The residual gas amount in the cylinder can be decreased by delaying intake valve opening timing or increasing the turbocharger turbine area. These measures will influence charge air pressure, trapped air mass and engine efficiency. Controlling the residual gas percent without significantly changing engine operation is not possible in the concepts, unlike in conventional exhaust gas recirculation, where the residual gases are simply mixed with the charge air before admission to the working cylinder.

The effective working cylinder compression ratio will be much lower than the in the W20. Due to this, in theory the concepts would operate with considerably lower compression temperature than the W20. This would be advantageous for HCCI, since it is always easier to heat the charge air to reach the required compression temperature rather than cool it.

As described in chapter 7.3, the residual gases increase the in-cylinder temperature so much that the air is well above the autoignition temperature of light or heavy fuel oil. The 35—43 % residual gas would decrease the ignition delay considerably, but also slow down the combustion. It is safe to assume that even though the relative air-fuel ratio is low, the combustion would be relatively slow due to the very high residual gas amount. Due to the very high temperature of the mixed charge air and residual gases in the beginning of compression, it is safe to assume that HCCI would not work with these simulation parameters without additional cooling of the charge air. The problem is that the mixture would ignite too early during compression. (Axelsson 2017.)

7.4.4 Realising the concepts

By their construction, the concepts do not differ considerably from the four-stroke engine. In theory components such as pistons, cranktrain, fuel system and exhaust valve train, could be existing Wärtsilä hardware. However, it is safe to assume that none of the Wärtsilä in-cylinder components withstand the heat load caused by the Z gas exchange cycle. The cooling system, and the in-cylinder components and their materials would require a complete redesign.

The sensitivity analysis revealed that valve train actuation speeds like in existing Wärtsilä engines are not enough for the Z gas exchange. The Z gas exchange cycle, as well as the Hoos engine cycle (which was not studied) require a special intake valve train that was discussed in chapter 3. A considerable amount of research work is done already regarding the valve train, however realising it in a Wärtsilä engine would require additional development efforts, since such a technology is not an existing Wärtsilä solution.

The highest rate of turbocharging in a Wärtsilä engine is implemented in the Wärtsilä 31, which is two-stage turbocharged (Åstrand et al 2016.). The two-stage turbocharger can produce charge air at a pressure level of 10 bar (a), which is not quite enough by itself for the operation of the concepts.

In addition to the piston compressor, a two-stage turbocharging setup is required by the Z-engine to operate it on the optimum area that was discovered in the optimizations in chapter 6.3. The four-stage turbocharging system of the Hoos Variant would take considerable amounts of development work, and the system will be expensive. However, turbochargers are a well-studied and established technology. Therefore, the charge air production on both concepts should be realisable with additional development work.

7.5 Comparison summary

Brake specific fuel consumption of the engines with the different boundary conditions is summarized in table 7.4. With the standard boundary conditions, the Z-engine and the Hoos Variant are less fuel efficient than the W20 engine. However, with the standard boundary conditions the concepts have significant margin to increase the maximum cylinder pressure to the general level of the medium-speed engines (~200 bar). If a fast combustion like HCCI is used to increase the concepts' maximum cylinder pressure, then both concepts are more fuel efficient than the W20. If the maximum pressure margin is utilized, the Hoos Variant engine has roughly 8 g/kWh lower brake specific fuel consumption than the W20, and even outperforms the four-stage turbocharged W20 with a 4 g/kWh lower BSFC. This is the single most important advantage of the concepts.

Table 7.4. Summary of the brake specific fuel consumption of the engines with the different boundary conditions.

Engine Brake Specific Fuel Consumption (g/kWh)				
Comparison Boundary Conditions	**Hoos Variant**	**Z-engine**	**Wärtsilä 20**	**W20 4-stage**
Standard	197	206	194	190
Standard HCCI	186	192	-	
Ideal IC + VT	194	202.4	193	189

In the beginning of combustion, 35—43% of the trapped cylinder mass are residual gases in the concepts. The concepts operate with a relative air-fuel ratio of 1.3—1.4, which is significantly lower than the industry standard, 2.2. The low air-fuel ratio and the high amount of residual gases are linked together; due to the high amount of residual gases, the air-fuel

ratio remains low. Due to the low air-fuel ratio, the residual gases are extremely hot. This causes an unreasonably high heat load. This is also the main reason why the concepts are less fuel efficient with the standard boundary conditions.

As described in chapter 2.6, external compression engines have potential to increase the internal combustion engine's efficiency. The improvement in fuel consumption can be achieved with similar mechanisms as in the Atkinson and Miller cycle.

Based on the simulation results, the total compression efficiency and the turbocharging efficiency are indeed higher in the concepts than in the W20 due to the more compression stages used in the concepts. Efficient external compression lowers the compression temperature, which gives margin to increase engine efficiency when tuning engine NOx emissions. Compression temperature should in theory be lower in the concepts; however, this is not the case due to the high residual gas amount. The compression temperature is roughly 400ºC higher in the concepts, which is why there is no possibility of increasing the engine efficiency by NOx tuning, like with Miller cycle.

The combination of the low compression temperature and the unique two-stroke cycle means that HCCI could be operable in an external compression engine, producing full cylinder output. However, the high compression temperature also prevents the use of HCCI with light or heavy fuel oil.

Indicated efficiency can be improved by decreasing the compression ratio of the engine, while keeping the expansion ratio. This is true for the Z-engine; it has a considerably better indicated efficiency than the W20. However, the power required to drive the piston compressor overcomes the advantage in indicated efficiency.

8 Conclusion

8.1 Conclusion

The object of this thesis was to evaluate the engine performance potential of the two engine concepts, the Z-engine and the Hoos engine, within medium-speed boundary conditions. Finally, the Z-engine and a simplified version of the Hoos engine, the Hoos Variant, were compared against the reference engine, the Wärtsilä 20. The thesis aims to answer the four research questions:

1. Are the Z-engine and Hoos engine concepts more fuel efficient than a comparable four-stroke medium-speed engine?
2. What are the possible bottlenecks of the concepts?
3. Can the concepts be realised with existing Wärtsilä designs and solutions?
4. Is it a good idea for Wärtsilä to start developing these engine concepts?

With the standard boundary conditions, the Z-engine and the Hoos Variant are not more fuel efficient than a comparable four-stroke engine. However, the concepts' greatest potential is the maximum pressure margin; if the margin can be utilized by using a fast heat release, the concepts will be considerably more fuel efficient. The concepts therefore have potential to be more fuel efficient than a comparable four-stroke engine. Whether the Hoos engine, as defined by the developer, is more fuel efficient than the W20 is left unanswered by this thesis work.

Regarding the second research question of the thesis, the bottleneck of the Z-engine and the Hoos Variant is the working cycle. The high amount of high-temperature residual gases causes high heat transfer losses throughout the whole cycle, and an unreasonably high heat load, and very high heat transfer losses. The high heat transfer losses are the main reason why the concepts are less fuel efficient than the W20 with the standard boundary conditions.

Additional development work is required to realise an intake valve train fast enough for the working cycle of the Z-engine, as existing Wärtsilä valve actuation speeds are not enough. Regarding the third research question of this thesis, the special valve train required for a successful gas exchange prevents the realisation of the Z-engine and the Hoos Variant with existing Wärtsilä solutions.

Even if the maximum cylinder pressure margin is utilized to increase the efficiency of the Z-engine and the Hoos Variant, a solution must be developed to solve the heat load problem. Furthermore, the W20 should be tested with charge air pressure and Miller timing comparable to the concepts and see how fuel efficient they are before making any conclusion about which engine ultimately is the most efficient. Until these points are investigated, it is not recommended for Wärtsilä to start developing these engine concepts.

8.2 Suggestions and final words

Instead of starting the development of the concepts, it would be much easier for Wärtsilä to continue developing their existing engines towards stronger and stronger Miller timing, higher charge air pressure and more efficient turbocharging. After all, this is also what the external compression engines are about. Development of the concepts would mean solving the problems of the Z-engine working cycle and developing new technologies. There would be no guarantee of a more efficient engine, compared to a situation where the same development work would be targeted to Wärtsilä's existing engines.

Unfortunately, there was no time to do certain studies that would have been important for the conclusion for this thesis. The original plan was to test out more charge air production methods than the ones in the Z-engine and the Hoos engine, such as a two-stage turbocharger combined with a piston compressor, or a three-stage turbocharger.

According to the simulation results, the Hoos Variant engine has more performance potential than the Z-engine. The scope of the thesis was set so that the Hoos engine was not simulated as it was defined by its developer. It would be interesting to simulate the Hoos engine with the gas exchange suggested for it, and with the recuperator. Since the gas exchange of the Z-engine proved to be problematic, it would be interesting to see how the gas exchange suggested for the Hoos engine would perform.

The comparisons in this thesis were in one aspect flawed: in practice, the four-stage W20 would be run with considerably higher charge air pressure and much stronger Miller timing. If the four-stage was operated with the same charge air pressure as the Hoos Variant engine, with according Miller timing, the fuel consumption improvement from the single-stage W20 would have been greater. It would be essential to simulate the W20 with the same charge air pressure and Miller timing as the concepts before any conclusion about the concepts' performance can be made. If the W20 fuel efficiency is even at the same level as the concepts with these boundary conditions, then it can be concluded that the concepts are not worth developing.

The Z-engine concept is still being improved and developed by Mr. Janhunen. The latest developments can be followed on Aumet Oy's website (2018). Future developments of the Hoos engine are unknown.

References

Anderson, M. K. & Assanis, D. N. & Filipi, Z. S. 1998. First and Second Law Analyses of a Naturally-Aspirated, Miller Cycle, SI Engine with Late Intake Valve Closure. [Online]. SAE Technical Paper 980889. [Retrieved 25.1.2018]. ISSN 0148-7191.

Aumet Oy. 2018. Front page. [Aumet Oy's website]. Updated 2018. Retrieved 9.2.2018. From: www.aumet.fi

Axelsson, M., Manager, Engine Performance and Control. 2017. Wärtsilä Finland Oy. Järvikatu 2, 65100 Vaasa, Finland. Interview 9.11.2017.

Brayton Ready Motor Hydrocarbon Engine. [Old Machine Press' website]. Updated on December 5, 2016. [Retrieved 20.1.2017]. From: https://oldmachinepress.com/2016/12/05/brayton-ready-motor-hydrocarbon-engine/

Campbell, J. M. 2014. Gas Conditioning and Processing, Volume 2: The Equipment Modules, Norman, USA: JMC Press. 398 p. ASIN B00JUAM1ZI.

Cengel, Y. A. & Boles, M. A. 2007. Thermodynamics: An Engineering Approach, Sixth Edition (SI Units). New York, NY, United States: McGraw-Hill Education. ISBN 978-007-125771-8.

Chapman, W. A. J. 1972. Workshop Technology, Part 1. Burlington, MA: Elsevier Butterworth-Heinemann. ISBN 978-0713132694.

Clarke, J. M. 2009. How the CCI Mechanism Enables Higher Efficiency. [Online]. Updated in October, 2009. From: https://dreamer3000.files.wordpress.com/2008/07/extreeme-expansion-cycle-ccipaper521.pdf

Coney, M. W. & Linnemann, C. & Greenwood, A. L. & Hogg, C. R. 2003. First test results of a novel large high-efficiency reciprocating piston engine. In: Spring Technical Conference of the ASME Internal Combustion Engine Division. Salzburg, Austria, 11—14.5.2003. The American Society of Mechanical Engineers. From: http://proceedings.asmedigitalcollection.asme.org/

Coney, M. W. & Linnemann, C. & Abdallah, H. S. 2004. A thermodynamic analysis of a novel high efficiency reciprocating internal combustion engine—the isoengine. Energy. [Online]. Vol. 29:2004. P. 2585–2600. [Retrieved 31.1.2017]. DOI:10.1016/j.energy.2004.05.014

Cummins, C. L. 1989. Internal Fire. Warrendale, PA, USA: Society of Automotive Engineers, Inc. 357 p. ISBN 0-89883-765-0.

External Company. 2015. An engine market Benchmark study done for Wärtsilä. Unpublished.

Gamma Technologies. 2017. GT-Power User Manuals.

Gurr, A. & Atkins, A. & Rawlins, D. & Morgan, R. 2016. The 60% Efficiency Reciprocating Engine: A Modular Alternative to Large Scale Combined Cycle Power. Technical Paper No. 267. In: CIMAC World Conference. Helsinki, Finland. 6—10.6.2016. Gesellschaft zur Förderung des Maschinenbaues mbH. From: http://www.cimac.com/publication-press/technical-database/index.html

Grönlund, T. 2003. Valve Train of a New Type of Engine. Master's Thesis. Helsinki University of Technology, Department of Mechanical Engineering. Espoo. 111 p.

Grönlund, T. & Larmi, M. 2004. Valve Train Design for a New Gas Exchange Process. [Online]. SAE Technical Paper 2004-01-0607. [Retrieved 27.4.2017]. 13 p. ISBN 0-7680-1319-4.

Hattar, C., Chief Expert, Engine Performance and Control. 2017. Wärtsilä Finland Oy. Järvikatu 2, 65100 Vaasa, Finland. Interview 16.11.2017.

Hattar, C., Chief Expert, Engine Performance and Control. 2018. Wärtsilä Finland Oy. Järvikatu 2, 65100 Vaasa, Finland. Interview 12.1.2018.

Hattar, C., Chief Expert, Engine Performance and Control & Järvi, A., General Manager, Product Performance. 2018. Wärtsilä Finland Oy. Järvikatu 2, 65100 Vaasa, Finland. Interview 29.1.2018.

Heywood, J. B. 1988. Internal Combustion Engine Fundamentals. New York, USA: McGraw-Hill. 930 p. ISBN 0-07-028637-X.

Hoos, Frank. 2015. Development of a new generation combustion engine. Presented 9.11.2015. Unpublished.

Hyvönen, J. 2005. The Performance of a Multi Cylinder HCCI Engine using Variable Compression Ratio and Fast Thermal Management. Doctoral Thesis. Lund Institute of Technology, Department of Energy Sciences. Lund, Sweden. 259 p.

International Maritime Organization - Nitrogen Oxides (NOx) – Regulation 13. 2018. [IMO's website]. Updated in 2018. [Retrieved 30.1.2018]. From: http://www.imo.org/en/OurWork/environment/pollutionprevention/airpollution/pages/nitrogen-oxides-(nox)-%E2%80%93-regulation-13.aspx

Isaksson, S. 2017. Manager, Engine Performance and Control. Wärtsilä Finland Oy. Järvikatu 2, 65100 Vaasa, Finland. Interview 24.11.2017.

Janhunen, T., Managing Director, Aumet Oy & Nyyssönen, S., Research Scientist, VTT Oy. 2017. Innopoli 1, Tekniikantie 12, 02150 Espoo, Finland. Interview 25.4.2017.

Master's Thesis. 2018. Friction Modelling of Medium Speed Engines. Unpublished.

Kuleshov, A. & Mahkamov, K. & Janhunen, T. & Akimov, V. & Kuleshov, A. 2015. New Downsized Diesel Engine Concept with HCCI Combustion in High Load Conditions.

[Online]. SAE Technical Paper 2015-01-1260. [Retrieved 27.4.2017]. 17 p. DOI: 10.4271/2015-01-1791.

Lam, N. & Tunér, M. & Tunerstål, P. & Andersson, A. & Lundgren, S. & Johansson, B. 2015. Double Compression Expansion Engine Concepts: A Path to High Efficiency. 2015. [Online]. SAE Technical Paper 2015-01-1260. [Retrieved 3.2.2017]. 17 p. DOI: 10.4271/2015-01-1260.

Lampinen, M. J. 1997. Termodynamiikan perusteet. Helsinki, Finland: Hakapaino Oy. 182 p. ISBN 951-672-324-1.

Mazda Announces Long-Term Vision for Technology Development, 'Sustainable Zoom-Zoom 2030'. [Mazda's website]. Updated on 8.8.2017. [Retrieved 4.10.2017]. http://www2.mazda.com/en/publicity/release/2017/201708/170808a.html

Mollenhauer, K. & Tschöke, H. 2010. Handbook of Diesel Engines. Heidelberg, Germany: Springer-Verlag. 636 p. ISBN 978-3-540-89082-9.

Motiv Engines. 2012. [Motiv Engine's website]. Updated 2012. From: http://www.motivengines.com/AboutMotiv.html

Musu, E. & Rossi, R. & Gentili, R. & Reitz, R. D. 2010. Clean Diesel Combustion by Means of the HCPC Concept. [Online]. SAE Technical Paper 2020-01-1256. [Retrieved 30.3.2017]. 18 p. DOI: 10.4271/2010-01-1256.

Philips, F. & Gilbert, I. & Pirault, J-P. & Megel, M. 2011. Scuderi Split Cycle Research Engine: Overview, Architecture and Operation. [Online]. SAE Technical Paper 2011-01-0403. [Retrieved 24.1.2017]. 17 p. DOI: 10.4271/2011-01-0403.

Stanglmaier, R. H. & Roberts, C. E. 1999 Homogeneous Charge Compression Ignition (HCCI): Benefits, Compromises, and Future Engine Applications. [Online]. SAE Technical Paper 1999-01-3682. [Retrieved 16.1.2018]. 10 p. ISSN 0148-7191.

The Tour Engine Technology. [Tour Engine, Inc.'s website]. Updated 2017. From: http://www.tourengine.com/technology/design.html

Tiainen, J. & Saarinen, A. & Grönlund, T. & Larmi, M. 2003. Novel Two-Stroke Engine Concept, Feasibility Study. [Online] SAE Technical Paper 2003-01-3211. [Retrieved 27.1.2017]. 15 p. ISSN 0148-7191.

US 1062999 A. 1913. Gas-engine. Samuel J. Webb, Minden, Louisiana, United States. (Webb, S. J., Webb, R. D.) US 129428, 30.10.1902. Published 27.5.1913. 5 p.

US 1372216. 1921. Internal combustion engine. James O. Casaday, South Bend, Indiana, United States. (Casaday, J. O.) US 282236, 12.3.1919. Published 22.3.1921. 5p.

US 2011/0303185 A1. 2011. Split cycle engine and method with increased power density. Zajac Optimum Output Motors, Inc., San Jose, California, United States. (Zajac, J., Moran, J.) US 61/353572, 10.6.2010. Published 15.12.2011. 10 p.

US 2017/0045230 A1. 2017. Combustion cycle process. Frank Hoos, Mijnsheerenland, Netherlands. (Hoos, F.) US 61/980764, 17.5.2014. Published 16.2.2017. 1p.

US 3688749. 1972. Supercharged rotary combustion engine. Audi NSU, Neckarsulm, Germany. (Wankel, F.) US 136120, 21.4.1971. Published 5.9.1972. 7 p.

US 961059. 1910. Gas engine. William G. Jr. Abbot, Philadelphia, Pennsylvania, United States. (Abbot, W. G. Jr.) US 293992, 30.12.1905. Published 7.6.1910. 7p.

van Basshuysen, R. & Schäfer, F. 2004. Internal Combustion Engine Handbook - Basics, Components, Systems, and Perspectives. Warrendale, PA, USA: SAE International. 811 p. ISBN 978-0-7680-1139-5.

Wiksten, R. 2009. Virtauskoneet. Helsinki, Finland: Edita Prima Oy. 254 p. ISBN 978-951-22-9892-1.

Wärtsilä. 2017. Wärtsilä 20 Product Guide. [Retrieved 15.1.2018.] From: https://cdn.wartsila.com/docs/default-source/product-files/engines/ms-engine/product-guide-o-e-w20.pdf?sfvrsn=6

Zima, S. & Ficht, R. 2010. Ungewöhnliche Motoren. Germany: Vogel Business Media. 608 p. ISBN 10 3834331406.

Åstrand, U. & Aatola, H. & Myllykoski, J-M. 2016. Wärtsilä 31 – World's most efficient four-stroke engine. Technical paper nr. 225. In: CIMAC World Conference. Helsinki, Finland. 6—10.6.2016. Gesellschaft zur Förderung des Maschinenbaues mbH. From: http://www.cimac.com/publication-press/technical-database/index.html

List of appendices

Appendix 1. Sensitivity analysis charge air pressure predictions

To predict, what charge air pressure is required for the Z gas exchange at different intake valve opening timings and exhaust pressure levels, a simple ideal gas calculations were done with Microsoft Excel as a part of the sensitivity analysis. The theory used is described here.

First step is to determine, what amount of air per cycle the engine requires at a certain operating point. This can be determined, if the load, engine efficiency, air-to-fuel ratio, fuel heat content, cylinder geometry and engine speed are known. First the needed fuel amount per cycle is determined, and from there the needed air amount is calculated:

$$P_{fuel} = \frac{p_{me} V_d n}{n_c \eta_e} \quad 14)$$

$$\dot{m}_{fuel} = \frac{P_{fuel}}{H_u} \quad 15)$$

$$\dot{m}_{air} = L_{st} \cdot \lambda \cdot \dot{m}_{fuel} \quad 16)$$

$$m_{air} = \frac{\dot{m}_{air}}{n} \quad 17)$$

where P_{fuel} is the fuel power, p_{me} the brake mean effective pressure, V_d the cylinder swept volume, n the engine operating speed, n_c revolutions per working cycle (1 for two-stroke engines) and η_e the engine efficiency. H_u is the lower heating value of the fuel, L_{st} the stoichiometric air-fuel-ratio and λ the relative air-fuel-ratio. (van Basshuysen and Schäfer 2004, p. 19.)

The following assumption is made here: the intake period is instant, meaning its duration is 0 °CA, and during the intake period, the cylinder is filled up with the required air amount so that the cylinder pressure level rises to that of the charge air. The cylinder volume depends on the intake valve opening timing. To calculate the momentary cylinder volume, the piston stroke equation can be used:

$$s_\alpha = r \cdot \left(1 + \frac{l}{r} - \cos\alpha - \frac{l}{r} \cdot \sqrt{1 - \left(\frac{r}{l}\right)^2 \cdot (\sin\alpha)^2}\right) \quad 18)$$

$$V_{min} = \frac{V_d}{\varepsilon - 1} \quad 19)$$

$$V_c = V_{min} + s_\alpha \cdot \pi \cdot \left(\frac{D}{2}\right)^2 \quad 20)$$

where s_α is the momentary stroke of the piston, r the crank radius ($s/2$), l the connecting rod length and α the momentary crank angle. V_{min} is the minimum cylinder volume that can be calculated using the cylinder displacement V_d and the compression ratio ε. What is still needed to calculate the total cylinder volume V_c is the engine bore D. (van Basshuysen and Schäfer 2004, p. 15—16.)

When the available cylinder volume is known, the needed charge air pressure can simply be calculated using the ideal gas law:

$$\frac{(m_{air}+m_{exhaust})RT_3}{M_3 p_3} = \frac{m_{exhaust}RT_{exhaust}}{M_{exhaust}p_{exhaust}} \quad 21)$$

$$m_{exhaust} = \frac{p_{exhaust}MV_c}{M_{exhaust}p_{exhaust}} \quad 22)$$

where the molar masses of the exhaust gases $M_{exhaust}$ and the combination of the two M_3 can be assumed to be the same. Here T_3 is the charge air temperature, $T_{exhaust}$ the exhaust gas temperature and R is the gas constant. Finally, the charge air pressure p_3 can be calculated:

$$p_3 = \frac{p_e(m_{air}+m_{exhaust})T_3}{m_{exhaust}T_{exhaust}} \quad 23)$$

Appendix 2. Hoos Variant engine optimization results

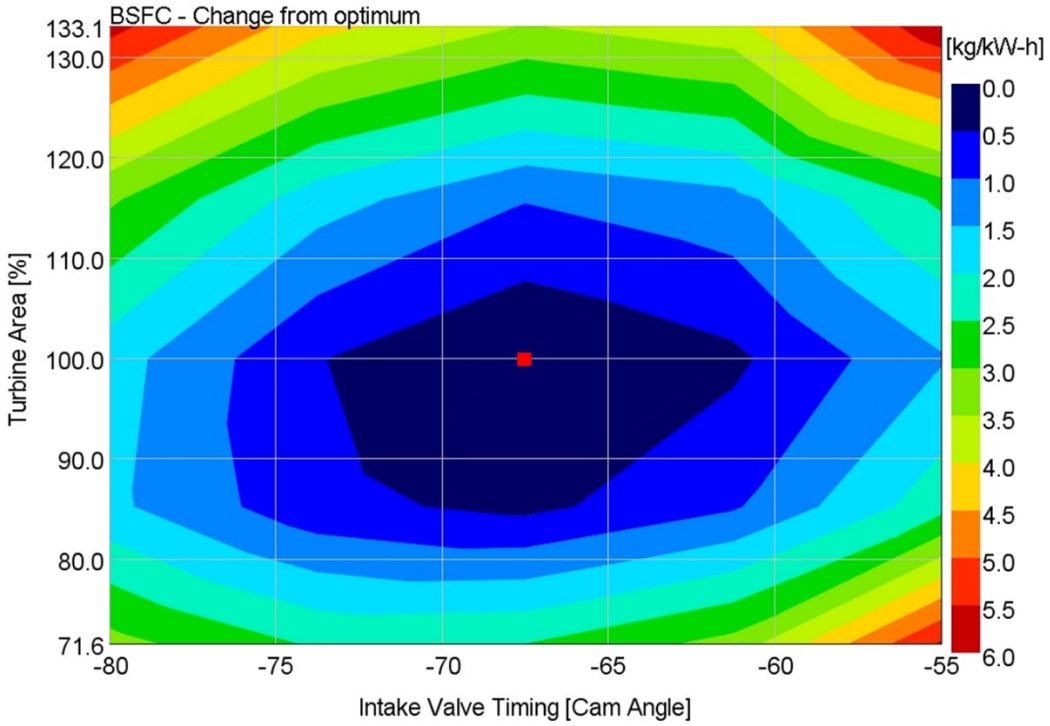

Figure 1. Brake specific fuel consumption. The optimum point is highlighted in red.

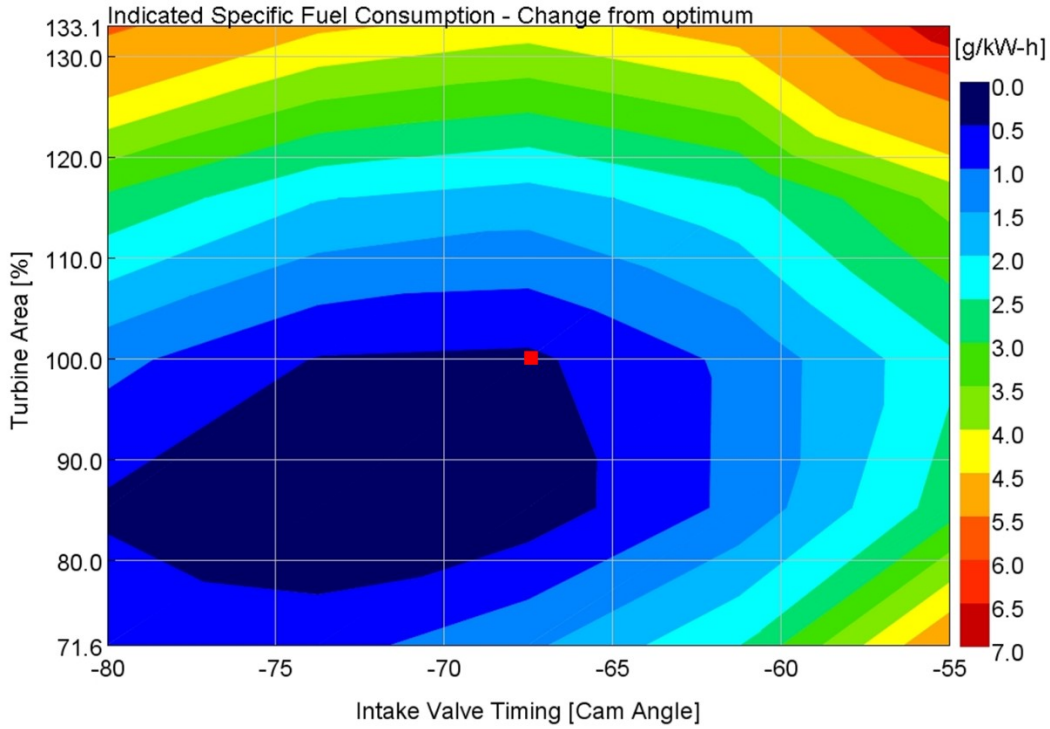

Figure 2. Indicated Specific Fuel Consumption, with the optimum BSFC point highlighted.

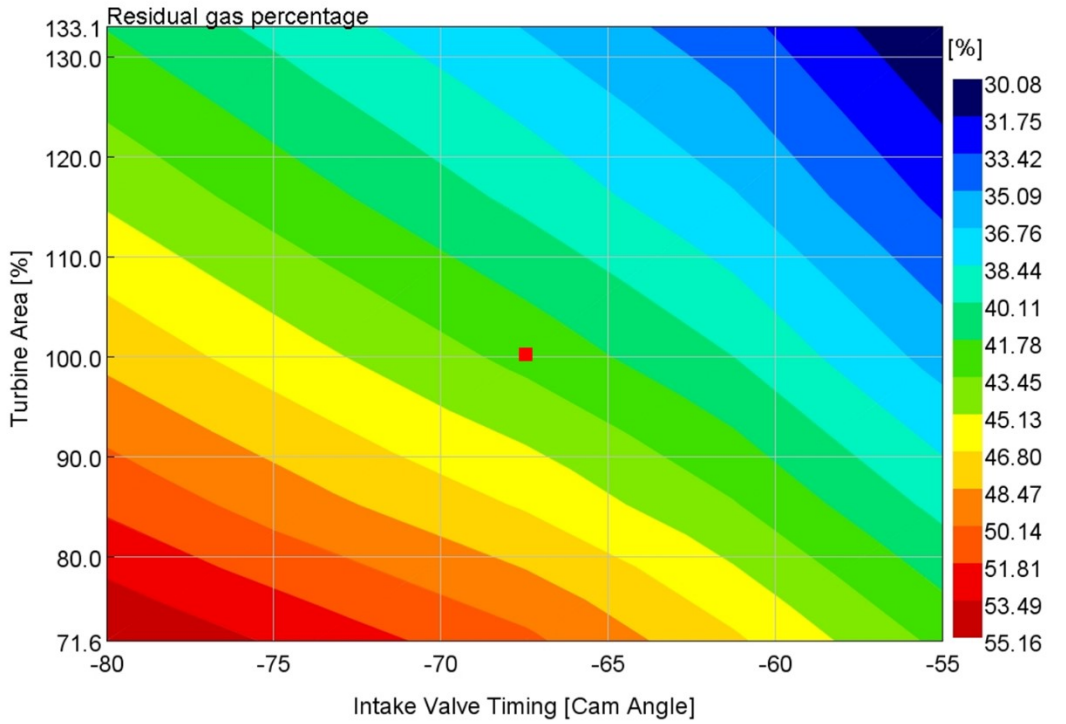

Figure 3. The residual gas percentage in the cylinder.

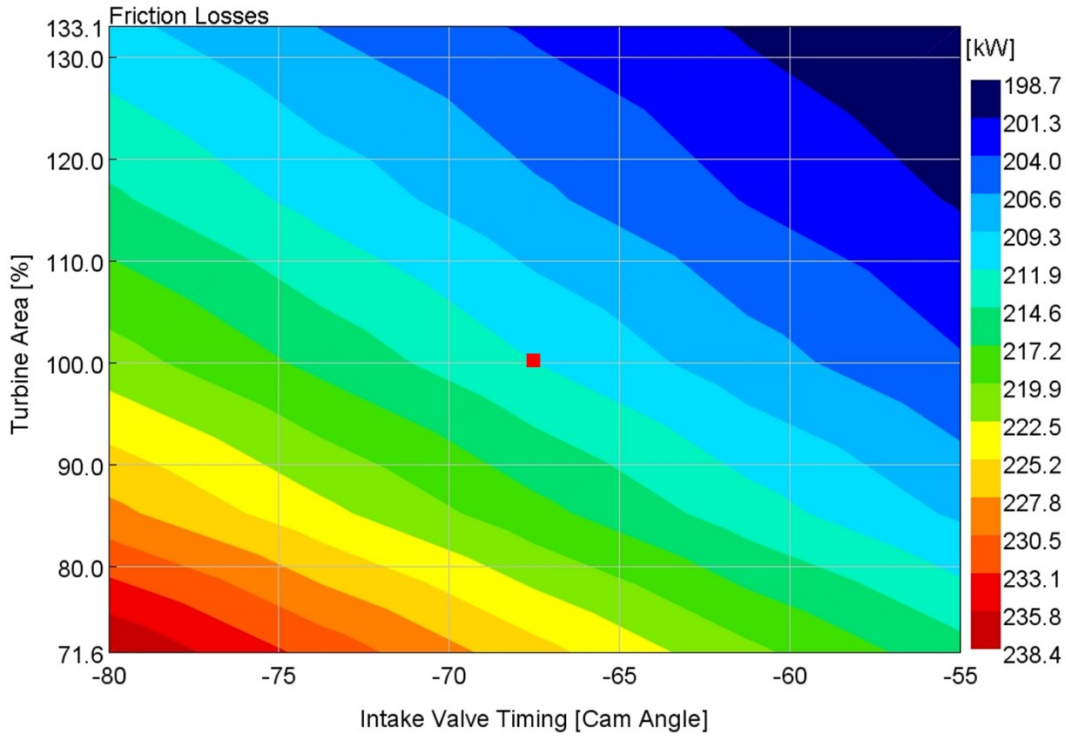

Figure 4. Friction losses.

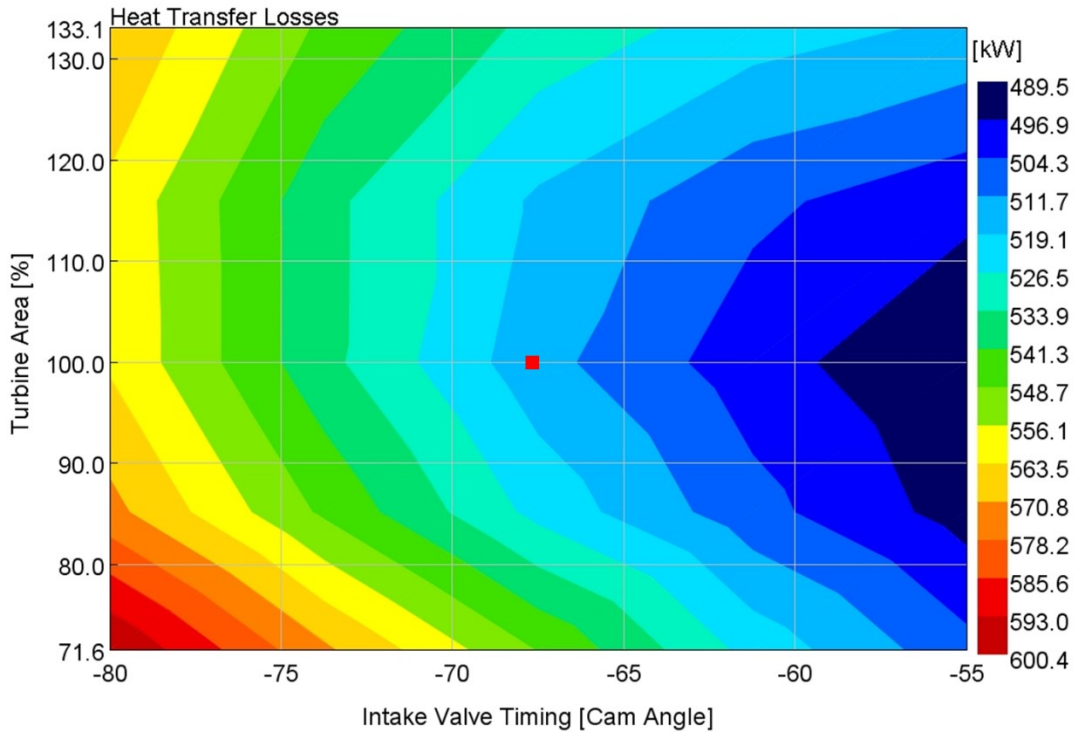

Figure 5. Heat transfer losses.

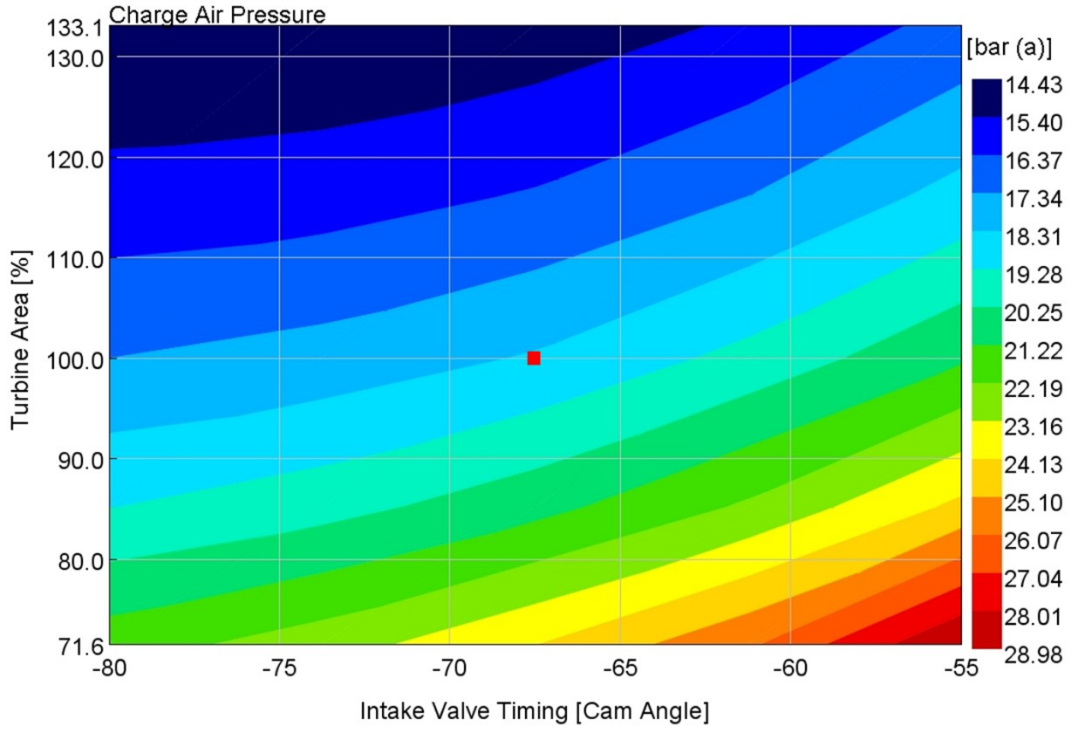

Figure 6. Charge air pressure.

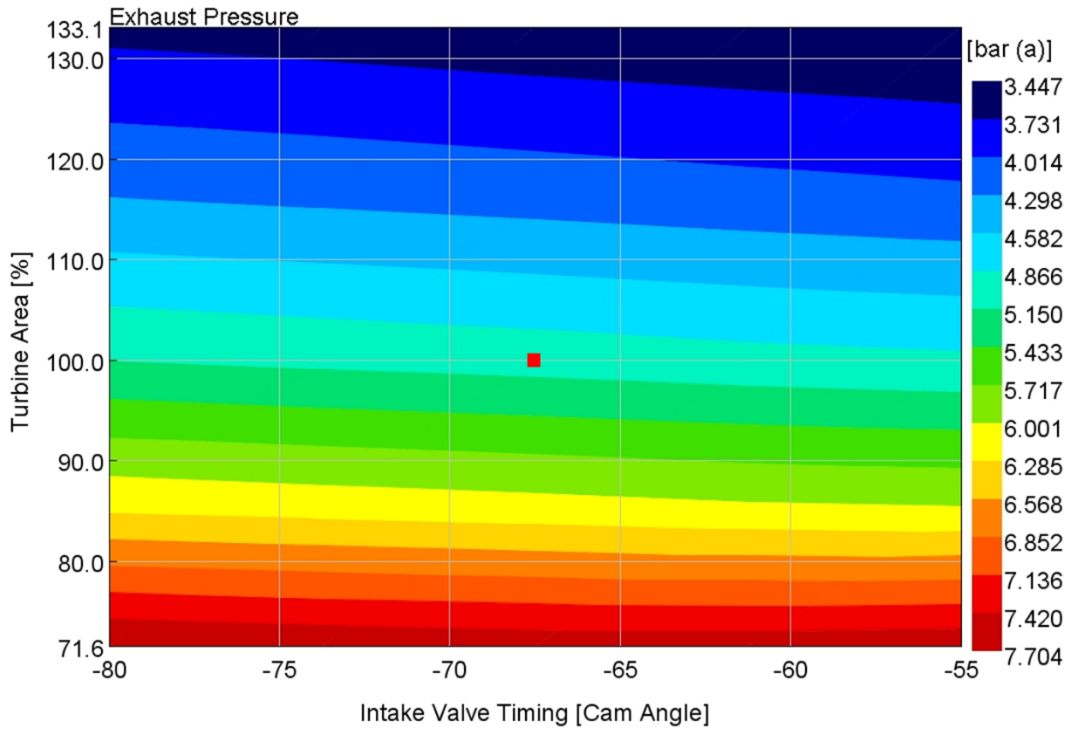

Figure 7. Exhaust pressure.

Appendix 3. Z-engine optimization results

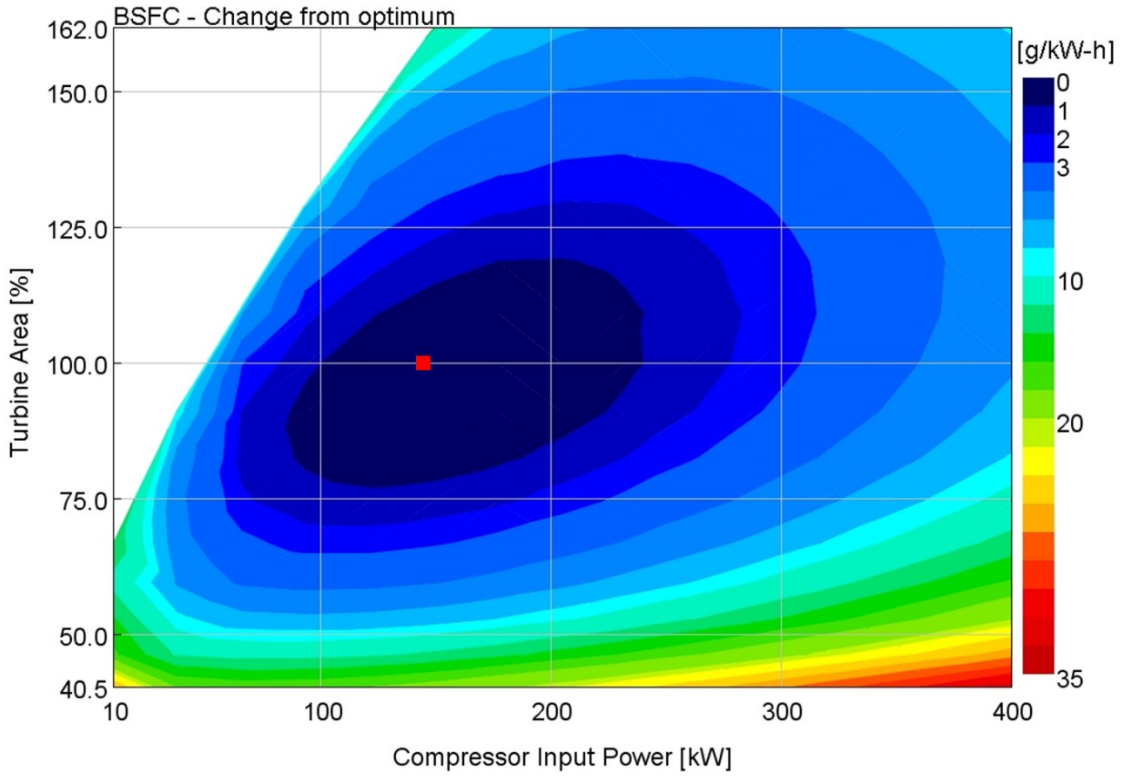

Figure 1. Brake Specific Fuel Consumption, where the optimum point is highlighted in red.

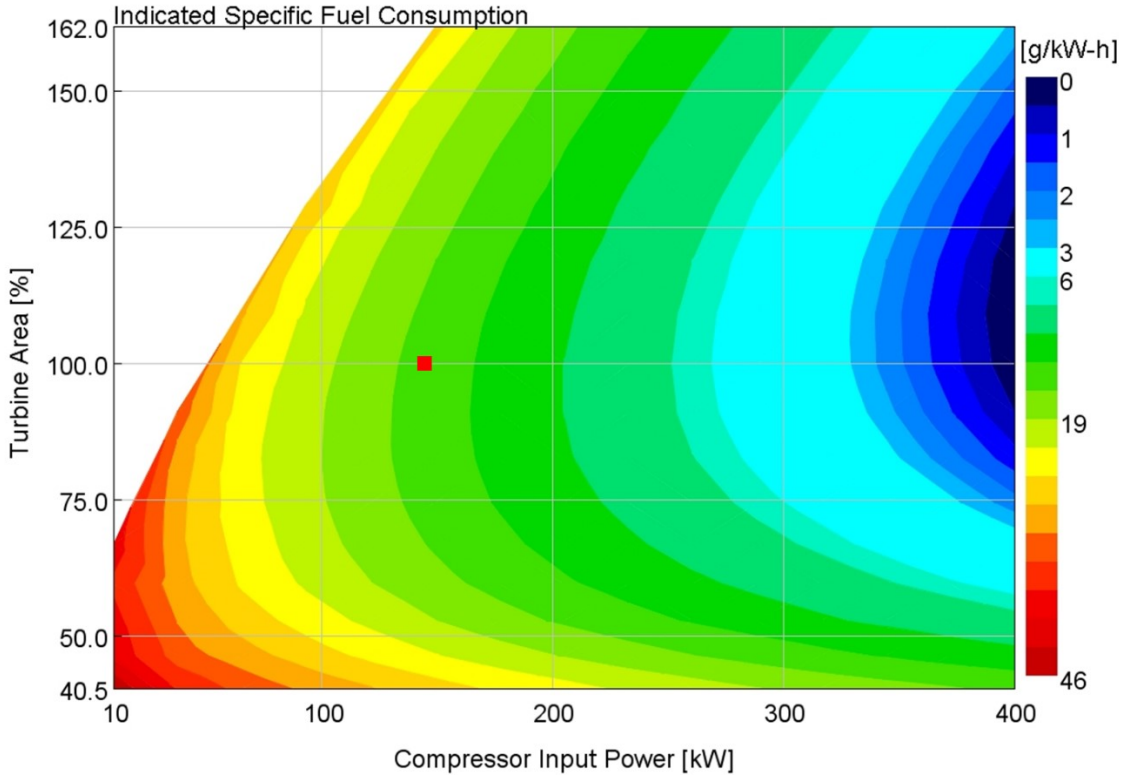

Figure 2. Indicated Specific Fuel Consumption, where the optimum BSFC point is highlighted in red.

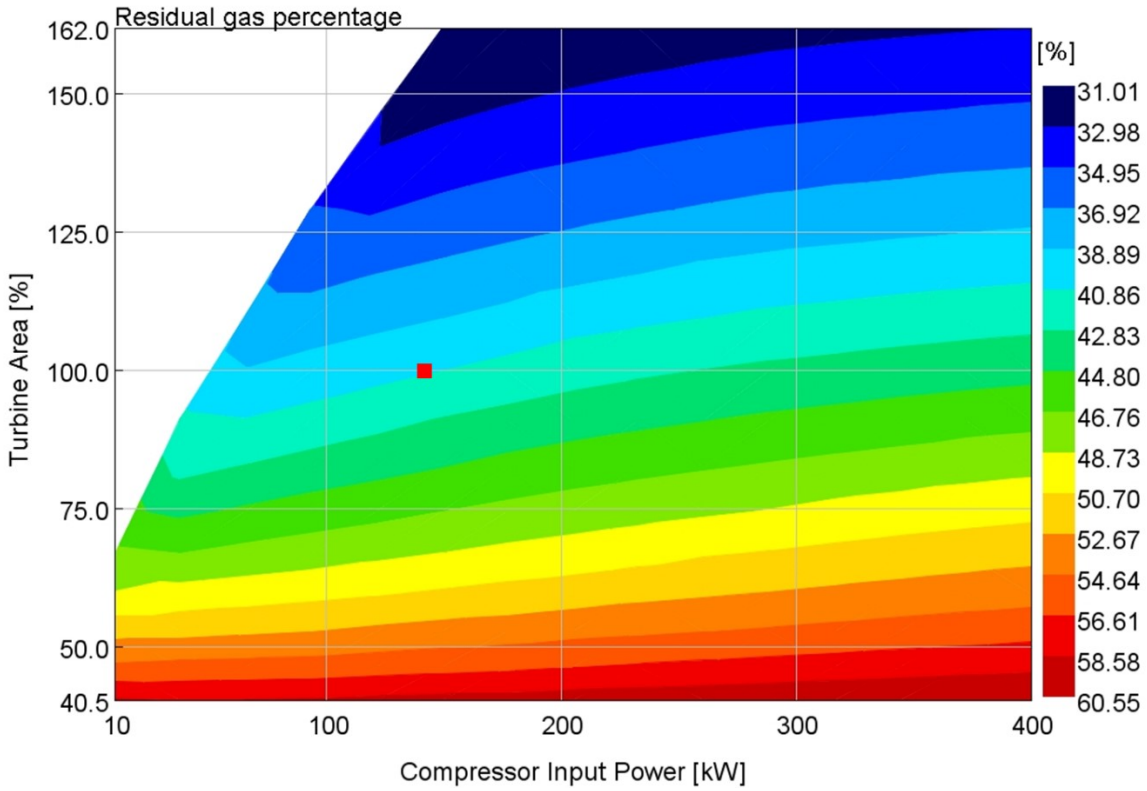

Figure 3. Residual gas percentage, with the optimum BSFC point highlighted in red.

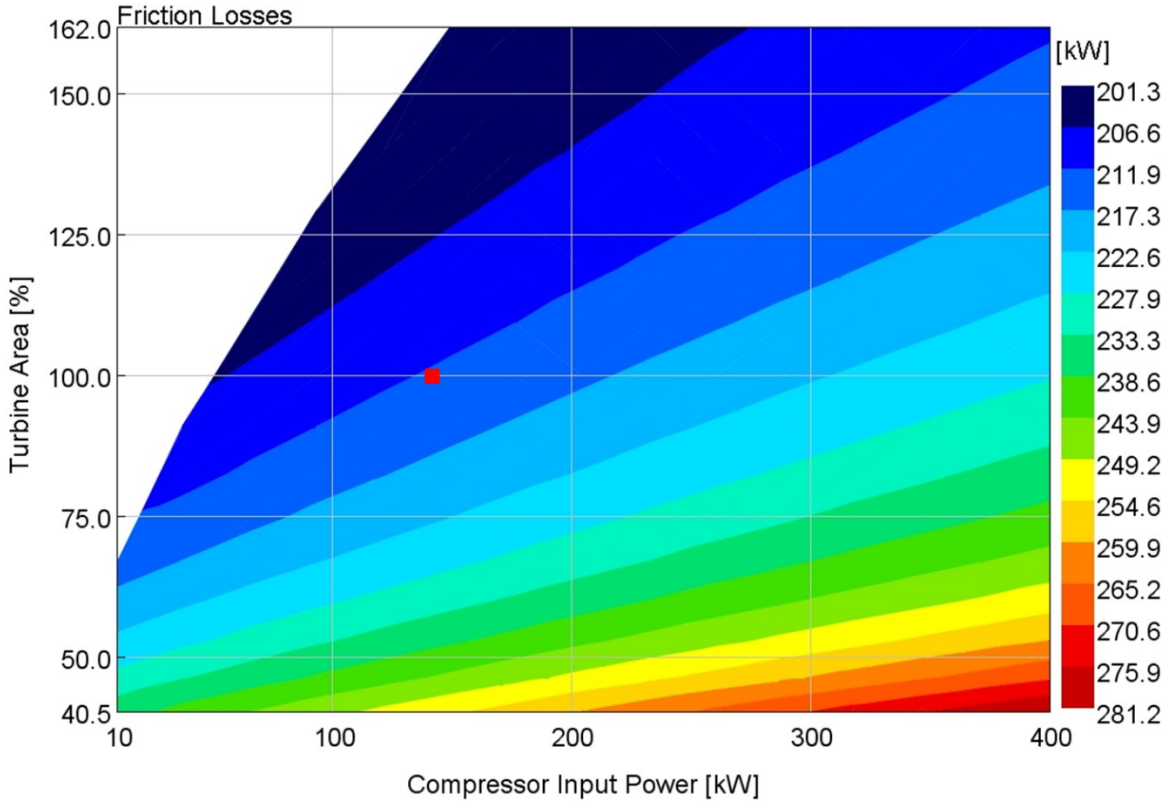

Figure 4. Friction losses, with the optimum BSFC point highlighted in red.

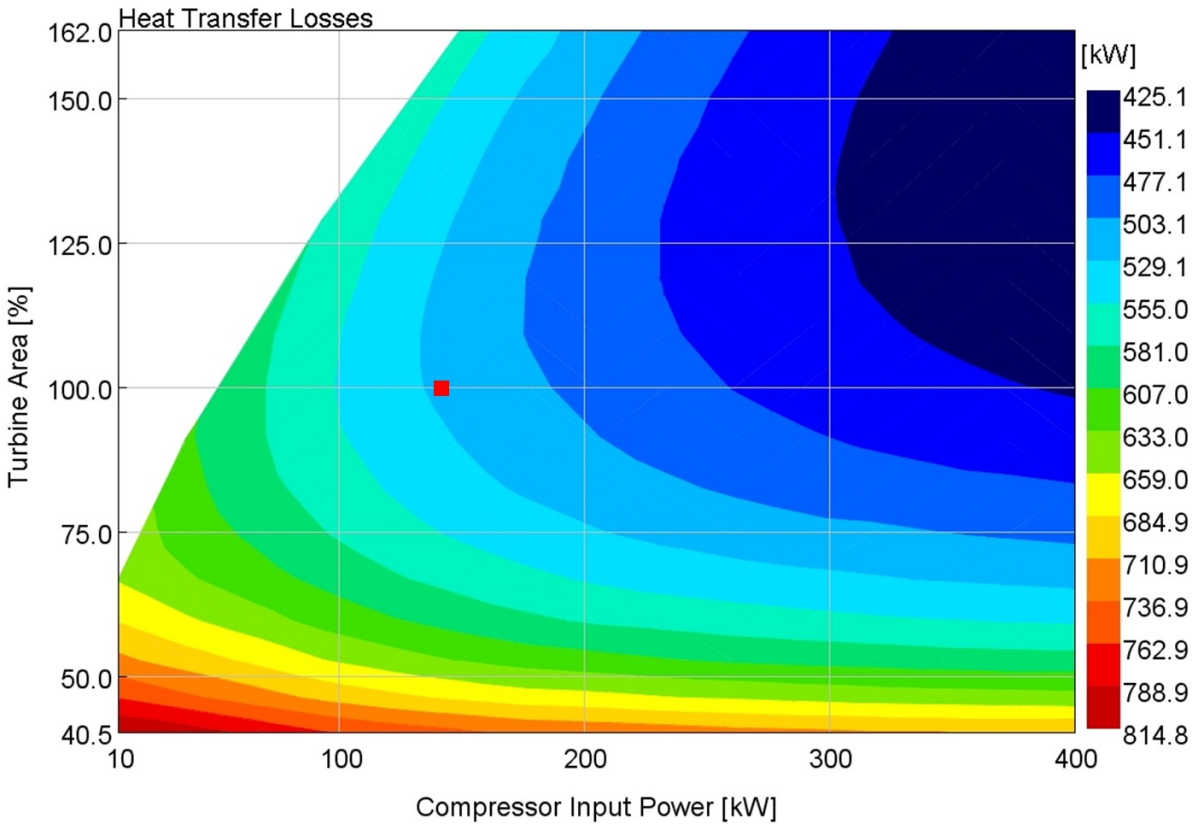

Figure 5. Heat transfer losses, with the optimum BSFC point highlighted.

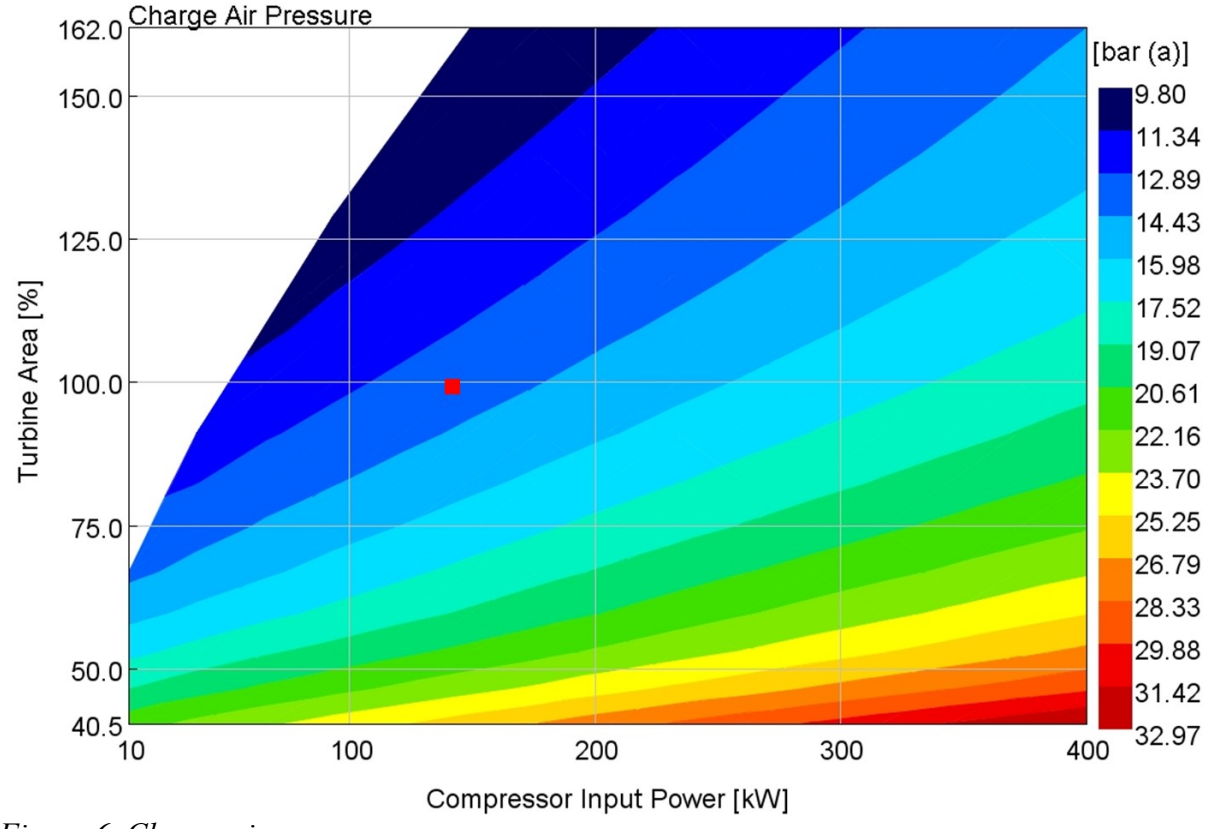

Figure 6. Charge air pressure.

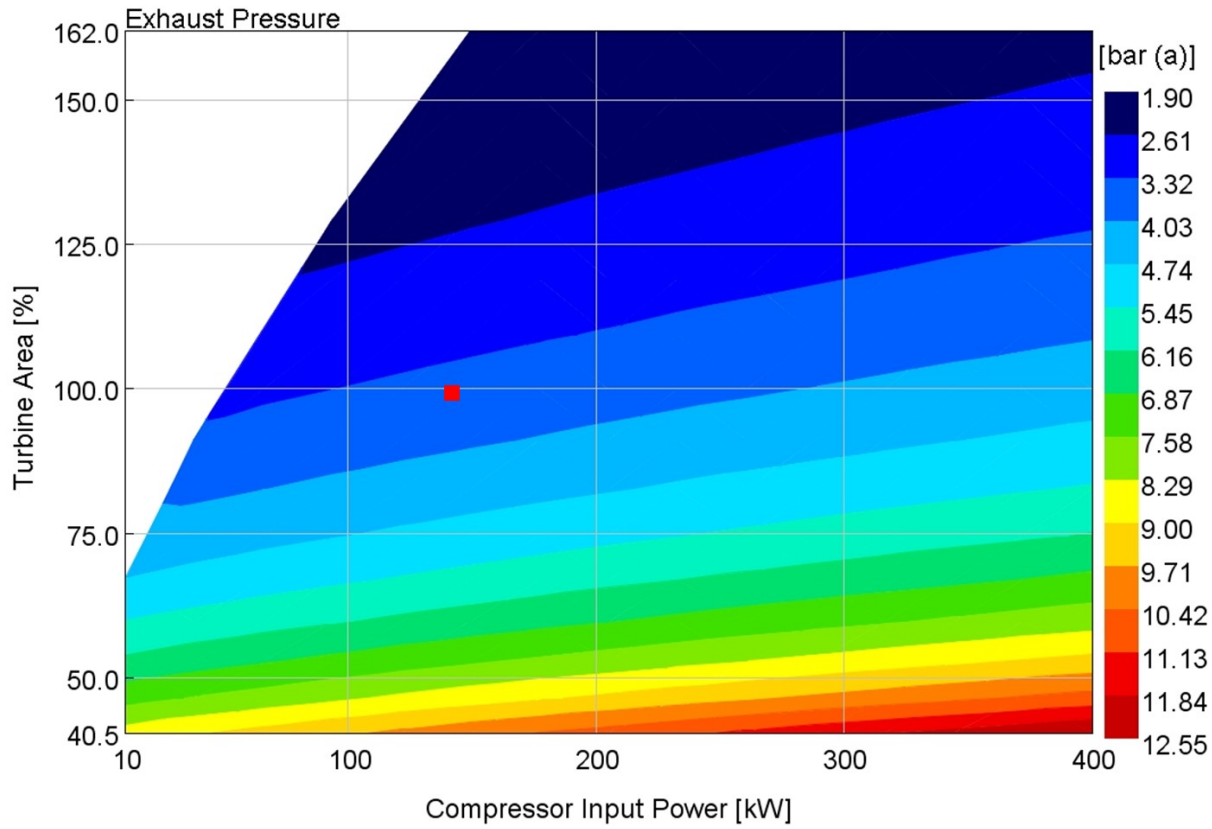

Figure 7. Exhaust pressure.

Appendix 4. Sankey diagrams

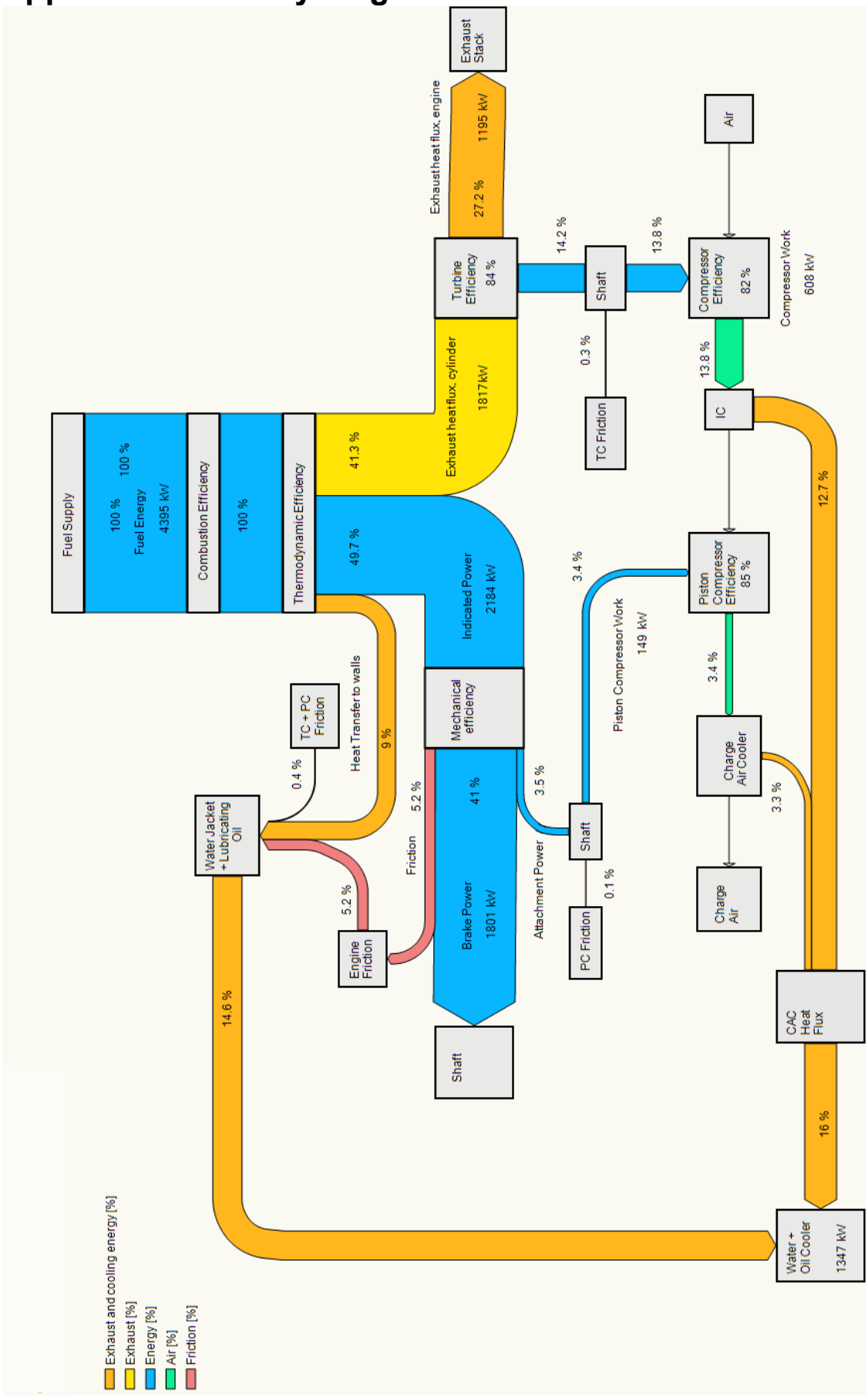

Figure 1. The Z-engine Sankey diagram.

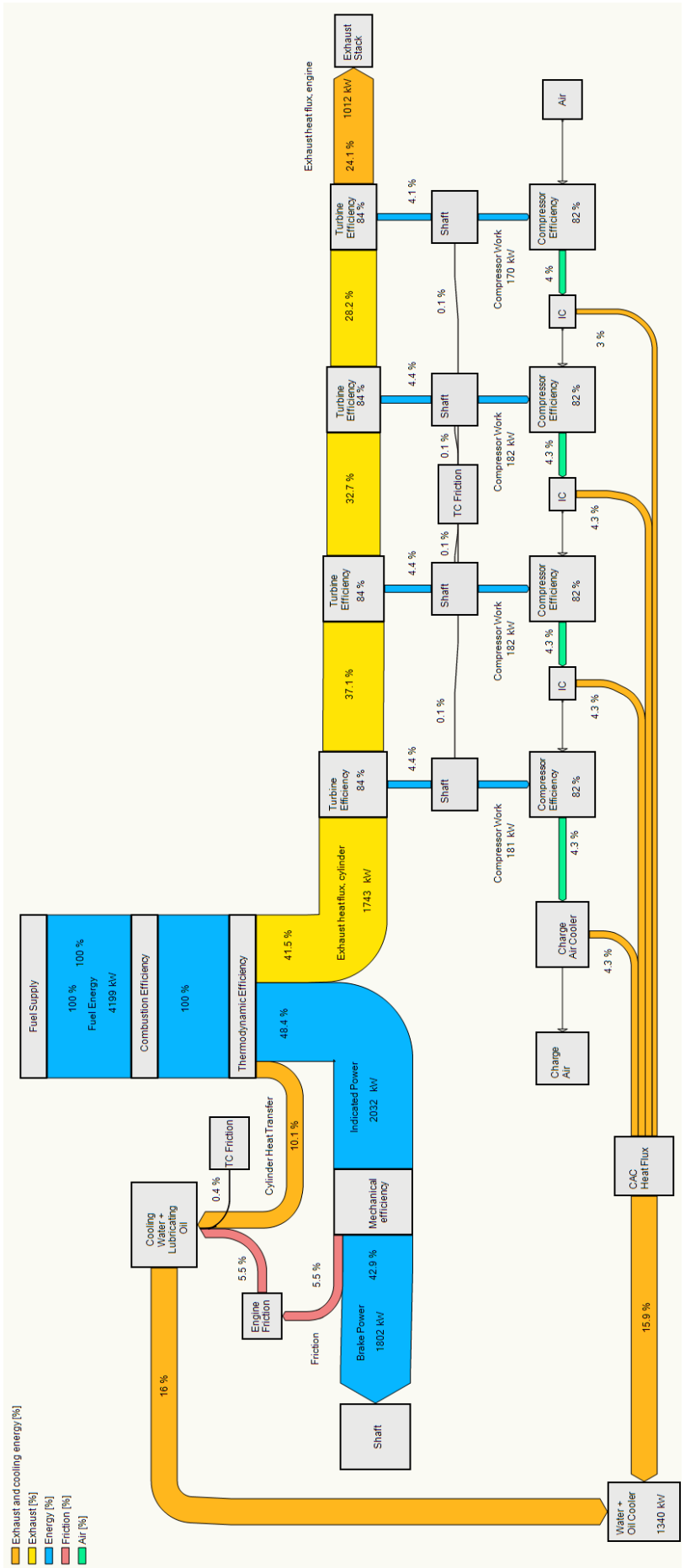

Figure 2. The Hoos Variant engine Sankey diagram.

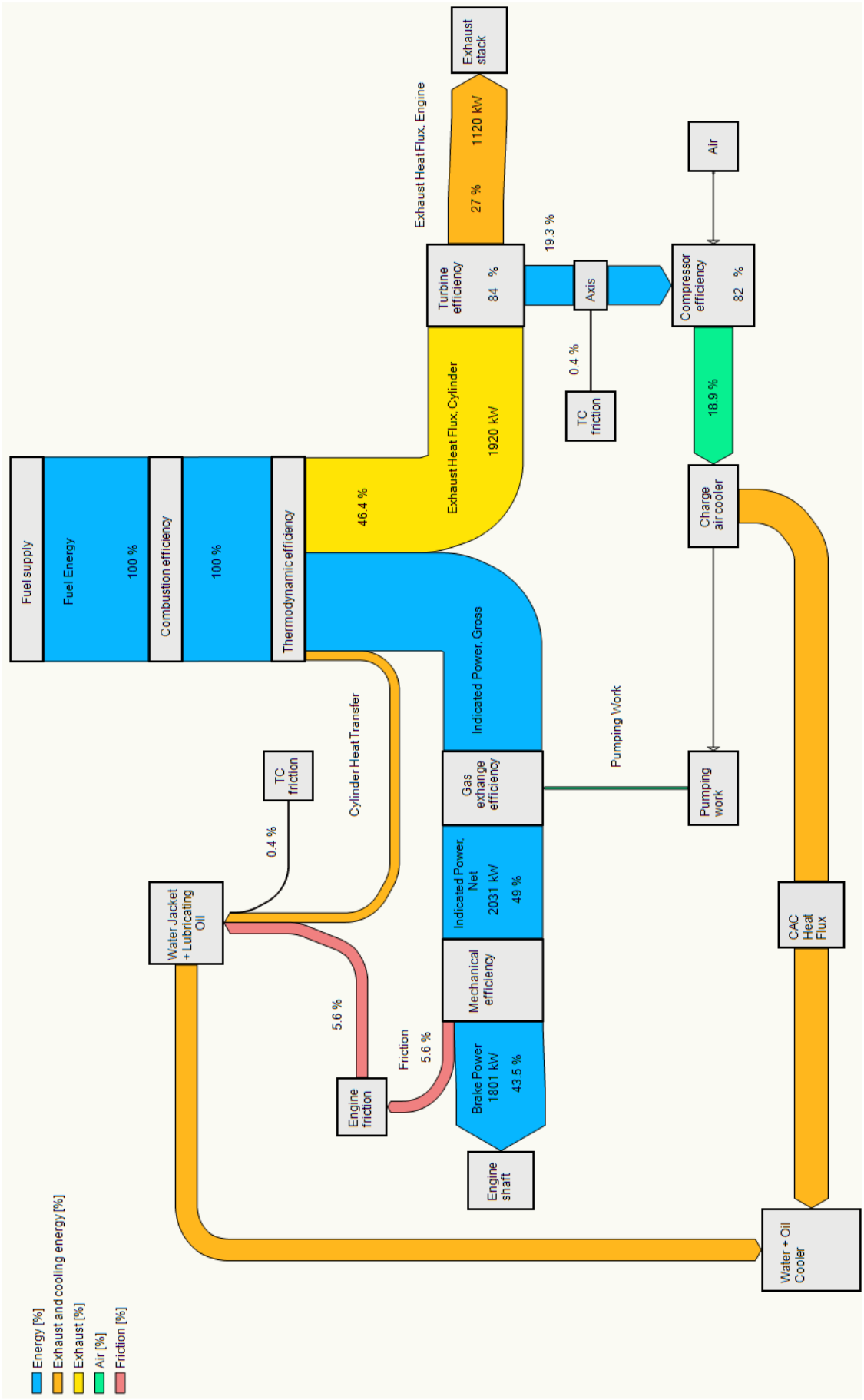

Figure 3. The W20 Sankey diagram.

Appendix 5. Heat load

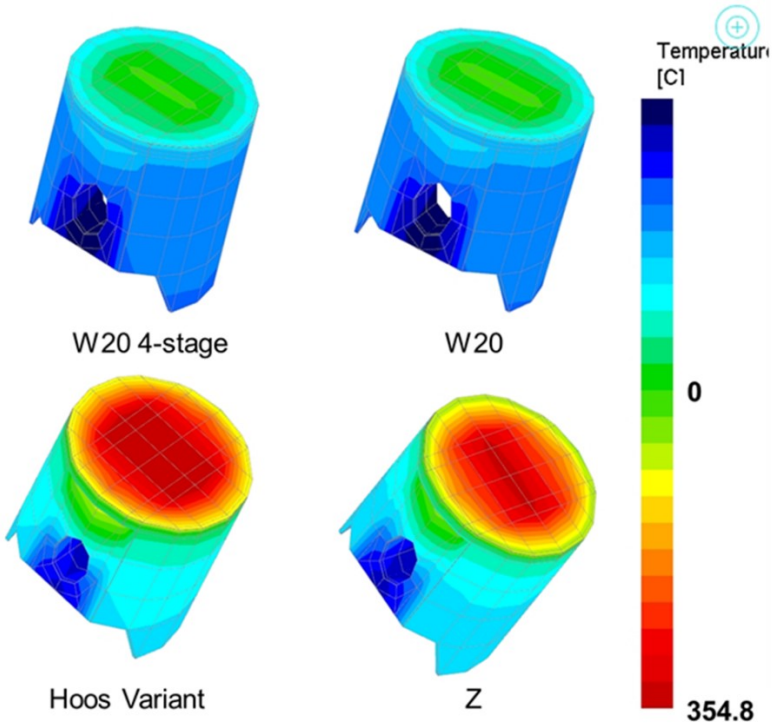

Figure 1. The piston temperature distribution in the engines. The scale is shown as change in temperature from a reference point.

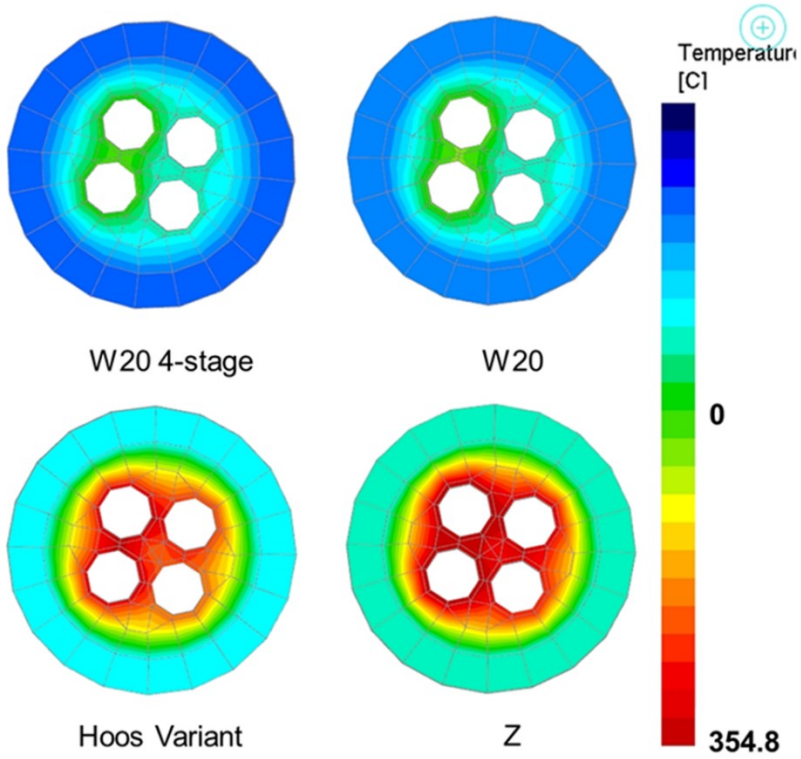

Figure 2. Temperature distribution in the cylinder head. The scale is shown as change in temperature from a reference point.

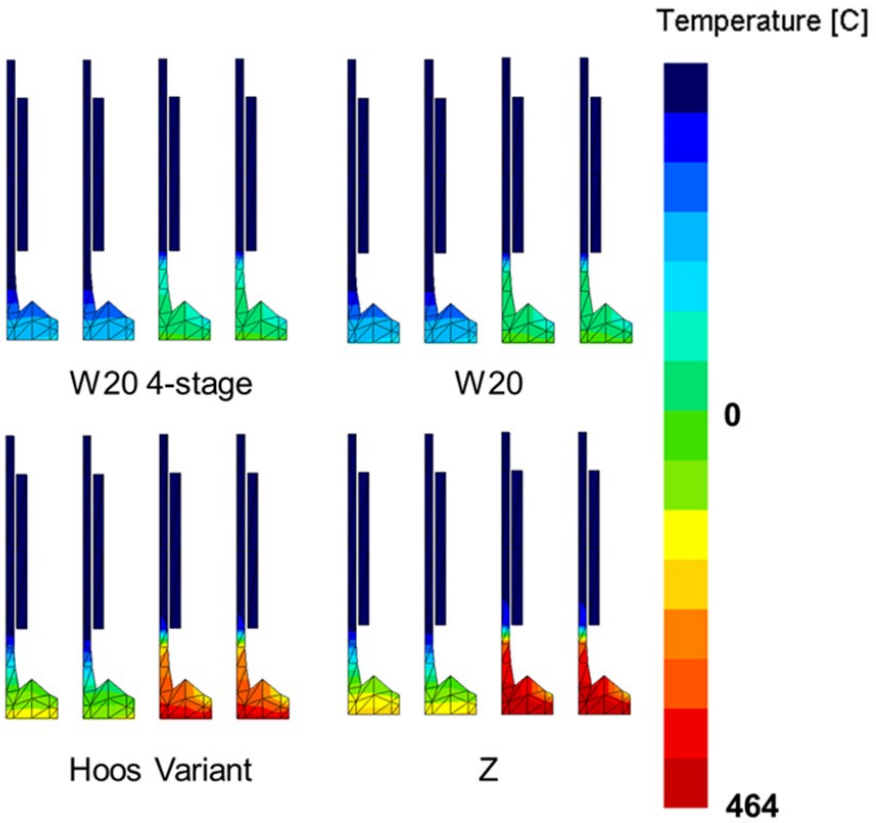

Figure 3. Temperature distribution in the intake (two leftmost valves) and exhaust (two rightmost) valves.